Aus der Medizinischen Klinik mit Schwerpunkt Kardiologie
der Medizinischen Fakultät der Charité – Universitätsmedizin Berlin

DISSERTATION

Protein transduction of $p21^{CIP1}$ inhibits angiotensin II-induced cardiac hypertrophy in mice

Zur Erlangung des akademischen Grades
Doctor medicinae (Dr. med.)

Vorgelegt der Medizinischen Fakultät der Charité-
Universitätsmedizin Berlin

von

Junfeng An

aus NingXia, China

Gutachter: 1. Prof. Dr. med. Rainer. Dietz

2. Priv.-Doz. Dr. med. Kai. C. Wollert

3. Priv.-Doz. Dr. med. Johann. Bauersachs

Datum der Promotion

CONTENTS

ABSTRACT

Myocardial hypertrophy is an early milestone during the clinical course of heart failure and an important risk factor for subsequent cardiac morbidity and mortality. Left ventricular wall stress, hormones, cytokines, growth factors and cardiovascular diseases increase cardiac workload and induce myocyte hypertrophy that often leads to overt heart failure. Reduction of left ventricular hypertrophy by anti-hypertensive treatment improves the prognosis of patients. However, only a partial reduction of cardiac hypertrophy is achieved with the available means. Previous studies have focused on the activation of maladaptive signalling pathways in the etiology of cardiac hypertrophy and adverse remodelling. Interestingly, recent results indicate that cardiac hypertrophy is associated with activation of the cell-cycle machinery or with the induction of cell cycle-related proteins and an increase in Cyclin-dependent kinase signalling. Therefore we hypothesized that overexpression of cell cycle inhibitor $p21^{CIP1}$ repressing Cyclin-dependent kinase signalling could be an effective molecular approach to inhibit cardiac hypertrophy. Due to low gene expression efficiencies by adenovirus or adeno-associated virus vectors *in vivo*, the TAT protein transduction technique was applied for somatic gene transfer. This method utilizes the ability of an amino-terminal 11 amino-acid protein transduction domain from the human immunodeficiency virus TAT protein to mediate protein transduction. The fusion protein TAT.$p21^{CIP1}$ was expressed in bacteria and purified under denaturation conditions employing *FPLC* equipment. Importantly, application of TAT.$p21^{CIP1}$ fusion protein provided efficient and homogenous gene transfer *in vitro* and *in vivo*, allowing assessment of the impact of $p21^{CIP1}$ on heart remodelling following angiotensin II administration. In contrast to inactive mutant TAT.$p21^{CIP1}\Delta C$, TAT.$p21^{CIP1}$ wild-type protein significantly inhibited features of cardiac hypertrophy such as reexpression of fetal cardiac genes, increased protein synthesis and cardiomyocyte surface area following angiotensin II administration.

In summary, we show by means of TAT protein transduction, that $p21^{CIP1}$ efficiently abrogates angiotensin II-induced hypertrophy *in vitro* and *in vivo*.

ZUSAMMENFASSUNG

Die kardiale Hypertrophie stellt einen frühen Meilenstein in der klinischen Entwicklung einer Herzinsuffizienz dar und ist mit erhöhter Morbidität und Mortalität vergesellschaftet. Dabei führen linksventrikulärer Wandstress, Hormone, Zytokine, Wachstumsfaktoren und kardiovaskuläre Erkrankungen zu einer erhöhten kardialen Belastung, die häufig zur Herzinsuffizienz führt. Durch blutdrucksenkende Therapie kann die linksventrikuläre Hypertrophie reduziert und die Prognose des Patienten verbessert werden. Dennoch kann mit der verfügbaren pharmakologischen Therapie in der Regel maximal eine partielle Reduktion der Hypertrophie erreicht werden. Die Kenntnis molekularer Mechanismen der linksventrikulären Hypertrophie erlaubt die Entwicklung neuer molekularer Therapieansätze. Vorausgegangene Studien haben sich meist mit der Aktivierung maladaptiver Signalwege in der Entstehung der linksventrikulären Hypertrophie und des myokardialen Remodelling beschäftigt. Interessanterweise weisen neuere Studien auf eine Induktion Zellzyklus relevanter Gene und erhöhte Zyklin-abhängige Kinaseaktivitäten in der Hypertrophieentstehung hin. Daraufhin entwickelten wir die Hypothese, dass eine Hemmung Zyklin-abhängiger Kinaseaktivitäten durch den Zyklin-abhängigen Kinaseinhibitor $p21^{CIP1}$ ein bedeutsamer molekularer Ansatz in der Behandlung der myokardialen Hypertrophie sein könnte. Aufgrund nur geringer Effizienzen der Expression eines Transgens nach adeno- oder adeno-assoziiert-viralem somatischem Gentransfer *in vivo*, verwendeten wir die TAT Protein-Transduktionstechnik. Hierbei wurde der Inhibitor Zyklin-abhängiger Kinasen, $p21^{CIP1}$, als Fusionsprotein kloniert, das an seinem aminoterminalen Ende die 11 Aminosäuren umfassende Protein-Transduktionsdomäne des humanen HIV TAT-Proteins enthält (TAT.$p21^{CIP1}$). TAT.$p21^{CIP1}$ wurde in Bakterien exprimiert und unter denaturierenden Bedingungen mit Hilfe eines *FPLC*-Verfahrens bis zur Homogenität aufgereinigt. Proteintransduktion von TAT.$p21^{CIP1}$ führte zu einem homogenen Proteintransfer sowohl in Zellkulturexperimenten neonataler Rattenkardiomyozyten als auch nach intraperitonealer Injektion adulter Mäuse. Dabei inhibierte TAT.$p21^{CIP1}$ in einer Dosis-abhängigen Weise Angiotensin II induziertes hypertrophes Wachstum *in vitro* und *in vivo*. Dies wurde bestimmt durch Northernblott-Analysen zur Expression der molekularen Hypertrophiemarker ANF und β-MHC, der Kinaseaktivität von Cdk2 sowie Bestimmung der Proteinsynthese und Kardiomyozytengröße. Keinen Einfluss auf die Entwicklung der Hypertrophie hatte ein mutiertes TAT.$p21^{CIP1}\Delta C$, in dem der Carboxylterminus deletiert wurde.

Zusammenfassend lässt sich sagen, dass TAT.$p21^{CIP1}$ Proteintransduktion zu einer Inhibition Angiotensin II induzierter Hypertrophie *in vitro* und *in vivo* führt.

1 INTRODUCTION

1.1 The mammalian cell cycle

The mammalian cell cycle is a highly coordinated complex process mediated by internal and external signals. Growth factors stimulate the replication process, but it is an intrinsic control mechanism that determines whether the cell is ready to proceed through the ordered set of events, the cell cycle, which culminate in the production of two daughter cells (Regula et al., 2004; Verschuren et al., 2004) **(Figure 1.1, page 3)**.

Cell cycle phases 1-4

The cell cycle consists of four different phases: the time window between mitosis and successive deoxyribonucleic acid (DNA) replication (G_1 phase), the phase of DNA duplication (S phase), the gap after DNA synthesis (G_2 phase) and the phase which results in cell division or mitosis (M phase). Generally, there is a division in mitosis and interphase. Mitosis describes the cell division itself, whereas interphase serves as a generic term for all other states. After mitosis the cell enters the first gap phase, known as G_1, where it starts producing ribonucleic acid (RNA) and synthesizing proteins. This state is accompanied by an increase in size and can lead to another gap phase, known as G_0. This phase may represent an end-stage of development, a sign that the cell will no longer divide. Many cells are able to leave G_0 again, re-entering G_1 and continue the cell cycle. These cells enter the so-called S phase, where DNA is completely duplicated providing two identical genomes for two daughter cells. Before dividing, cells have to cross a third gap phase: G_2. In G_2, cells grow further and synthesize more protein to prepare for mitosis. Finally the cell enters the M phase and divides into two daughter cells. During this period of the cell cycle, the nuclear envelope breaks down and nuclear division occurs in a carefully orchestrated manner. Chromosomes condense and align at the metaphase plate and duplicated chromosomes are segregated to opposite poles of the cell, cytokinesis marks the end of mitosis **(Figure 1.1, page 3 B)**. The period between two subsequent mitotic cycles is known as interphase and consists of the G_1, S, and G_2 phases of the cell cycle. After having completely divided, the cell enters G_1 again in response to appropriate mitogenic signals.

Cell cycle control mechanisms

Cell cycle progression is tightly controlled by a diverse panel of factors that coordinate the biochemical events within the cell necessary for cell division. These factors include Cyclins

(also called CYC or Cyc), Cyclin-dependent protein kinases (Cdks), Cdk-activating kinase (CAK), Cdk inhibitors (CKIs), both members of the retinoblastoma family (Rb, also called pRB or pRb) and the E2Fs. Cyclins are nuclear proteins without intrinsic enzymatic activity. Each Cyclin contains a region called the Cyclin box which is involved in the binding of specific Cdks (Kobayashi et al., 1992). In complex with Cyclins, Cdks phosphorylate proteins at critical serine and threonine residues to drive the cell cycle. The progression through the cell cycle depends on sequential binding of Cyclins to distinct Cdks, which represent the functionality of the Cyclin/Cdk complex (Borriello et al., 2002). Cyclins can be divided into four main classes, depending on the phase of the cell cycle where they occur. In mitosis CyclinB is found, Cdk4 and its close relative Cdk6 function early in G_1 and are activated by D-type Cyclins: (i.e. CyclinD1, D2 and D3). Complexes of D-type Cyclins with Cdk4 and Cdk6 play a critical role in the cellular transition from G_0 to G_1. Growth factors induce synthesis of D-type Cyclins via the Ras/Raf/ERK signalling pathway (Regula et al., 2004). In contrast, CyclinE specifically activates Cdk2 and starts to accumulate late in G_1. It peaks at the $G_1 \rightarrow S$ transition and can be detected until middle S phase (Keyomarsi et al., 1997). From early S phase to beginning G_2, CyclinA is found complexed with Cdk2 (Grana et al., 1998). Then, the activated Cyclin/Cdk complexes regulate the activity of their target molecules. The primary target of Cdk activities are Rb and the related pocket proteins (p107 and p130) that serve as transcriptional repressors (Grana et al., 1998). In contrast, the E2F family of transcription factors is required for transcription of many genes involved in DNA and deoxyribonucleotide synthesis such as Cdk2 and CyclinA and E. The transcription-activating ability of E2Fs is inhibited by their binding of Rb protein and two related proteins, p107 and p130. Indeed, binding of Rb to E2Fs converts them from transcriptional activators to repressors because Rb interacts with histone deacetylase complexes. Phosphorylation of Rb protein inhibits its repressing function, permitting activation of the genes required for entry into the S phase by E2Fs. Phosphorylation of Rb protein is initiated by Cdk4/CyclinD and Cdk6-CyclinD in mid G_1. Once expression of Cdk2 and CyclinE is stimulated, Cdk2/CyclinE further phosphorylates Rb in late G_1. Since E2Fs also stimulate their own expression, these processes form positive feedback loops for the phosphorylation of Rb protein. Initial phosphorylation of Rb leads to generation of Cdk2/CyclinE, which accelerates further phosphorylation of Rb. At this point, passage through the cell cycle is independent of Cdk4,6/CyclinD activity, so that progression occurs even when mitogens are withdrawn and CyclinD levels fall (Grana et al., 1998; Regula et al., 2004).

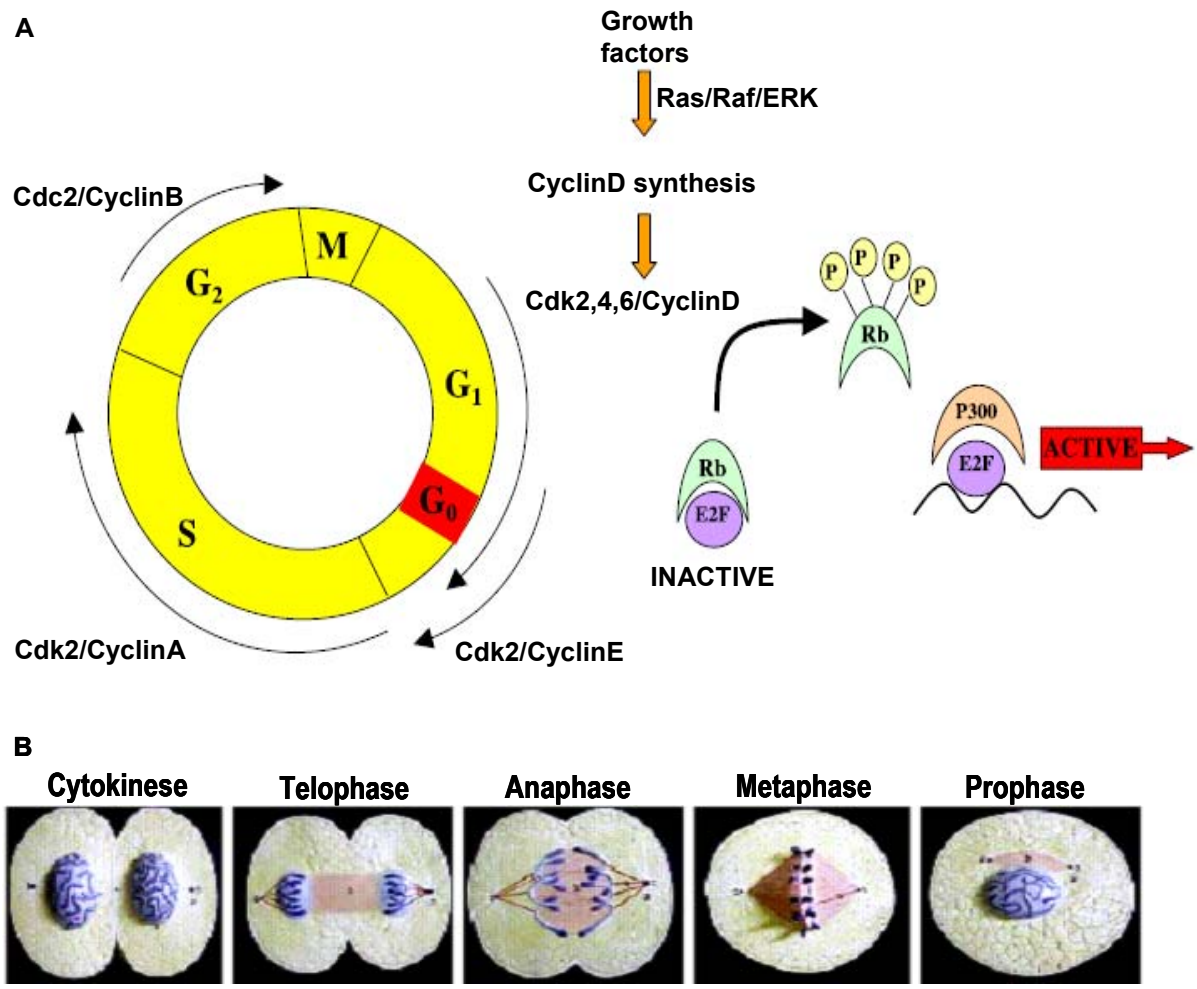

Figure 1.1: A. The mammalian cell cycle. Cyclins/Cdk complexes control entry and exit through the 4 phases of the cell cycle. Growth factors trigger the synthesis of D-type Cyclins which complex with Cdk4 or Cdk6 to regulate cell cycle progression through G_0. The phosphorylation of pRb by G_1 Cyclins (D1, D2, D3, and E)/Cdk complexes promotes the release of E2F1 from Rb. Through its association with p300, E2F1 activates the transcription of genes important for the G_1 transition to S phase (Regula et al., 2004). B. Schematic figures of the mammalian cell mitosis.

1.2 Cyclin-dependent kinase inhibitors (CKIs)

Progression through the cell cycle is controlled by the Cyclin/Cdk complexes. Numerous mechanisms have evolved to regulate this important function (Obaya and Sedivy, 2002). Cyclins display a periodic pattern of expression (Verschuren et al., 2004). They accumulate during different phases of interphase and then rapidly degrade before the next round of the cell cycle. Once the Cyclin has associated with its Cdk partner, it is not catalytically active

until it is phosphorylated on a threonine around position 160 (Regula et al., 2004). The Cyclin/Cdk activities are in turn constrained by CKIs, which bind to and inhibit the activity of Cyclin/Cdk complexes. All CKIs involved in eukaryotic cell cycle control require phosphorylation at a conserved threonine (or serine) residue within the activation- or T-loop to attain full enzymatic activity. The enzyme responsible for this activating phosphorylation of Cdks is therefore essential for normal proliferation of all eukaryotic cells (Larochelle and Fisher, 2005). There are proteins that inactivate Cdks by binding them and thus prevent them from phosphorylating their targets. These inhibitory proteins are referred to as inhibitors of Cyclin-dependent kinases or CKIs. Several studies have identified two classes of CKIs: the CIP/KIP and the INK4 families. The CIP/KIP family is formed by three members: $p21^{CIP1}$, $p27^{KIP1}$ and $p57^{KIP2}$. The INK4 family is composed of four members: $p16^{INK4A}$, $p15^{INK4B}$, $p18^{INK4C}$ and $p19^{INK4D}$ (Brooks et al., 1998), henceforth referred to as p15, p16, p18 and p19. This classification is based on the protein sequence, as well as on the affinity for the Cdk target. INK4 inhibitors are narrow-spectrum CKIs, they only specifically bind to and inhibit the activity of Cdk4/6 (Brooks et al., 1998). The members of the CIP/KIP CKI family show significant amino acid homology at their amino-terminal domains building the Cdk binding/inhibitory domains. Furthermore, they all have a nuclear localization signal (NLS) near the carboxyl-terminus but no other motifs in common (Nakayama and Nakayama**,** 1998). The carboxyl-terminal region of $p21^{CIP1}$ possesses a unique region for contacting with proliferating-cell nuclear antigen (PCNA, a subunit of DNA-polymerase delta). $p21^{CIP1}$ was found to block the ability of PCNA to promote DNA synthesis (Nakayama and Nakayama**,** 1998). The $p21^{CIP1}$ family can bind and inhibit a broad range of Cyclin/Cdk complexes **(Figure 1.2, page 6)**, with a preference for those containing Cdk2, compared with the narrow-spectrum of the INK4 family (Xiong et al., 1993; Harper et al., 1995; Brooks et al., 1998). CKIs prevent the phosphorylation of pRb/p107/p130 by binding Cyclin/Cdk complexes, thus arresting cells in G_1 (Medema et al., 1995; Harper et al., 1995; Grana et al., 1998). To overcome the G_1 arrest, they can be sequestered from their binding partners by means of accumulation of more Cdks, or the CKIs can be cleaved by caspases. Among them, caspase-3 activation results in translocation of the protein into the cytoplasm (Rosato et al., 2001). The CIP/KIP family inhibits the activity of complexes containing D-type Cyclins and Cdk4 or Cdk6, CyclinE and Cdk2, and CyclinA and Cdk2 (Brooks et al., 1998). When active, these complexes implement G_0/G_1 progression and S phase entry. DNA synthesis begins with the Cdk4- and/or Cdk6-mediated phosphorylation of Rb protein. Phosphorylated Rb is released from its complex with E2F. The released E2F then promotes the transcription of numerous

genes required for cellular progression through S phase (Grana et al., 1998; Regula et al., 2004).

1.2.1 $p21^{CIP1}$

$p21^{CIP1}$ is also named $p21^{CIP1/KIP1}$ (for Cdk interacting protein/kinase inhibitory protein) or $p21^{CIP1/Waf1}$ (wild-type p53-activated fragment) and will be henceforth referred to as p21. p21 was the first member of the CIP/KIP family, which was identified and cloned (Xiong et al., 1993; Brooks et al., 1998). This CKI appears to be a universal inhibitor of Cyclin/Cdk activity (Xiong et al., 1993; Harper et al., 1995), primarily acting in G_1 and at the G_1–S phase transition **(Figure 1.2, page 6)**. The level of p21 mRNA has been shown to fluctuate during the cell cycle, peaking on the exit from G_0 phase (Brooks et al., 1998), Increased levels of p21 protein can bind and inhibit G_1 phase Cyclin/Cdk complexes and result in a G_1 arrest (Brugarolas et al., 1995). Overexpression also leads to G_2 and S phase arrest (Stein et al., 1999). It has been proposed that the induction of p21 on exit from G_0 is to reduce Cyclin/Cdk activity in G_1 and to act as a threshold, above which Cyclin/Cdk complexes need to accumulate to enable cell cycle progression (Brooks et al., 1998). The levels of p21 mRNA and protein are elevated in quiescent and differentiated cells (Brooks et al., 1998). Despite the observation that mice with a targeted homozygous inactivation of the p21 gene are essentially normal, inactivation of p21 increased cell proliferation (Yang et al., 2005). This finding is consistent with the depiction that overexpression of p21 prevents cellular proliferation (Xiong et al., 1993). One of its first identified functions was its binding of PCNA resulting in the direct inhibition of DNA-replication (Perkins, 2002). p21 is a molecule with two domains and multiple functions: At one level, p21 can inhibit the kinase activity of Cyclin/Cdk complexes and these have been shown to regulate the activity of a number of transcription factors. The best example of this straightforward mechanism is found with members of the E2F and Rb families of transcriptional regulators. Phosphorylation by Cdks relieves repression of E2F complexes by Rb family members during cell cycle progression. Expression of p21 will reverse this effect leading to repression of E2F regulated genes. However, mutants of p21 that no longer inhibit Cyclin/Cdk activity are still capable of inhibiting E2F transactivation (Perkins, 2002). Interestingly, this study also reported that p21 could bind directly to E2F1 and its partner DP-1. These results demonstrate that p21 is capable of affecting transcription by mechanisms other than those merely acting as inhibitor of both Cyclin/Cdk complexes and PCNA.

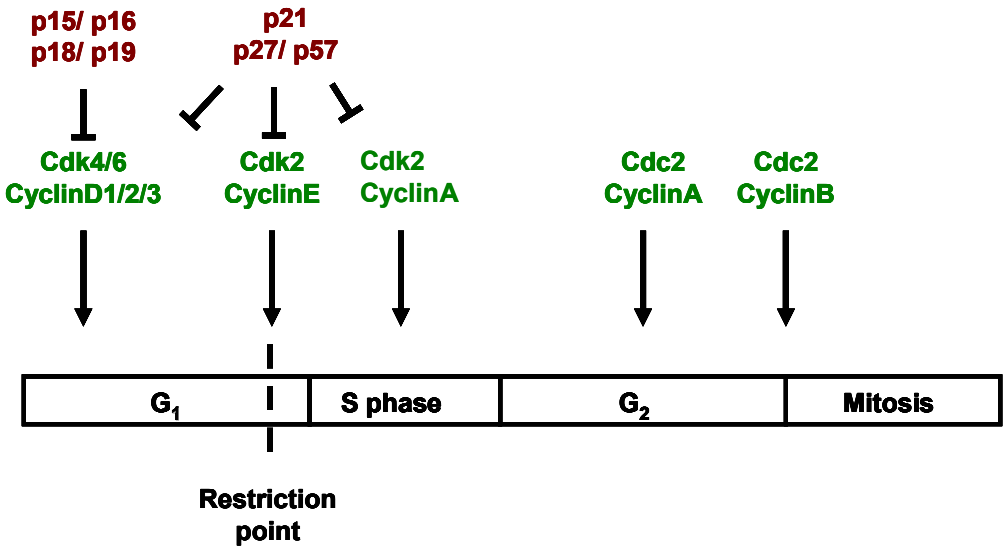

Figure 1.2: Diagram to show the progression of the mammalian cell cycle through different phases and its regulation by specific Cyclin/Cdk complexes and CKIs.

1.3 Expression of p21 during cardiac myocyte development

The result of an extensive developmental study using cardiac myocytes obtained from fetal, neonatal and adult rats demonstrated a differential expression of the CKI p21 during development of the rat myocardium (Poolman et al., 1998). The mRNA and protein expression of p21 is up-regulated in freshly isolated adult cardiac myocytes compared with fetal and neonatal cardiomyocytes (Poolman et al., 1998). In contrast to the results obtained for p21, levels of p27 are up-regulated in neonatal myocytes, when compared to fetal myocytes, but then are expressed at lower levels in the adult cardiac myocyte, a finding that is consistent with a recent report by Koh and colleagues (Koh et al., 1998). Other studies also show a significant upregulation of p21 mRNA and protein expression during cardiac myocyte development. Flink et al. have reported that p21 inhibitory activities increased markedly in cultured two-day-old neonatal cardiomyocytes when compared with cultured fetal cells (Flink et al., 1996). p21 protein obtained from adult myocytes was able to inhibit significantly the histone H1 kinase activity of Cdk2 obtained from neonatal rat cardiomyocytes. In addition, immunodepletion of p21 from adult myocyte lysates prior to incubation with neonatal myocyte lysates led to a loss of inhibitory activity (Poolman et al., 1998). Therefore, it is possible that the up-regulation of the CIP/KIP family of CKI molecules, especially p21, during cardiac myocyte development could contribute to the progressive withdrawal of maturing cardiac myocytes from the cell cycle. The precise mechanisms that control the cardiac myocyte cell cycle still remain to be fully understood. However, these studies have shown that certain inhibitory elements of the cell cycle (p21 and p27), especially p21, are

crucial for controlling the progressive withdrawal of cardiac myocytes from the cell cycle during cardiac myocyte development.

1.4 The role of p21 in cardiac myocyte cell cycle withdrawal

The ability of the mammalian cardiomyocyte to divide and proliferate is lost just after birth when a switch from cardiomyocyte hyperplasia (cell division) to hypertrophy (an increase in cell size) occurs (Brooks et al., 1998). The cessation of proliferation of the cardiac myocyte has previously been attributed to a blockade at the G_0 and/or G_1 phases of the cell cycle (Capasso et al., 1992). It is known that the G_0/G_1 phase blockade produced is due to a loss of Cyclin/Cdk complex activity during the development that is associated with an upregulation of p21 (Brooks et al., 1998). Other studies also showed that both mRNA and protein expression levels of p21 are upregulated during cardiac development in both rat and man, which is consistent with a direct role of p21 in cardiac myocyte cell cycle withdrawal (Burton et al., 1999). The precise mechanisms that control the cardiac myocyte cell cycle and therefore regulate myocyte proliferation and differentiation still remain to be fully understood. However, it is know that the major function of all CKIs molecules is to inhibit the activity of Cyclin/Cdk complexes (Brooks, et al., 1998). Previous reports have shown that over 85% of adult cardiac myocytes are found in the G_0 or G_1 phases of the cell cycle. Other observations of inhibitory elements of the cell cycle suggest that certain CKIs, especially p21, are crucial for controlling the progressive withdrawal of cardiac myocytes from the cell cycle during development of the rat cardiomyocyte (Brooks et al., 1998). Since p21 and p27 were the only two CKIs detected in myocytes and since these molecules can inhibit the activity of G_1 phase Cdks and potentially cause a G_1 phase cell cycle arrest, it is possible that one or both of these molecules are involved in arresting adult cardiomyocytes (Brooks et al., 1998). In addition, p21 mRNA expression levels have been shown to peak on exit from G_0 (Brooks et al., 1998). In addition to an upregulation of the expression of inhibitory proteins of p21 and p27, there is a concomitant downregulation in G_1 phase Cdks during development of the rat cardiac myocyte (Brooks et al., 1997). It is possible that during normal cardiomyocyte development, p21 may contribute to the progressive loss of myocyte proliferation by inhibiting the transcriptional activity of E2F1. The blockade of cells at G_1/S is generally attributed to a lack of complete Rb phosphorylation and the subsequent release of E2F family members (Clark et al., 2000). Other studies show that p21 can bind directly with multiple Cyclins and Cdks and inhibit Cdk activity *in vitro* and *in vivo* (Xiong et al., 1993; Harper et al., 1995).

1.5 Cardiac hypertrophy and heart failure

Myocardial hypertrophy is an early milestone during the clinical course of heart failure and an important risk factor for subsequent cardiac morbidity and mortality (Hunter and Chien, 1999). In response to a variety of mechanical, hemodynamic, hormonal, and pathologic stimuli, the heart adapts to increased demands for cardiac work by increasing muscle mass through the initiation of a hypertrophic response. A growing body of evidence indicates that the local angiotensin system plays a critical role in the development of cardiac hypertrophy. Angiotensin II induces activation of protein kinases, including ERKs, and expression of immediate early genes, such as c-fos and c-jun, as well as an increase in protein synthesis through the Ang II type 1 receptor (AT1) (Sadoshima et al., 1993; Frey and Olson, 2003). Hypertrophic agonist Ang II exerts it`s effects through the Raf (Ras/Raf/MEK/ERK) signalling pathway. Many cells respond to a variety of environmental stimuli by ion channels in the plasma membrane (Frey and Olson, 2003). The importance of Ca^{2+} in the development of cardiac hypertrophy was recently highlighted when it was reported that overexpression of constitutively active mutants of a Ca^{2+}-dependent phosphatase calcineurin, and of its downstream transcription factor NFAT3, induced marked cardiac hypertrophy in transgenic mice, and that phenylephrine- and Ang II-induced cardiomyocyte hypertrophy *in vitro* was inhibited by calcineurin inhibitors (Molkentin et al., 1998). Moreover, Ang II also has been implicated in the activation of the JAK/STAT pathway in pressure overloaded hearts and mechanically stretched cardiac myocytes (Pan et al., 1997; Pan et al., 1999). Other factors involved in hypertrophic signalling are IL-6 and Gp130 (Frey and Olson, 2003). Long lasting maladaptive cardiac signalling ultimately leads to cardiac failure. Characteristics of the biology of cardiac hypertrophy and heart failure are illustrated in **Figure 1.3, page 9**.

1.6 Cell cycle regulators and cardiac myocyte hypertrophy

Cardiomyocytes undergo terminal differentiation soon after birth, irreversibly withdrawing from the cell cycle (Poolman et al., 1998). They do not divide any longer and augmentation of the heart muscle does only occur in the form of hypertrophic cell expansion. Thus, a heart injured by a number of stimuli, including infarct (Takeishi and Walsh, 2001) and pressure overload (Takaoka et al., 2002) is not able to regenerate damaged tissue by proliferation. Instead, cardiac myocytes try to compensate for loss of tissue by further outstretching. During this process cells re-enter the cell cycle and synthesize DNA but do not undergo mitosis (Marino, 1991).

Recent evidence suggests that cell cycle regulatory mechanisms participate in cardiac hypertrophy. Hypertrophic stimuli induce many cell cycle regulatory proteins in cardiac myocytes (Sadoshima et al., 1997; Tamamori et al., 1998; Poolman et al., 1998; Nozato et al., 2000). The hypertrophic response leads to enlargement of cardiac myocytes and is regulated by multiple signalling pathways (Frey and Olson, 2003).

Characteristics of cardiac hypertrophy and transition to overt heart failure

Morphology

Concentric hypertrophy	Pronounced increase in wall thickness
Eccentric hypertrophy	Pronounced ventricular dilatation
Heart weight/body weight ratio	↑

	Compensated hypertrophy	**heart failure**
Systolic function	↔	↔/↓
Diastolic function	↔/↓	↔/↓
End-systolic diameter	↔/↓	↑
End-diastolic diameter	↔	↑
Fibrosis	↔/↑	↔/↑
Arrhythmias	↔/↑	↔/↑
Apoptosis	↔/↑	↑
Fetal gene program induction	↔/↑	↑

Figure 1.3: Characteristics of cardiac hypertrophy and the transition to overt heart failure.

In the process, D-type Cyclins play a crucial role. D-type Cyclins (D1-3) act as growth factor sensors, with CyclinD transcription, assembly, nuclear transport, and turnover being regulated in a mitogen-dependent manner (Sherr, 1993). Similar responses are observed in various cell types in response to mitogenic stimuli. It appears likely that hypertrophic and mitogenic stimuli share certain intracellular responses (Busk and Hinrichsen, 2003). D-type Cdk activity is a prerequisite for cardiomyocyte hypertrophy and provides direct evidence of a new role for G_1 Cdks in terminally differentiated cells in addition to their known critical functions in proliferating cells (Sadoshima et al., 1997; Tamamori et al., 1998). The most recognized function of Cdks is phosphorylation of Rb (negative regulator of G_1 and S phase progression). The generally accepted view is that Cdks initiate Rb phosphorylation in mid-G_1 phase after

which CyclinE/Cdk2 becomes active and completes this process by phosphorylating Rb on additional sites (Meyerson and Harlow, 1994; Taya, 1997), thereby activating E2F transcription factors that are required for S phase entry for DNA synthesis (Ohtsubo et al., 1995).

Link of angiotensin and Cyclins

Based on intensive *in vitro* and *in vivo* investigations, it is now clear that Ang II plays an important role in the pathogenesis of cardiac hypertrophy via a variety of proliferative signal transduction pathways, such as RAS/RAF1/MAPK, PI3-K, and JAK/STAT (Sadoshima et al., 1993; Kodama et al., 1998; Nozato et al., 2000) **(Figure 1.4, page 11)**. Generally, D-type Cyclins, which are the first transducers of the cell cycle, are induced in response to mitogenic signals via the Ras/Raf1/ERK and PI3-K pathways (Gille and Downward, 1999). As cells progress through the G_1 phase, the Cyclins assemble with their catalytic partners Cdk4 and Cdk6 (Gille and Downward, 1999; Regula et al., 2004). Other studies have shown that Ang II increases the transcription of D-type Cyclins leading to the phosphorylation of pRb. These results indicate that the hypertrophic factor Ang II activates cell cycle regulators in non-proliferating cardiac myocytes in a manner similar to that in proliferating cells (Nozato et al., 2000). At present, the underlying mechanisms of the G_1 Cyclin/Cdk-related hypertrophy remain unclear. Tamamori et al. have shown that serum stimulation promoted the G_1 Cyclin-dependent Cdk activity without induction of DNA synthesis in cardiomyocytes (Tamamori et al., 1998). Furthermore, overexpression of the Cdk inhibitor p21 effectively prevented cell enlargement and depressed serum-induced protein synthesis and expression of fetal cardiac genes *in vitro* (Tamamori et al., 1998).

Unresolved role of p21

Some experiments found that both the mRNA and protein levels of p21 are downregulated during the development of pressure overload-induced left ventricular hypertrophy. This finding is consistent with a concomitant upregulation in the expression and activities of certain Cyclin/Cdk complexes during this period of left ventricular growth (Brooks et al., 1998). Furthermore, the results have demonstrated that the expression of p21 is tightly regulated during the development of left ventricular hypertrophy (Brooks et al., 1998). However, others have shown that the expression of the p21 is upregulated significantly at the time of the transition from myocyte hyperplasia to hypertrophy, whereas p27 expression remains relatively constant (Poolman and Brooks, 1998; Koh et al., 1998). Recently, Nozato et al. reported that the p21 gene product inhibited cardiac myocyte hypertrophy *in vitro*

(Nozato et al., 2000). The *in vitro* results, while providing important clues, do not establish whether p21 can in fact affect cardiac myocyte hypertrophy *in vivo*. To resolve this issue, we developed a new approach that allows us to study the role of p21 specifically in relation to cardiac myocyte hypertrophy.

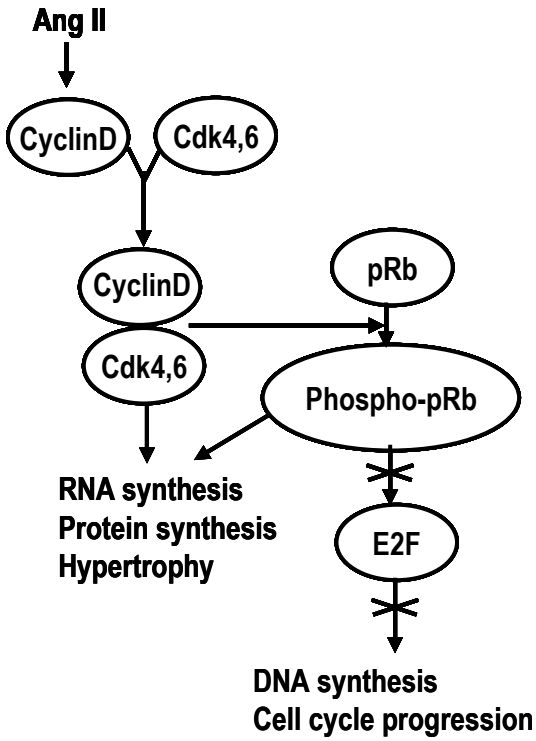

Figure 1.4: Possible mechanism of Ang II-induced cardiac myocyte hypertrophy via the G_1 Cyclin/Cdk pathway.

1.7 Transduction of TAT fusion proteins

The transfer of genetic material into eukaryotic cells either by adenovirus or adeno-associated viral vectors through intravenous or intracavitary injection or by non-viral mechanisms such as microinjection, electroporation, or chemical transfection remains problematic. Use of anti-sense approaches to manipulate intracellular processes has both specific gene and cell-type restrictions. Moreover, *in vivo* gene therapy approaches relying on adenoviral vectors are associated with significant difficulties relating to a lack of target specificity, massive overexpression, broad cell-to-cell intracellular concentration ranges of expressed proteins, low transfection efficiencies and toxicity (Nagahara et al., 1998; Lea et al., 2003; Wadia and Dowdy, 2005). In 1988, Green and Frankel discovered independently that HIV-1 TAT protein is able to cross cell membranes (Green and Loewenstein, 1988; Frankel and Pabo, 1988). In

1994, Fawell et al. demonstrated that chemically cross-linking of a 36-amino acid domain of TAT to heterologous proteins conferred the ability to transduce into cells (Fawell et al., 1994). The methodology to generate transducible, full-length TAT fusion proteins was greatly advanced by Dowdy and co-workers (Nagahara et al., 1998; Schwarze and Dowdy, 2000; Wadia and Dowdy, 2005). In this system, in-frame polyhistidine-TAT fusion proteins are purified from a bacterial lysate under denaturing conditions through a series of affinity, ion-exchange, and desalting steps. Isolated TAT fusion proteins are made soluble in an aqueous buffer and can be transduced into cells simply by adding them directly to the cell culture medium or by intraperitoneal injection in mice (Schwarze and Dowdy, 2000). After their exogenous application to cultured cells, misfolded TAT fusion proteins, purified under denaturing conditions, are internalized and refolded *in vivo* in a rapid, concentration-dependent manner to achieve maximum intracellular concentration in less than 10 min with nearly equal intracellular concentrations between all cells (Nagahara et al., 1998; Becker-Hapak et al., 2001). Mechanistic studies suggest that TAT-mediated transduction directs penetration across the lipid bilayer through a rapid, temperature- and energy-independent process. The PTD first interacts with cell membrane lipid rafts in a receptor-independent manner, stimulating a rapid internalization by macropinocytosis, followed by a pH drop and destabilization of the integrity of the macropinosome vesicle lipid bilayer that ultimately results in the release of TAT-cargo into the cytosol and/or nuclear transport. Both TAT-fusion proteins and TAT peptides transduce into cells by macropinocytosis (Wadia et al., 2004). Studies have shown that TAT-fusion proteins can transduce into all cells and tissues present in mice, including those present across the blood–brain barrier (Schwarze and Dowdy, 2000).

1.8 Objective

Objective of the study was to analyse the effects of ectopic p21 on Ang II-induced cardiac hypertrophy *in vitro* and *in vivo* by means of TAT-mediated protein transduction.

2 MATERIALS

2.1Laboratory equipment

• Balance	Mettler-Toledo GmbH, Giessen
• Centrifuges	Super T21, RC-2B, Sorvall GmbH, Bad Homburg Avanti J20, Beckmann Coulter GmbH, Krefeld 5417C, Eppendorf AG, Hamburg
• Filmprocessor	Curix, Agfa-Gevaert, NV, Mortsel, Belgium
• Freezer, -80°C	Forma, ThermoQuest Analytische Systeme GmbH, Egelsbach
• Gel electrophoresis equipment	Amersham Pharmacia Biotech Europe GmbH, Freiburg
• Gel documentation system for ethidiumbromide-stained agarose gels	Herolab GmbH, Wiesloch
• GeneAmp PCR system 9600	PE Biosystems, The Perkin Elmer Corporation, CA, USA
• Hitrap desalting column	Amersham Biosciences
• Hybridization oven	Oncor, Appligene, UK
• Incubator	Heraeus Instruments GmbH, Wiesloch
• Incubator shaker	New Brunswick scientific GmbH, Nürtingen
• MonoQ HR 5/5, 10/10	Amersham Pharmacia
• NiNTA Superflow column	Amersham Pharmacia
• Pipettes, adjustable	Abimed Analysen Technik GmbH, Langenfeld
• Pipettes, adjustable, multichannel	Dunn Labortechnik, GmbH, Asbach Corning Costar, Acton, MA, USA Eppendorf AG, Hamburg
• PhosphorImager	Molecular Dynamics GmbH, Krefeld
• Plasmid isolation robot	PI-100Σ Kurabo Industries Ltd. Osaka, Japan
• Plate sealer	Genetix, Christchurch, Dorset, UK
• Power supply	Bio-Rad Laboratories GmbH, München
• Q-Fill	Genetix, Christchurch, Dorset, UK
• Sequence Detection system ABI Prism 7700	PE Biosystems, The Perkin Elmer Corporation, CA, USA
• Shaker	Rocky, Fröbel Labortechnik, Wasserburg
• Sonifier W250 (Ultraschall Desintegrator)	Branson, Dietzenbach, Germany
• Spectrophotometer	Shimadzu Deutschland GmbH, Duisburg
• Thermocycler	PTC100, PTC200, PTC225, MJ Research, Inc.; Watertown, USA
• Thermomixer	Eppendorf AG, Hamburg
• UV crosslinker	Stratagene, La Jolla, CA, USA
• Vortex	Vortex Genie 2, Bender und Hobein AG, Zürich, Switzerland
• Water bath	Köttermann, Germany
• ÄKTA *FPLC*	Amersham Pharmacia

2.2 Chemicals and enzymes

• Agarose	Gibco Life Technologies, Karlsruhe
• Agarose, low melting point	FMC SeaPlaque GTG, Biozym, Hessisch Ohlendorf
• Ampicillin	Sigma, Deisenhofen
• ATP, [γ-^{32}P]ATP	Amersham Pharmacia Biotech Europe GmbH, Freiburg
• Bacto Agar	Difco, Becton Dickinson, Sparks, MD; USA
• Bacto trypton	Difco, Becton Dickinson, Sparks, MD; USA
• Bacto yeast extract	Difco, Becton Dickinson, Sparks, MD; USA
• Betaine, anhydrous	Fluka, Taufkirchen
• Bromophenol blue	Sigma, Deisenhofen
• Casamino acids	Difco, Becton Dickinson, Sparks, MD; USA
• dATP, dCTP, dGTP, dTTP sodium salt	Amersham Pharmacia Biotech Europe GmbH, Freiburg
• [γ-^{32}P]dCTP	Amersham Pharmacia Biotech Europe GmbH, Freiburg
• DNA molecular weight standards	MBI Fermentas, St. Leon-Roth Promega GmbH, Mannheim
• DNA Polymerase I (E. coli), Large (Klenow) Fragment	New England Biolabs GmbH, Schwalbach/Taunus
• DNA Taq-Polymerase	Promega, Mannheim
• DNA Taq-Polymerase, AmpliTaq Gold	PE Applied Biosystems, Weiterstadt
• DNase (RQ1 DNase)	Promega, Mannheim
• DTT	Serva, Heidelberg
• EDTA (Titriplex® III)	Merck, Darmstadt
• Ethidium Bromide, 1% solution	Fluka, Taufkirchen
• Formaldehyde	Sigma, Deisenhofen
• Glucose	Merck, Darmstadt
• Glycerol	Merck, Darmstadt
• HEPES	Sigma, Deisenhofen
• Imidazole	Sigma-ALDRICH
• IPTG	Sigma, Deisenhofen
• Isopropanol	Merck, Darmstadt
• LB medium	Bio 101, Vista, CA, USA
• Lysozyme	Boehringer Mannheim GmbH
• Lyticase	Sigma, Deisenhofen
• β-Mercapto-ethanol	Sigma, Deisenhofen
• Nonidet P-40(NP-40)	Sigma, Deisenhofen
• pd(NTP)$_6$, random hexamer primer, Na salt	Amersham Pharmacia Biotech Europe GmbH, Freiburg
• Phenol	Roti-Phenol, Carl Roth GmbH & Co. KG, Karlsruhe
• PMSF	Sigma, Deisenhofen
• Proteinase K	Boehringer Mannheim GmbH

• Restriction Enzymes	New England Biolabs GmbH, Schwalbach/Taunus
• Reverse Transcriptase (Superscript II)	Gibco Life Technologies, Mannheim
• SeaPlaque GTG low melt agarose	FMC Bioproducts, Rockland, ME
• Tris	Merck, Darmstadt
• Tryptone	Gibco Life Technologies, Mannheim
• Tween 20	Roth
• Urea	CALBIOCHEM
• Yeast extract	Gibco Life Technologies, Mannheim

Salts, acids, bases and solvents not mentioned in the table were *pro analysi* quality from Merck (Darmstadt) or Sigma (Deisenhofen).

2.3 Oligonucleotides

Standard primers:

• 3´-wtp21	GAGATGTCAGAACCGGCTGGGGATGTCCG
• 5´-wtp21	GAGATGTCAGAACCGGCTGGGGATGTCCG
• 3´-p21ΔC	GCCAGGCCGCCTGCCTTATCCCAACTCATCCCGGCCTCG
• 5´-p21 ΔC	GAGATGTCAGAACCGGCTGGGGATGTCCG
• 3´-ANF	TGGGCTCCAATCCTGTCAATC
• 5´-ANF	CATCACCCTGGGCTTCTTCCT
• 3´- β-MHC	CCTCGGGTTAGCTGAGAGATCA
• 5´- β-MHC	ATGTGCCGGACCTTGGAA
• 3´- β-actin	CAAAGAAAGGGTGTAAAACG
• 5´- β-actin	AGATTACTGCTCTGGCTCCTA
• 3´- GAPDH	GAAGACACCAGTAGACTCCACGACA
• 5´- GAPDH	ATGTTCCAGTATGACTCCACTCACG

2.4 Kits

• ABI PRISM BigDye Terminator Cycle Sequencing Ready reaction kit	PE Applied Biosystems, Foster City, CA, USA
• Dynabeads mRNA DIRECT™ kit	Dynal AS, Oslo, Norway
• PCR select cDNA subtraction kit	Clontech Laboratories, Palo Alto, CA, BD Biosciences, Heidelberg
• Plasmid Mini- und Maxipräparation	Qiagen, Hilden
• Qiaquick DNA-Aufreinigung	Qiagen, Hilden
• RNeasy Kit:	Qiagen, Hilden
• SYBR Green PCR core reagent kit	PE Applied Biosystems, Foster City, CA, USA
• TaqMan universal PCR master mix	PE Applied Biosystems, Foster City, CA, USA

2.5 Animals

C57BL/6 mice were obtained from the animal house of the Max Delbrück Center for Molecular Medicine (TVA G0202/04).

2.6 Other materials

• ABI PRISM BigDye Terminator Cycle Sequencing Ready reaction kit	PE Applied Biosystems, Foster City, CA, USA
• Coomassie® protein assay reagent kit	PIERCE Germany
• MicroAmp optical 96-well reaction plates and caps	PE Applied Biosystems, Foster City, CA, USA
• Microseal TM "A" film	Biozym, MJ Research, Inc. Watertown MA, USA
• MicroSpin G-50 columns	Amersham Pharmacia Biotech
• Microtitre plates, 384-well	Genetix, Christchurch, Dorset, UK
• Nylon filters, 222 x 222 mm Hybond-N+	Amersham Pharmacia, Biotech Europe GmbH, Freiburg
• PCR plates, 96-well	Abgene, Surrey, UK
• Polypropylene tubes 15ml and 50 ml, sterile	Greiner Labortechnik GmbH, Frickenhausen
• Replicators, 384-pin	Genetix, Christchurch, Dorset, UK
• Sterile filters	Cellulose nitrate membrane, pore size 0.2 µm, Nalgene, Hamburg
• Size standard, DNA marker PhiX174 DNA/BsuRI	MBI Fermentas, Germany
• Lambda ladder PFG marker	New England Biolabs, Schwalbach/Taunus

2.7 Solutions, buffers and media

1.5% agarose gel: 1.5 g agarose, top up to 100 ml with TAE buffer.

1% acetic acid solution: 1 ml glacial acetic acid and 99 ml destilled water.

Aniline blue solution: 2.5 g aniline blue, 2 ml glacial acetic acid and 100 ml destilled water.

Antibiotics (1000 x): 50 mg/ml ampicillin, 30 mg/ml kanamycin.

Antifade: 10 ml glycerin, 2.5% DABCO (w/v).

Antifade 1: 1, 4-phenylene-diamine. Reagents: 1, 4-phenylene-diamine; 86% glycerol; 1 x phosphate buffered saline (PBS); sodium bicarbonate; sodium carbonate. Preparation: carbonate-bicarbonate buffer (pH 9.0); 40 ml Sodium bicarbonate, 0.5 M (pH 8.13); 10 ml Sodium carbonate, 0.5 M (pH 11.32), filter sterilize. Procedure: Prepare carbonate-bicarbonate buffer (pH 9.0), dissolve 100 mg 1,4- phenylenediamine in 4 ml 1 x PBS, adjust pH with carbonate-bicarbonate buffer to 8.0, add 1 x PBS to 10 ml, mix with 90 ml 86% glycerol.

Antifade 2: DABCO (1, 4 diazabizyclo [2.2.2] octane). Reagents: DABCO (1, 4-diazabicyclo[2.2.2]octane); 86% glycerol; 1 M Tris-HCl, pH 8.0; H_2O, sterile. Preparation: Components amount, 0.233 g DABCO, 200 µl Tris-HCl, 1 M pH8.0, 800 µl sterile water, 9 ml 86% glycerin. Procedure: combine components, dissolve by warming to 70°C, vortex.

Biebrich scarlet-acid fuchsine solution: 90 ml 1% Biebrich scarlet, 10 ml 1% acid fuchsine and 1 ml glacial acetic acid.

Blocking Buffer: 100 ml PBS, 0.2% Tween 20 (v/v), 5% BSA (w/v).

Buffer Z (1000 ml): 20 mM HEPES (4.76 g to 500 ml destilled water), adjust pH value to 8.0 with 1 N HCl, add 100 mM NaCl (5.85 g) and 8 M urea (480 g), bring volume up to 1000 ml.

Cardiomyocyte medium: 500 ml DMEM/F12, 5 ml penicillin/streptomycin (stock GIBCO concentrate), 5 ml L-glutamine (stock GIBCO concentrate), 15 ml of 100 mM sodium-pyruvate, 0.5 ml of 100 mM ascorbate, FW 176.1, 3.0 ml 35% BSA.

Detection solution: 1:1 detection reagent 1 and detection reagent 2 (ECL Plus western blotting detection reagent, AMERSHAM).

DTT: FW 154.2 g/M; 1.6 µl/ml buffer; 100 mg/ml stock in deionised water.

Electrophoresis sample buffer (10 ml): 5 ml 50% glycerine, 50 mg 0.5% orange acid, 0.5 ml 0.5 M EDTA and 4.5 ml destilled water.

Ethidium bromide bath (300 ml): 3 g in 300 ml destilled water.

HEPES buffer: 50 mM HEPES, pH 7.4 (FW 238.3 g/M), 50 mM KCl (FW 74.56 g/M), 8 mM $MgCl_2$ (FW 95.3 g/M).

Hybridization-buffer: Prehybridization buffer with 5% dextransulfate (Na-salt, MW 500,000, 50% stock-solution) and without non-homologous DNA.

2 M imidazole solution (100 ml): bring up 13.62 g imidazole with destilled water to 90 ml, adjust pH value to 7.4, fill up volume to 100 ml and filter through a 0.45 µm sterile filter.

IPTG: 1.0 g/10 ml in deionised water; use 240 mg/L (liter) TB medium for 1000 µM IPTG.

LB-Ampicillin agar (1000 ml): 10 g NaCl, 10 g tryptone, 5 g yeast extract, 20 g agar; adjust pH to 7.0 with 5 N NaOH; add destilled water to 1000 ml; autoclave; cool to 50ºC; add 5 ml (50 µg/ml) of filter-sterilized ampicillin.

LB Broth (1000 ml): 10 g NaCl, 10 g tryptone, 5 g yeast extract; add deionised water to a final volume of 1000 ml; adjust pH to 7.0 with 5 N NaOH; autoclave.

1 x ligation buffer: 50 mM Tris-HCl, 10 mM $MgCl_2$, 10 mM DTT, 1 mM ATP, 25 µg/ml BSA.

Loading Buffer: 1 x MOPS; 18.5% formaldehyde; 50% formamide; 4% Ficoll400; bromophenolblue.

Lysis buffer (50 ml): 50 ml buffer Z with 500 µl PMSF, 80 µl DTT and 50 µl lysozyme.

Lysozyme: 100 mg/ml in deionised H_2O.

MOPS buffer (mild): 20 mM MOPS, pH 7.0 (FW 209.27 g/M), 5 mM $MgCl_2$ (FW 95.21).

10 x MOPS: 0.4 M morpholinopropanesulfonic acid (free acid); 0.1 M Na-acetate-3 x H_2O; 10 mM EDTA; adjust to pH 7.2 with NaOH.

PBS (rinsing excised ventricles): 0.15 g Na_2HPO_4 x 2 H_2O, 0.06 g KH_2PO_4, 7.00 g NaCl, 0.34 g KCl, 2.10 g $NaHCO_3$, pH 7.5, bring up to 1000 m with waterl, autoclave a add 2.5 ml of 2 M glucose.

10 x PCR buffer (standard): 500 mM KCl, 350 mM Tris Base, 150 mM Tris HCl, 15 mM $MgCl_2$, 1% w/v Tween, 1.5 mM Cresol red.

Permeabilization Buffer: 15 ml PBS, 0.1% Triton X-100.

PMSF: 10 mg/ml in a-propanol.

Prehybridization-buffer: 5 x SSC; 50% formamide; 5 x Denhardt's-solution; 1% SDS; 100 ug/ml heat-denatured sheared non- homologous DNA (Salmon sperm DNA or yeast tRNA), 100 ml: 25 ml 20 x SSC, 50 ml formamide, 5 ml 100 x Denhardt's, 1 g SDS, 1 ml 10 mg/ml DNA.

Prehybridization/Hybridization solution: 0.1% SDS, 50% formamide, 5 x SSC, 50 mM $NaPO_4$, pH 6.8, 0.1% sodium pyrophosphate, 5 x Denhardt's Solution, 50 ug/ml sheared herring sperm DNA.

10 x restriction buffer NEB2: 50 mM NaCl, 10 mM Tris-HCl, 10 mM $MgCl_2$, 1 mM DTT, pH 7.9.

Restriction buffer NEB3: 100 mM NaCl, 50 mM Tris-HCl, 10 mM $MgCl_2$, 1 mM DTT; pH 7.9.

RNA loading buffer: 50% glycerol, 1 mM EDTA, 0.25% bromophenolblue.

5 x running buffer = electrode buffer: 25 mM Tris, 192 mM glycine, 0.1% SDS in destilled H_2O; adjust pH to 8.3 prior to use.

Sadomix (digestion of shopped ventricles for 1000 ml): 20 ml of 1 M HEPES, pH 7.6 (20 mM final) 13.82 g/50ml, 65 ml of 2 M NaCl (130 mM final) 23.4 g/200 ml, 3 ml of 1 M KCl (3 mM final) 3.73 g/50 ml, 10 ml of 100 mM NaH_2PO_4 (1 mM final) 0.6 g/50 ml, up to 1000 ml, autoclave and add 2 ml of 2 M glucose (19.817 g/50 ml; 4 mM final) to 300 ml Sadomix add 600 mg trypsin, 100 mg pancreatin and 450 µl DNase I (containing 4.5 µl 1 M $MgCl_2$ 10 mM final) (10 mg/ml stock, Roche, 1284932).

Sample buffer: 62.5 mM Tris-HCl (pH 7.0 at 25°C), 1 mM EDTA, 2% SDS, 50 mM DTT, 30 mM NaCl, 1 mM NaN_3, 0.01% bromophenol blue and 50% glycerol.

3 x SDS loading buffer buffer: 20 mM Tris, pH 7.5, 50 mM NaCl, 0.5 % SDS, 1 mM dithiothreitol.

SOC medium (1000 ml): 20 g tryptone, 5 g yeast extract, 0.5 g NaCl; autoclave; add 10 ml 1 M $MgCl_2$, 10 ml 1 M $MgSO_4$ and 10 ml 40% glucose to the medium prior to use, filter sterile.

20 x SSC: 3 M NaCl; 0.3 M Na-citrate, 175.3 g NaCl, 88.2 g Na-citrate.

Stripping solution: 5 mM Tris pH 8; 0.2 mM EDTA; 0.05% Na-pyrophosphate; 0.1 x Denhardt's solution. 500 ml: 2.5 ml 1 M Tris, 200 µl 0.5 M EDTA, 5 ml 5% NaPP, 1 ml 50 x Denhardt's.

1 x TAE buffer: 40 mM Tris-acetate, 1 mM EDTA.

TB medium (1000 ml): 12 g tryptone, 24 g yeast extract, 4 ml glycerol, 50 ml 0.17 M KH_2PO_4, 50 ml 0.72 M K_2HPO_4, add deionized H_2O to a final volume of 1000 ml; autoclave.

TBS-plus (100 ml) : 92 ml 1 X TBS, 5 ml 10% Triton X 100, 3 ml goat serum and 0.5 ml Tween 20.

TBS washing buffer + 5% BSA blocking buffer (500 ml): 500 ml 1 x TBS; add 25 g BSA.

TBS washing buffer + 5% milk blocking buffer (500 ml): 500 ml 1 x TBS; add 25 g milk powder.

10 x TBS (1000 ml): 24.2 g Tris, 80.7 g NaCl; adjust pH to 7.6.

TBST (1000 ml): 100 ml 10 x TBS, 900 ml destilled water, 1 ml Tween 20 (= 0.1%).

1 x TE buffer: 10 mM Tris-HCl, adjust pH to 7.5, 1mM EDTA, autoclave.

10 x transfer buffer (1000 ml): 30 g Tris, 144 g glycine; bring up volume to 1000 ml with destilled H_2O; adjust pH to 8.3.

Wash buffer (250 ml): 250 ml PBS, 0.1% NP-40.

Weigert's Iron Haematoxylin Solution: Stock Solution A: 1 g Haematoxylin and 100 ml 95% Alcohol; Stock Solution B: 4 ml 29% $FeCl_3$ in H_2O, 95 ml distilled water and 1ml conc. HCl.

Weigert's Iron Haematoxylin Working Solution: Mix equal parts of stock solution A and B.

Glycerol stocks from PAC and cDNA clones were prepared in 10% glycerol and stored at –80°C.

2.8 Software

- ANOVA
- Image Quant:
- PhosphorImager and TINA
- Sigma-STAT
- Molecular Dynamics, Sunnyvale, USA
- Raytest

3 METHODS

3.1 Cloning strategy and recombinant protein expression and purification by *FPLC*

Genetic TAT.p21 fusions were generated by insertion of the p21 open reading frame DNA into the pTAT-HA plasmid. The pTAT-HA vector was obtained from S. Dowdy (Howard Hughes medical Institute, La Jolla, California, USA). The human p21 cDNA was provided by L. Hauck (MDC, Berlin, Germany) and was amplified with gene-specific primers including *Xho*I restriction sites. Following *Xho*I restriction of the p21 PCR product, the p21 open reading frame DNA was ligated into the pTAT-HA vector by single digestion of the multiple cloning site within pTAT-HA with *Xho*I. After ligation, plasmids were transformed into DH5α bacteria. The pTAT-HA vector contains an ampicillin resistance marker for selection after transformation, a T7 polymerase promoter, an N-terminal 6-histidine leader before the TAT domain, and an HA tag. Individual clones were isolated and analyzed for the correct p21 insert size. Correct orientation of the construct was confirmed by restriction analysis with *Bgl*II. Human TAT.p21- and TAT.p21ΔC-cDNA plasmids were transformed into *E.coli* BL21(DE3)pLysS (Promega) and then isolated and purified under denaturing conditions employing *FPLC* equipment (ÄKTA, Amersham) as described (Becker-Hapak et al., 2001). Briefly, a 800 ml Terrific Broth (TB) overnight culture supplemented with appropriate ampicillin was inoculated into 5 liter of TB induced with 1000 µM isopropyl-ß-D-thiogalactoside (IPTG) and cultured at 37°C overnight (up to 12 hours) while shaking at 200 rpm. After centrifugation the bacterial pellet was lysed in 8.0 M urea-buffer (Buffer Z) and sonicated six times for 50 s (seconds) on ice. The sonicate was clarified by centrifugation at 12,000 rpm, 4°C for 60 min (minutes) and the supernatant fraction was collected. Next, the clarified sonicate was equilibrated in 15 mM imidazole and applied to a preequilibrated Ni^{2+}-NTA column (10 ml, Amersham) connected to a *FPLC* with binding buffer (buffer Z) plus 15 mM imidazole. The column was washed with 10 bed volumes of binding buffer plus 15 mM imidazole and then the enriched TAT-fusion protein was eluted by one single-step addition of 1 bed volume of buffer Z containing 500 mM imidazole. Then, the sample from the pooled Ni^{2+}-NTA fractions was injected into ionic exchanger chromatography columns (Mono Q 5/10 column, Amersham Biosciences) and equilibrated in buffer Z. Following two washing steps with 20 ml buffer Z and 30 ml of buffer Z without urea, the sample was eluted with 2 M NaCl. Finally, 2.0 ml of protein from the ion exchange column was applied onto the desalting column preequilibrated with 10 ml of PBS, (G-25 column, Amersham Biosciences). Collection of fractions was started immediately after addition of the fusion protein onto the

column. 2.0 ml fractions were conveniently collected in micro centrifuge tubes. Purified TAT.p21 was adjusted to 10% (v/v) glycerol, aliquoted, snap-frozen in liquid nitrogen and stored at -80^{o}C. The protein concentrations in each fraction were quantified using the BCA Protein Assay Reagent (Pierce Chemical Co., Rockford, Illinois, USA). TAT.p21 was purified to near homogeneity as judged by Coomassie-gel staining following separation by SDS–PAGE and their identity was confirmed with antibodies directed against the cDNA-encoded product using either anti-His (anti-His antibody, mouse ascites monoclonal antibody, product code: 27-4710-01, Amersham Biosciences) or specific anti-p21 antibody (rabbit polyclonal antibody, sc-397, SantaCruz) by immunoblotting. We routinely obtained 5 ml recombinant TAT.p21 protein at 1.0 mg/ml from a single 5.0 L (liter) batch culture.

3.2 Immunopreciptation

The following antibodies were used: Cdk2 (610145; Pharmingen); sarcomeric MHC (MF20, University of Iowa, Hybridoma Bank), actin (sc-7210), p21 (C-19); all others from SantaCruz). Cellular extracts (500 µg of total protein in 500 µl of 1.0 mg/ml BSA in lysis buffer) were incubated with 50 µl of protein A-agarose (for mouse monoclonal antibodies) or protein G-agarose (for rabbit polyclonal antibodies) beads (Roche) preblocked with 1.0% (w/v) BSA in lysis buffer and incubated with antibodies (5.0 µg/ml) overnight at 4°C on a rotating wheel. For co-immunoprecipitation studies, immune complexes were dissociated in 25 µl of lysis buffer containing 1.0% (w/v) SDS. Lysis buffer was added to give a final concentration of 0.1% SDS, and the supernatant was incubated with 50 µl of protein A-agarose beads for 1 hr at 4°C. The supernatant was transferred to fresh protein A-agarose beads; antibodies used as negative controls were added and were incubated for 2 hr (hours) at 4°C. Immune complexes were then washed three times with lysis buffer and eluted in 50 µl of SDS sample buffer. Boiled samples (25 µl) were electrophoretically separated, transferred to polyvinylidene difluoride membranes, and blocked, and primary antibodies (0.2-1.0 µg/ml) were incubated overnight at 4°C on a rotary platform with gentle agitation. They were subsequently probed with secondary horseradish peroxidase (HRP)-conjugated anti-mouse or anti-rabbit immunoglobulin G antibodies (diluted 1:2500; Amersham). Equal loading was confirmed by resolving 50 µg of total protein by SDS-PAGE and probing with anti-sarcomeric actin antibody (diluted 1:200). Detection was carried out using the enhanced chemiluminescence assay (Amersham).

3.3 Western blot analysis and immune complex kinase assays

TAT-fusion protein transduced neonatal rat ventricular cardiomyocytes were lysed in NP40-buffer (50 mM Tris-HCl pH 7.5, 250 mM/L NaCl, 0.5% NP-40, 5 mM/L EDTA pH 8.0, 1 mM/L PMSF, 20 mM/L NaF, 1 mM/L Na_3VO_4, protease mixture (Roche)). Immunoprecipitations were done with 500 µl ventricular myocytes or total heart extract (2-3 mg/ml total protein) and 5 µg antibodies. Immunoprecipitations were carried out for 4 hr at 4°C. Immune complexes were washed twice with NP-40 buffer and boiled in 80 µl SDS-sample buffer (62.5 mM/L Tris-HCl pH 6.8, 50 mM/L DTT, 2.0% SDS, 10% glycerol, 0.01% bromophenol blue). 30 µl (50 µg total protein extract for plain Westerns) was subjected to SDS-PAGE (4-20% gradient Precise Protein Gels, Pierce) and immunoblotting procedure. Detection was carried out using the enhanced chemiluminescence assay (Amersham). Immune complex kinase assays were performed in 50 µl kinase buffer (20 mM/L Tris-HCl pH 7.4, 7.5 mM/L $MgCl_2$, 1 mM/L DTT, 5 mM/L ATP, 5 µg histone H1 (Sigma), 2 µl [γ-^{32}P]ATP (3000 Ci/mM, NEN) for 45 min at 37°C. Reactions were stopped by addition of 30 µl 3x SDS-sample buffer and 30 µl was subjected to SDS-PAGE. The amount of incorporated radioactive label was quantified with a PhosphorImager and TINA software (Raytest).

3.4 Histological examination and immunohistochemistry

Tissues were fixed in 4% paraformaldehyde overnight and immersed in 30% sucrose for cytoprotection. The Tissues were removed from the 30 % sucrose solutions, rinsed briefly in water and then rinsed with 1X TBS. Sections of 10-20 nm were prepared using standard protocols and adhered onto prepared slides. All steps were carried out at RT except where mentioned. Slides were briefly rinsed twice with 1X TBS for 5 min each. Sections were then permeabilized and blocked simultaneously by treatment with TBS-plus for 30 to 60 min with gentle agitation. Sections were incubated with primary antibody (normally F-50) in TBS-plus overnight at 4°C in the dark with mild agitation. Sections were rinsed twice with 1X TBS for 5 min each and antibodies were recovered and stored for reuse. Sections were treated with TBS-plus for 30 to 45 min with gentle agitation. Sections were incubated with fluorescence conjugated secondary antibody (normally F-50 - FITC, F-200 - TRITC) in TBS-plus for 4 hr at RT in the dark. Slides were rinsed thoroughly (6 times) with 1X TBS for 5 min to decrease background staining. If nuclear staining was necessary slides were treated with Hoechst 33258 (F 500 in water) for 10 min with gentle agitation in the dark. Slides were rinsed twice for 5 min each in water. DABCO antifade reagent was dropped onto the sections and covered with clean coverslips and the edges were sealed with clear nail polish. Slides were analysed

using a fluorescence microscope and digital images were saved. Sections were stained with hematoxylin/eosin. FITC-conjugated wheat germ agglutinine (WGA) was used to stain cell membranes of sections to outline cell size. Slides were stained for 30 to 60 min with WGA-FITC diluted F 5000 in PBS with Ca^{2+}/Mg^{2+} in darkness with gentle agitation. Slides were washed three times with PBS with $Ca^{2+/}Mg^{2+}$ for 10 min each.

3.5 Surgical procedure, isolation and culture of cardiac myocytes

Neonatal rat ventricular myocytes were enzymatically digested with collagenase and pancreatin as described (von Harsdorf et al., 1999). Cell suspensions were filtered through a nylon mesh (200 mm) and preplated in DMEM with 10% FCS for 90 min. Cardiomyocytes were incubated in serum-free medium in the presence of 10 mmol/L cytosine arabinoside (AraC; Sigma) that is toxic for proliferating cells for 36 hr. Cultures contained 3-8% non-myocyte cells as routinely monitored in parallel by indirect immunofluorescence staining with monoclonal antibody to sarcomeric myosin heavy chain (MF20). All immunofluorescence experiments were performed on three coverslips and repeated twice. For the quantitative analyses 200 nuclei were counted in random fields. Determination of cell surface area was done using NIH image. Statistical significance was determined using the unpaired t test (SigmaStat software). For hypertrophy studies, mice were continuously infused with Ang II (Sigma) (Alzet 2002 mini-osmotic pumps, Charles River) at 2 mg/kg for 14 days. Mini-osmotic pumps were placed under the skin to release 0.5µl/hr and 12µl total volume per day with 2mg/kg body weight/day. Recombinant TAT.p21 proteins (10 mg/kg daily for 14 days) were injected intraperitoneally. After euthanasia, the heart was excised, the atria and aorta were removed, and heart weight was determined. All animal studies were conducted according to the guidelines from the American Physiological Society and approved by local authorities (TVA G0202/04).

3.6 Immunocytochemistry analysis

Immunofluorescence experiments were carried out with cells grown on glass coverslips. The coverslips were collected and washed twice with PBS. The cells were fixed 15 min with 5% formalin in PBS. Three washes with PBS were followed by 60 min incubation at RT with 0.5% NP-40, 5% milk and 1% FCS in PBS to block and permeabilize the cells. This was followed by incubation with the appropriate primary antibody diluted in PBS containing 5% milk and 1% FCS for 60 min. Another three PBS washes were followed by 60 min incubation with PBS containing 5% milk, 1% FCS and the appropriate secondary antibody. Finally, three

washes with PBS were followed by 1 min incubation with 4', 6-diamidino-2-phenylindole dihydrochloride (DAPI, Sigma) diluted in water. Two washes with water were done before mounting the coverslips in 30% 1, 4-diazabicyclo-(2, 2, 2)-octane (DABCO, Sigma) 70% glycerol on glass slides and sealed with nail polish. Dilutions used for the antibodies were as follows: Anti-p21 1:100, all other primary antibodies were used at a 1:200 dilution whereas secondary antibodies were used at a 1:1000 dilution.

3.7 Northern blot analysis

Ventricular cardiomyocytes (10^6 cells) grown in six-well plates were washed once with ice-cold PBS and lysed with 1.0 ml of Trizol (Gibco). Total RNA was then isolated according to the manufacturer's procedure. Murine apical myocardium was lysed with Trizol (Gibco) and RNA isolated according to the manufacturer's procedure. A 20 μg portion of total RNA was resolved on a denaturing 1.5% agarose-formaldehyde gel, electro transferred onto nitrocellulose membrane (OPTITRAN BA-S85; Schleicher & Schuell, Dassel, Germany), and cross-linked (UV-Stratalinker, Stratagene). PCR-amplified full-length mouse and rat cDNAs for ANF and β-MHC were nick labelled with [γ-^{32}P] dCTP (111 MBq/mmol; NEN) and the multiprime DNA-labelling system (Pharmacia). Unbound radioactivity was removed applying Micro spin G-25 columns according to the manufacturer's instructions (Pharmacia Biotech). The membranes were reprobed to assess equivalent loading with a full-length rat glyceraldehyde-3-phosphate-dehydrogenase (GAPDH)-cDNA probe. The amount of incorporated radioactive label was quantified with a PhosphorImager and TINA software (Raytest).

3.8 Statistical analysis

Results are expressed as mean ± SEM. Throughout the text. A 2-way ANOVA was performed to evaluate the global statistical significance, and, if a significant F value was found, Bonferroni's post hoc test was performed to identify the difference among the groups. Differences in a single parameter among groups were evaluated using one-way ANOVA followed by Fisher's test for multiple comparisons. $P<0.05$ was considered to be statistically significant.

4 RESULTS

4.1 Preliminary analyses of TAT.p21 expression and solubility

The expression of the p21 gene in mammalian cells seems to be somewhat stochastic. The efficiency of transfection methods vary depending on the cell type and are difficult to reproduce. In order to introduce p21 into a cell in a more homogenous manner without using recombinant viruses or inducible cell lines, we applied a protein transduction method. It has been shown that fusing a TAT peptide sequence from HIV-1 to a target protein allows the fusion protein to enter the cell by freely diffusing through the plasma membrane of living cells (Schwarze and Dowdy, 2000; Becker-Hapak et al., 2001). In that perspective, a TAT.p21 fusion protein was designed and produced in the BL21 (DE3) pLysS strain of *E. coli*. The fusion protein comprises the TAT peptide followed by a histidine stretch (His-tag). **Figure 4.1, page 28** shows a diagram of the construct including the TAT domain and the His-tag. The construct was purified by using the His-tag and beads coated with Ni^{2+}. It was possible to obtain full length TAT.p21 as shown in **Figures 4.2-4.4, 4.6, 4.8, 4.10,** and **4.11**. As a negative control for further experiments, inactive TAT.p21ΔC in which the carboxyl-terminal PCNA-, the Cyclin-binding site, and the nuclear localization signal had been deleted, were generated in bacteria as N-terminal fusion proteins (Sherr and Roberts, 1999; Dotto, 2000; Besson et al., 2004) **(Figure 4.1, page 28)**. The purification procedure involved the collection of fractions of eluted proteins, they are referred to as pooled fractions in the **Figures 4.5, 4.7 and 4.9**.

Eukaryotic proteins that are overexpressed in *E. coli* are often insoluble, creating so-called inclusion bodies. This is connected to the loss of protein tertiary structure and consequently to the loss of the protein activity. It has been reported that 60% of fusion proteins are insoluble and inactive (Courtney et al., 1984). Furthermore, fusion protein expression varies from < 1%-25% of total cell proteins (Courtney et al., 1984). The major purification problem for directly expressed products is the development of techniques to release them from aggregates into stable active and soluble forms. First, we tried to find out expression conditions for TAT.p21 under which the resulting protein is biologically active. We not only tried to find such conditions but also tried to find out some factors that influence the levels of TAT.p21 expression to yield a high expression. Both TAT.p21 constructs in *E. coli* BL21 (DE3) pLysS bacteria were tested for expression. There are few factors that can directly influence the levels of TAT.p21 expression produced in *E. coli*. They include the temperature of the culture during the expression (25-37°C); optical density at which the culture is induced (OD600 = 0.5-1.0);

the inductor concentration used for induction (here: IPTG (isopropylβ-D-thiogalactopyranoside) 0.0-1000 µM, end concentration); the time after induction after which the culture is harvested (0-16 hr); and the incubation medium (ionic environment).

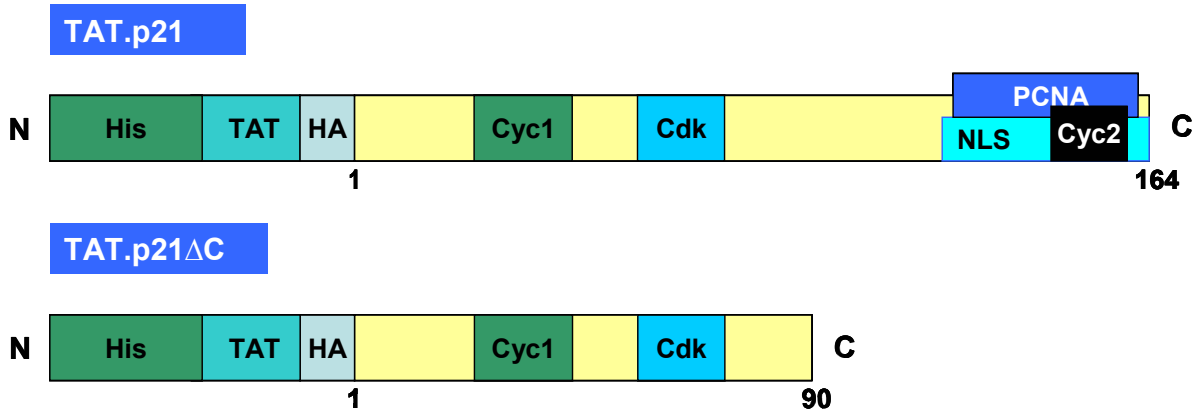

Figure 4.1: Domain structure of both TAT.p21 and TAT.p21ΔC. 11 amino acids that build the protein transduction domain (PTD) within TAT and 6 x His residues (His) as well as a hemagglutinine tag (HA) precede the N-terminus of the p21 cDNA. Control TAT.p21ΔC lacking the carboxyl-terminal PCNA-, the Cyclin-binding site, and the nuclear localization signal.

4.1.1 Effect of different IPTG concentrations on the expression of TAT.p21

10 ml of LB medium with different concentrations of IPTG (0, 20, 50, 100, 200, 500, and 1000 µM respectively) containing appropriate antibiotics was inoculated with a single bacterial colony from a fresh LB agar plate and incubated at 37°C overnight in a 14-ml tube with vigorous shaking (200 rpm). The samples were centrifuged for 20 min at 4°C with 6000 rpm after overnight culture incubation. The pellet was dissolved in 500 µl buffer Z with 10 mM PMSF, 1.0 mM DTT respectively for 60 min and then shortly sonicated for 2 x 10 s. The suspension was then centrifuged for 30 min at 4°C with 12000 rpm. 10 µl samples were taken for electrophoresis from the supernatant and each sample was mixed with 50 µl of 3 x SDS PAGE loading buffer. After heating for 5 min at 95°C, 30 µl from every sample was loaded onto the gel. The electrophoresed SDS-PAGE gels (4-20%) were transferred to immobilon membranes and finally probed with an anti-His mouse monoclonal antibody. An example of a gel is shown in **Figure 4.2, page 29**. One can see that the highest expression of the TAT.p21 fusion protein, which is expected at a size of about 28 kDa, was seen at a concentration of 1000 µM IPTG. Despite the fact that for reasons of convenience, usually overnight

incubations were used in the upcoming experiments, TAT.p21 expression was already evident after 12 hr of incubation.

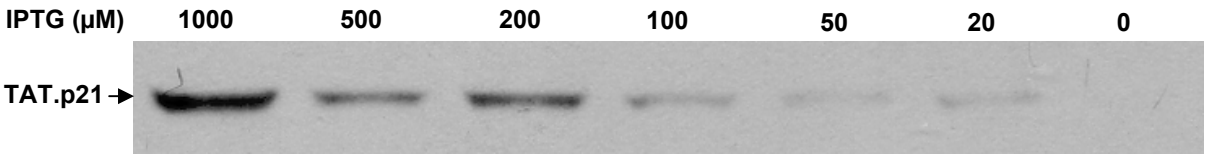

Figure 4.2: Expression of TAT.p21 depending on the IPTG concentration. The optimal dose of IPTG for TAT.p21 induction was determined by Western blotting of crude *E. coli* lysates that had been treated with IPTG concentrations from 0-1000 µM. The protein expression of His-tagged full length TAT.p21 (28 kDa) was detected by using an anti-His mouse monoclonal antibody.

4.1.2 Effect of the duration of incubation on TAT.p21 expression

Next 100 ml of LB medium containing appropriate antibiotics was inoculated with a single bacterial colony from a fresh LB agar plate, and incubated at 37°C overnight in a 250 ml flask with vigorous shaking (200 rpm). The following evening, the entire volume was inoculated in 500 ml of LB medium and cultured at 37°C. The OD600 was monitored until a value of 0.6-0.7 was reached. At that time (t=0) the culture was induced with 1000 µM IPTG (end concentration). The culture was grown overnight. Each 600-ml sample was taken before induction and at different time points after induction (hours 0, 2, 6, 10, 12) for electrophoresis. The samples were centrifuged and the pellet was lysed in buffer Z as stated above. Following sonification (6 x for 30 s on ice), the mixture was clarified by centrifugation at 12000 rpm for 30 min. The supernatant was equilibrated in 15 mM imidazole and applied at RT to a preequilibrated Ni^{2+}- column (1 ml, Amersham) connected to a *FPLC* with binding buffer Z plus 15 mM imidazole. The columns were washed with approximately 10 bed volumes of binding buffer plus 15 mM imidazole and then the enriched TAT-fusion protein was eluted by one single step addition of 1 bed volume of buffer Z containing 500 mM imidazole. 30 µl samples were taken from the selected fractions for electrophoresis and mixed with 50 µl 3 x SDS PAGE loading buffer each. After boiling for 5 min at 95°C, each sample was loaded onto the gel. Immunoblot detection was performed as mentioned before. An example of a gel is show in **Figure 4.3, page 30**. One can see that the full-length TAT.p21 fusion protein was being produced and purified at the expected size of ~28 kDa. Furthermore, our results indicate that the yield of TAT.p21 expression is strongest at 12 hr of incubation. However, these

results also indicated difficulties with regards to the purity of the anticipated fusion protein. Therefore, the stringency of the purification step was further improved by testing different media to obtain almost pure TAT.p21 fusion proteins.

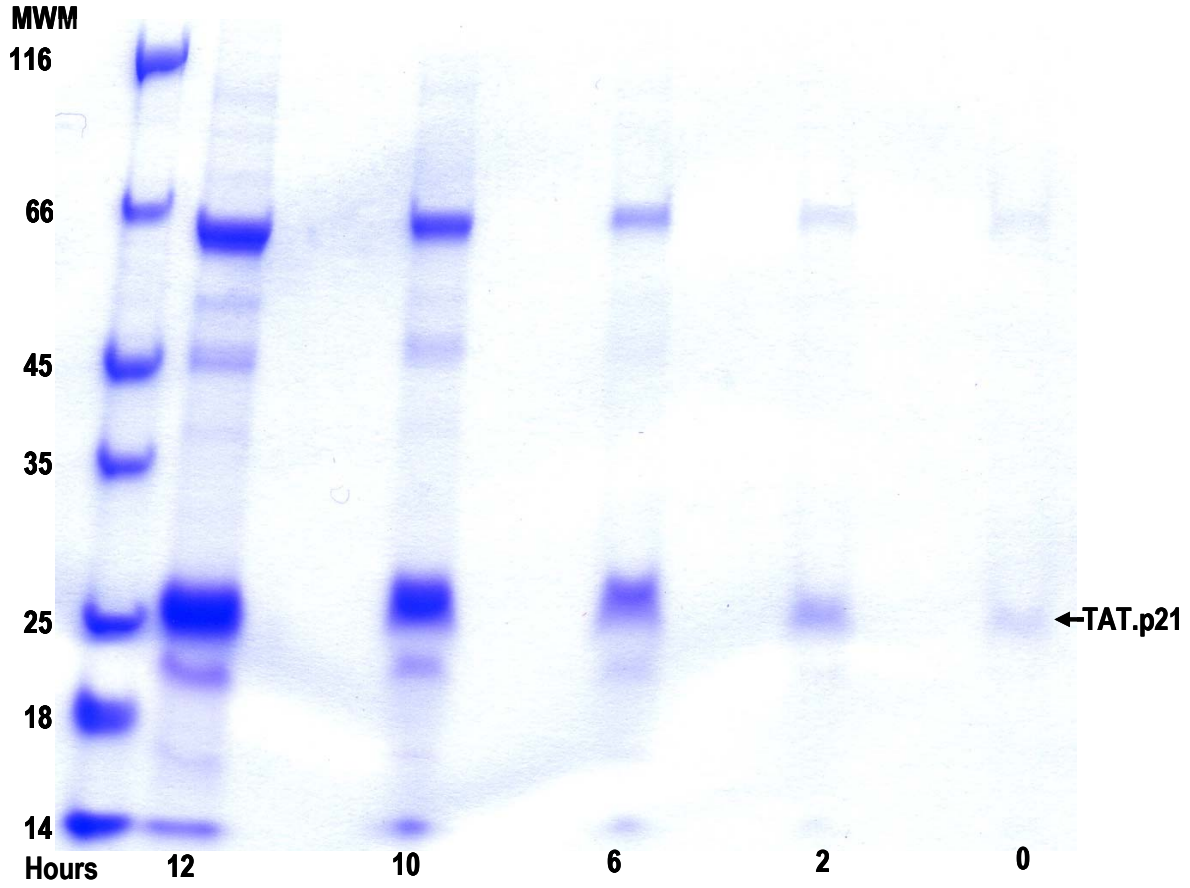

Figure 4.3: Effect of the duration of incubation on the expression of TAT.p21 (28 kDa). Coomassie stained SDS-PAGE gel. Samples were taken at the indicated time after induction with IPTG (hours 0–12). MWM: molecular weight marker (kDa).

4.1.3 Effect of different media on the expression of TAT.p21

A bacterial culture was grown exactly as mentioned before with a tested construct for the expression test, except that 3 different media were tested: LB, SOC and TB medium. At 12 hr of incubation after induction, the sample was prepared as usual for western blotting. 1 and 10 µl samples were taken from selected fractions for electrophoresis and mixed with 20µl of 3 x SDS PAGE loading buffer each. After heating the samples for 5 min at 95°C, 30 µl from each sample was loaded onto the gel (4-20%) and electrophoresed. An example of a gel is shown in **Figure 4.4, page 31**. Interestingly, the result shows a differential expression of TAT.p21 fusion protein, depending on the media used. Both, yield and purity of TAT.p21 are best in TB medium compared with LB and SOC medium **(Figure 4.4, page 31)**.

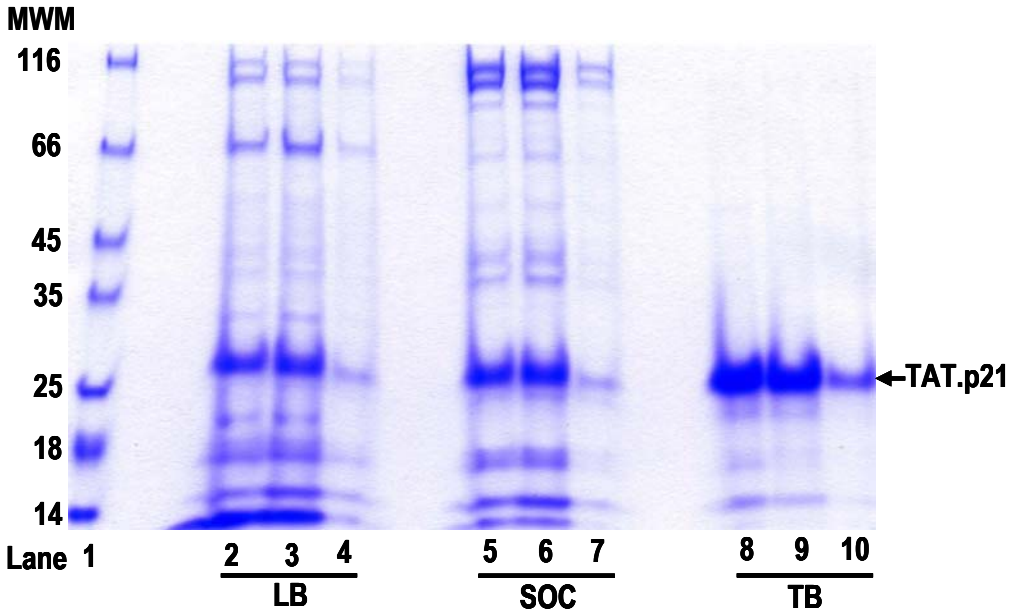

Figure 4.4: Effect of different media on the expression of TAT.p21. Coomassie blue stained SDS-PAGE (4-20%) gel for TAT.p21. Total bacterial protein extracts were affinity-purified on a Chelating sepharose charged with Ni^{2+} and separated on the gel. Loading was as indicated: 1) molecular weight marker (MWM, kDa), 2) Input, 10 µl eluted fraction, 3) 10 µl eluted fraction, 4) 1 µl eluted fraction (LB medium); 5) Input, 10 µl eluted fraction, 6) 10 µl eluted fraction, 7) 1 µl eluted fraction (SOC medium); 8) Input, 10 µl eluted fraction, 9) 10 µl eluted fraction, 10) 1 µl eluted fraction (TB medium).

4.2 Generation of TAT.p21 fusion proteins by *FPLC*

Proteins have evolved very complex structures in order to perform a diverse array of functions. As a result, their physicochemical properties vary greatly, posing difficulties when developing versatile purification protocols. Different purification methods have been developed that capitalize on the general physical properties of proteins. One of the quickest and easiest ways to purify a protein is to use affinity chromatography, since it is generally a more selective method of purification. This allows purification of the protein of interest in one or two steps. However, many proteins have not been characterized sufficiently, or do not have any known strong binding properties that can be utilized for purification. One way to circumvent this problem is to incorporate a purification tag into the primary amino acid sequence of a target protein, thus constructing a recombinant protein with a binding site, which allows purification under well-defined generic conditions. Histidines exhibit highly selective binding to certain metals and have great utility in an immobilized metal affinity

chromatography (IMAC). Under conditions of physiological pH, histidine binds by sharing electron density of the imidazole nitrogen with the electron-deficient orbitals of transition metals. Although only three histidines may bind transition metals under certain conditions, six histidines reliably bind transition metals in the presence of strong denaturants, such as urea or guanidinium (Hochuli et al., 1987). Such protein tags are commonly referred to as 6 x His tags. Those tags possess characteristics favourable for binding to IMAC resins and improve protein solubility and yield. Fast Protein Liquid Chromatography (*FPLC*) is a protein purification technique utilizing inert materials, such as glass or plastic, to purify proteins without any metal leaching from the instruments into the protein sample. This method allows running chromatography purification at flow rates of 10 ml/min/cm^2 under medium pressure (up to 3 MPA).

Downstream-processing of a recombinant expressed protein mainly consists of two different steps: extraction and purification, each of them increasing the purity and concentration of the product. Extraction: In this first step the cell membrane of the host organism is disrupted, releasing all cellular proteins. The cells are lysed either under native conditions or under conditions where the protein is denatured with urea. Inclusion bodies are destructed by treatment with the ultraTurax, and DNA is fragmented by sonification. Cells are harvested by centrifugation, washed with ice cold water and centrifuged again. Cell lysis is performed in lysis buffer of 8 M urea (providing denaturing conditions). The suspension is ultraTuraxed and sonificated. All components are segregated by adjusting to 15 mM imidazole followed by centrifugation. *FPLC* is performed for the supernatant. Purification: The steps performed for purification using *FPLC* consist of the HiTrap column, which allows abscission of His-tagged proteins, an ionic exchange column, which allows refolding of denatured proteins and a desalting column, which removes otherwise interfering ions. As the column is supplied free of metal ions it has to be charged with suitable metal ions before use. Therefore, following a washing step the column is loaded with $NiSO_4$, resulting in a matrix that represents a high affinity to His-tagged proteins. After rinsing with binding buffer to remove residual unbound metal ions and equilibrated, the protein sample is applied and binding is performed by washing with binding buffer. Binding buffer contains a low concentration of imidazole that competes with the histidine residues of proteins for binding to the nickel-chelate, thus allowing only His-tagged proteins to bind firmly to the matrix. The His-tagged protein is eluted from the column by washing with elution buffer containing a high concentration of imidazole, which is able to displace the His-tag. The resulting fractions leaving the column therefore contain the protein of interest.

4.2.1 Purification of TAT.p21 fusion proteins from the Ni-NTA column by *FPLC*

The Ni-NTA protein purification system is based on the remarkable selectivity of patented Ni-NTA (nickel-nitrilotriacetic acid) resin for proteins containing the 6 x His tag. This technology allows one-step purification of His-tagged protein under denaturing conditions. NTA, which has four chelation sites for nickel ions, binds nickel tightly. The extra chelation site prevents nickel-ion leaching and results in a greater binding capacity and protein preparations with higher purity than those obtained using other metal-chelating purification systems (Hochuli et al., 1987 and see a hand book for high-level expression and purification of 6 x His tagged proteins, The QIA expressionist ™). We can pool around 10 ml of TAT.p21 fusion protein at the first purifying step via Ni-NTA column by *FPLC* from 5 L bacterial cell culture as described in **Figure 4.5, page 33**.

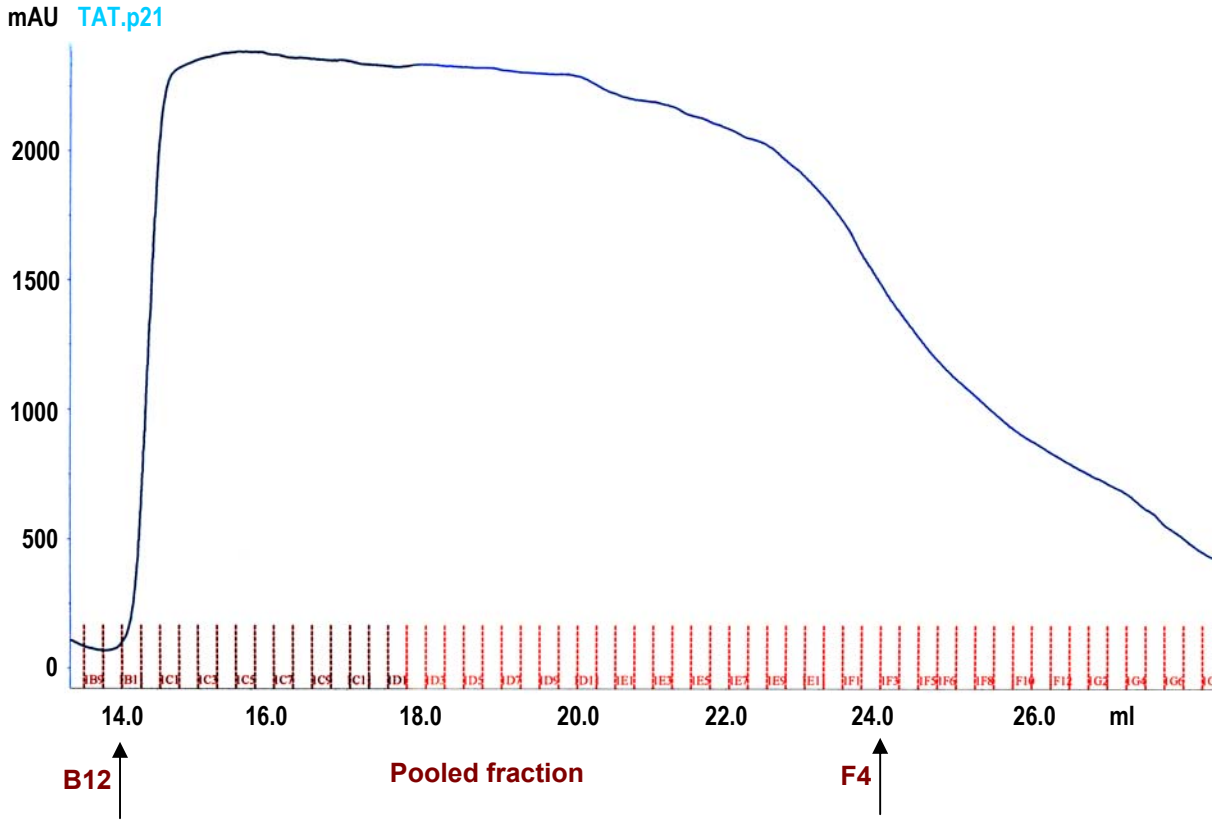

Figure 4.5: Elution and gradient profile of TAT.p21 from the Ni-NTA column by *FPLC*. His-tagged TAT.p21 was purified under denatured conditions on a 10 ml Ni-NTA Superflow column connected to an *FPLC* system at a flow rate of 1 ml/min. After applying the sample, the column was washed with 60 ml wash buffer (containing 15 mM imidazole) and eluted with 20 ml elution buffer (containing 500 mM imidazole).

The TAT.p21 expression represents approximately 5% of total soluble protein **(Figure 4.6 A, page 35)** as estimated by Coomassie blue staining and quantisation at 700 nm by infrared imaging (Li-Cor Odyssey). A one-step affinity purification with Ni-NTA resin gave a single dominant band with only traces of contaminating bands **(Figure 4.6 A, page 35)**. Most of the TAT.p21 was retained on the Ni-NTA resin, giving a final TAT.p21 preparation that was approximately 70% pure **(Figure 4.6 A, page 35)** compared with crude *E. coli* lysates. The protein composition of these fusion proteins was further confirmed using Western blot analysis probed with an anti-His antibody **(Figure 4.6 B, page 35)**. One can see that both the full-length TAT.p21 and TAT.p21ΔC fusion protein were being produced and purified at the expected sizes of ~28 kDa and ~20 kDa, respectively. For comparison purposes, different volumes of TAT.p21 and TAT.p21ΔC purified and eluted from Ni-NTA resin are shown.

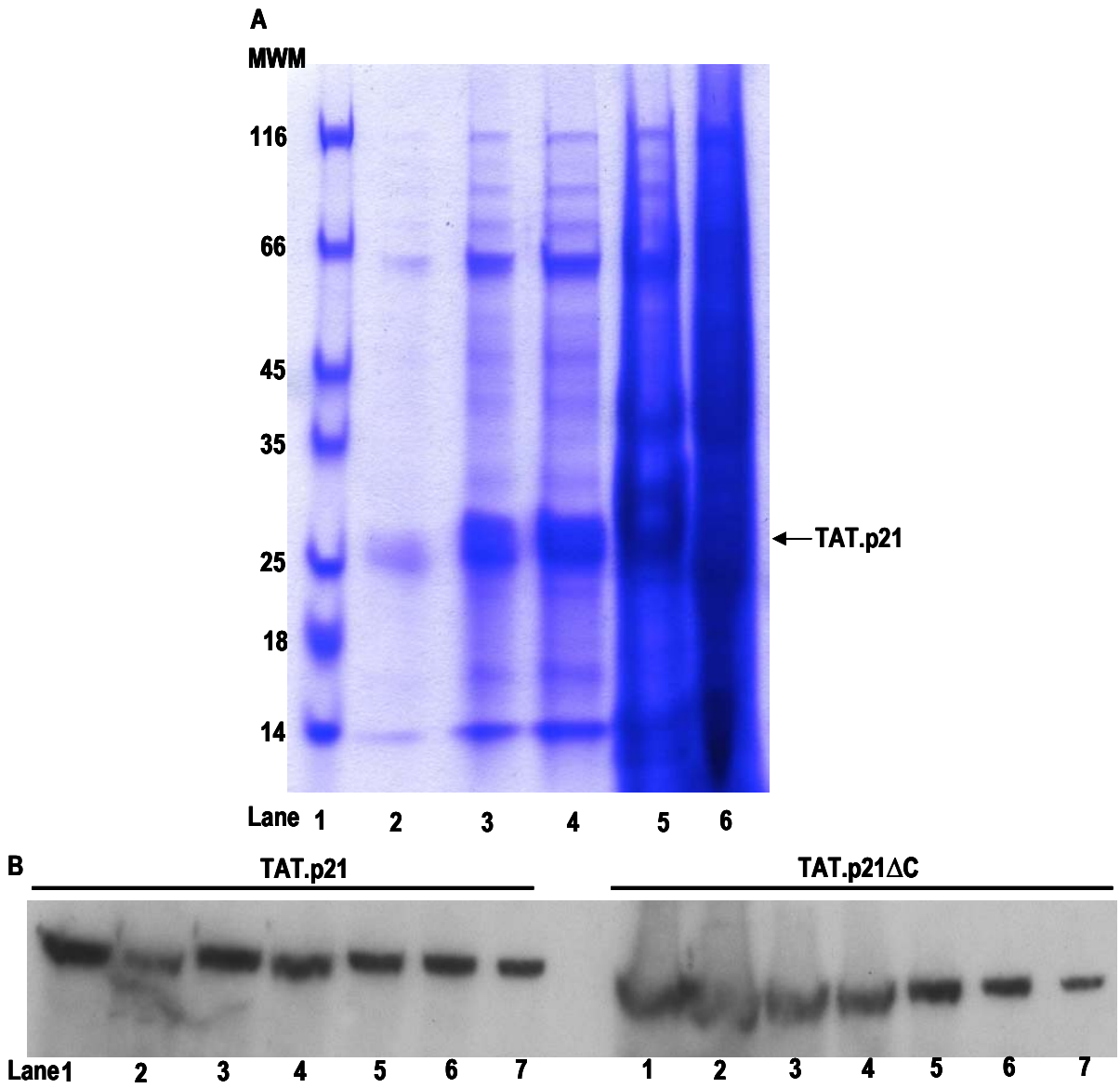

Figure 4.6: Expression of TAT.p21 fusion proteins affinity-purified from the Ni-NTA column by *FPLC*. **A**. Coomassie blue stained SDS-PAGE (4-20%) gel for TAT.p21. Lanes were loaded as indicated: 1) molecular weight marker (MWM, kDa), 2) Input, 1 µl eluted fraction, 3) 5 µl eluted fraction, 4) 10 µl eluted fraction, 5) Input, 0.1 µl crude lysate, 6) 1 µl crude lysate. **B**. Western blot analysis of both TAT.p21 (~28 kDa) and TAT.p21ΔC (~20 kDa) fusion proteins. Lanes were loaded as indicated: 1-2) 5 µl, 3-4) 2 µl, 5-6) 1 µl, 7) 0.5 µl.

4.2.2 Purification of TAT.p21 fusion proteins from the ion-exchange column (MonoQ)

If lysis takes place under denaturing conditions following the Ni-NTA column, the protein is refolded by performing an *FPLC* using an ion-exchange column (MonoQ). Hereby the concentration of urea in the column is decreased. Whereas denatured protein binds rather firmly to the anionic exchange material, refolded protein is eluted and can be collected. We can pool around 2 ml of TAT.p21 fusion protein at the second purifying step via MonoQ column from 10 ml of sample by Ni-NTA column as described in **Figure 4.7, page 36.**

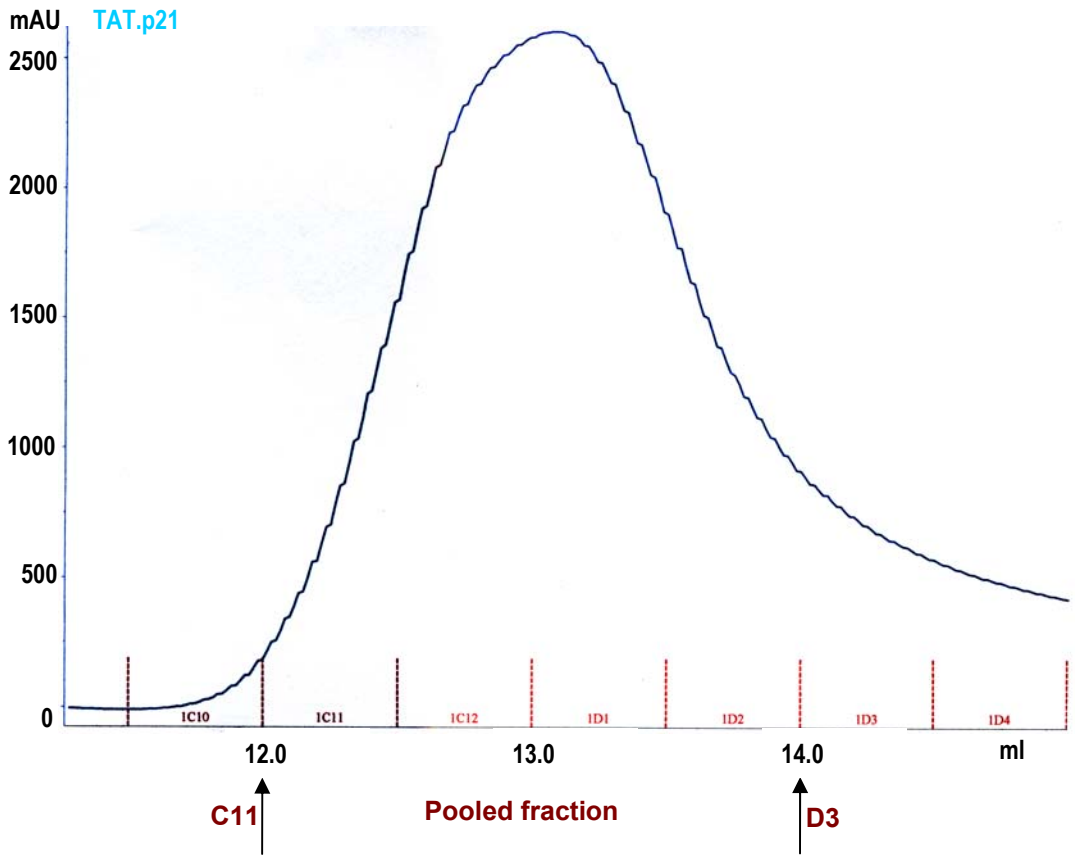

Figure 4.7: Elution and gradient profile of TAT.p21 fusion proteins from the ion-exchange column (MonoQ). Elution is shown with a step gradient using a MonoQ column. Around 10 ml TAT.p21 from the Ni-NTA Superflow column were applied to the column at a flow rate of 1 ml/min. After applying the sample, the column was washed with 20 ml binding buffer (100 mM NaCl, 20 mM HEPES, 8 M Urea, pH 8.0) and eluted with 10 ml elution buffer (2 M NaCl). Pooled factions from the elution peak for TAT.p21 fusion protein were collected and analyzed.

One-step affinity purification with the ion-exchange column gave a very strong band with only slight traces of contaminating bands **(Figure 4.8, page 37)**. Most of the TAT.p21 protein was retained on the MonoQ column, yielding a final TAT.p21 preparation that was approximately 95% pure **(Figure 4.8, page 37)** as estimated by Coomassie blue staining compared with the sample from the Ni-NTA column **(Figure 4.6 A, page 35)**.

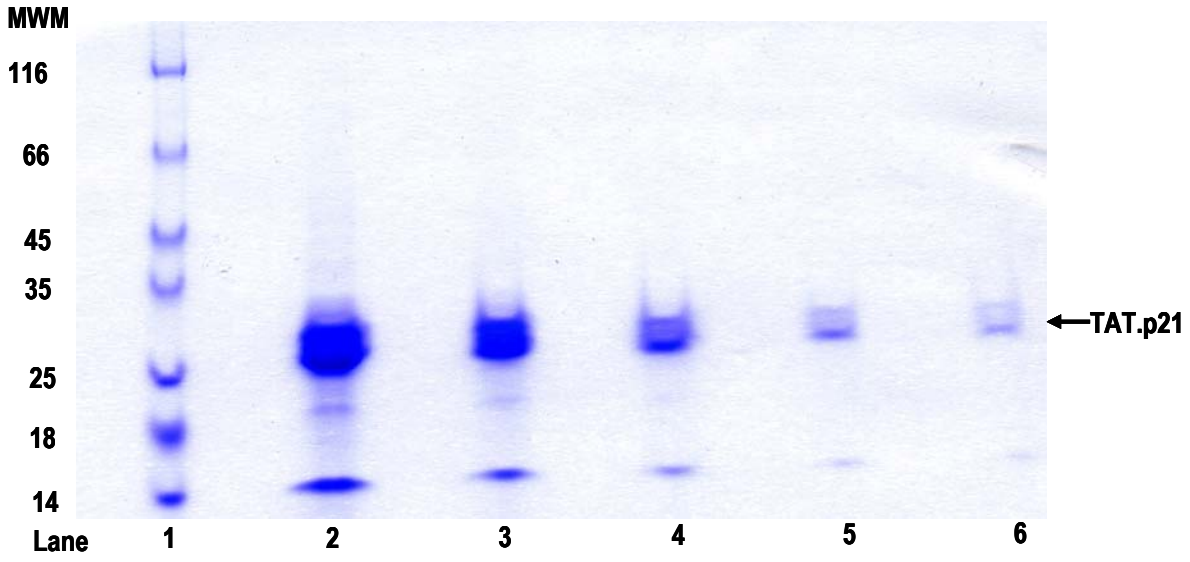

Figure 4.8: Expression of TAT.p21 fusion proteins following purification with the ion-exchange column (MonoQ). Coomassie blue stained SDS-PAGE (4-20%) gel for TAT.p21 (28 kDa). Lanes are loaded as indicated: 1) molecular weight marker (MWM, kDa), 2) Input, 20 µl eluted fraction, 3) 10 µl eluted fraction, 4) 2 µl eluted fraction 5) 0.5 µl eluted fraction, 6) 0.1 µl eluted fraction.

4.2.3 Purification of TAT.p21 fusion proteins from the desalting column

Desalting columns are used not only to remove low molecular weight contaminants such as salt, but also for buffer exchange before or after different chromatographic steps and for the rapid removal of reagents to terminate a reaction. This way, TAT.p21 protein can be separated from salts or other small molecules and be equilibrated in required buffer conditions (see for details publication: Affinity chromatography: Principle and Methods, Amersham pharmacia biotech). In total, we were able to pool ~5 ml of TAT.p21 or TAT.p21ΔC fusion protein at a concentration of 1mg/ml at the final purification step, which comes from 10 ml of sample from the Ni-NTA column **(Figure 4.9, page 38)**.

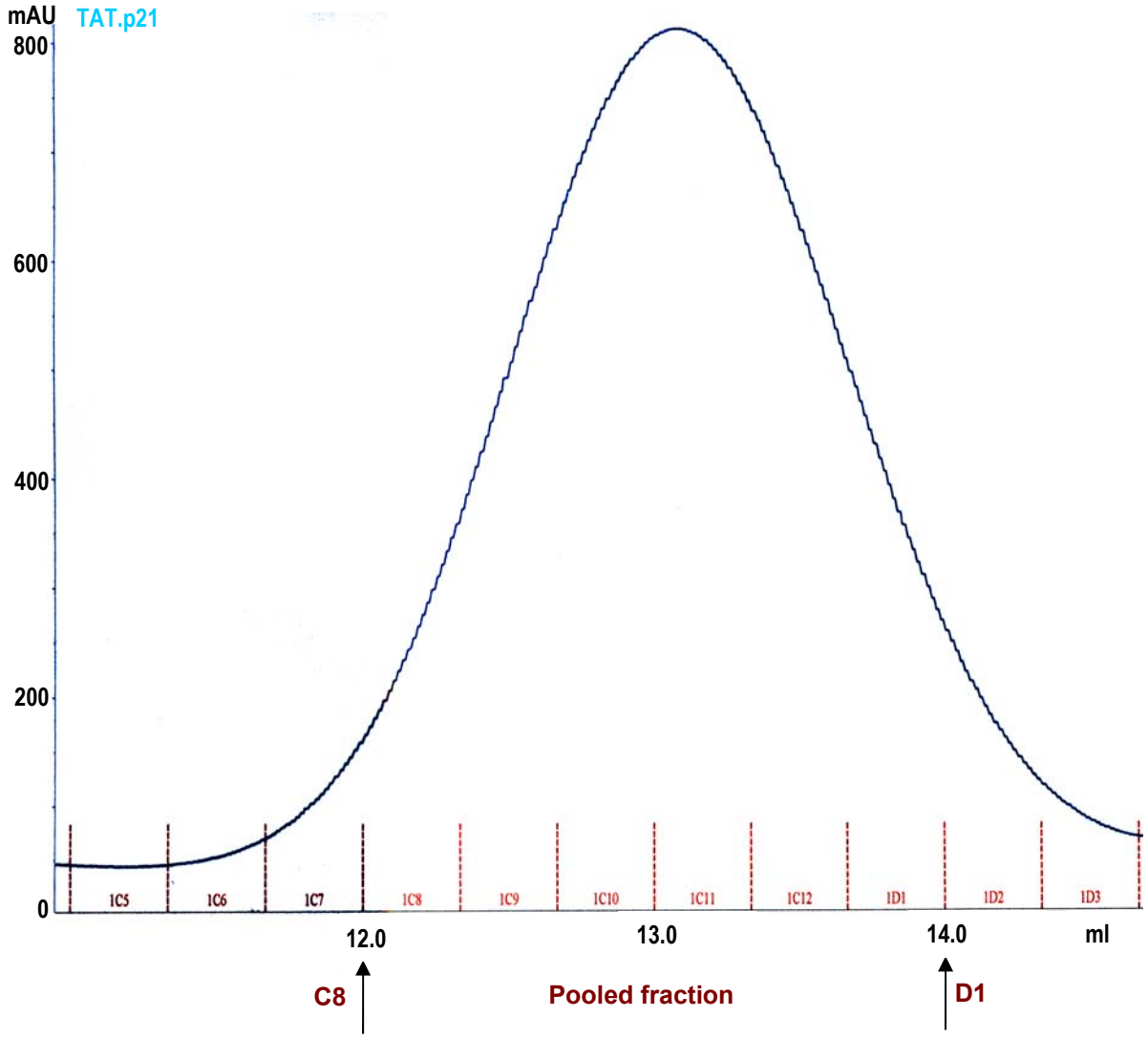

Figure 4.9: Elution and gradient profile of TAT.p21 fusion proteins from the desalting column. Elution was performed in a single step using the desalting column. The sample from the MonoQ column was applied to the desalting column at a flow rate of 1 ml/min. The sharp peak of the eluted fraction indicates TAT.p21.

Finally, we successfully obtained one dominant band of TAT.p21 or TAT.p21ΔC fusion protein from which salts and other small interfering molecules was removed. As expected, the concentration reached 1mg/ml in each case, which is similar to the concentration obtained at the second purification step. Most of the TAT.p21 was retained in the desalting column, yielding a final TAT.p21 preparation that was approximately 90% pure as estimated by Coomassie blue staining **(Figure 4.10 A and B, page 39)**.

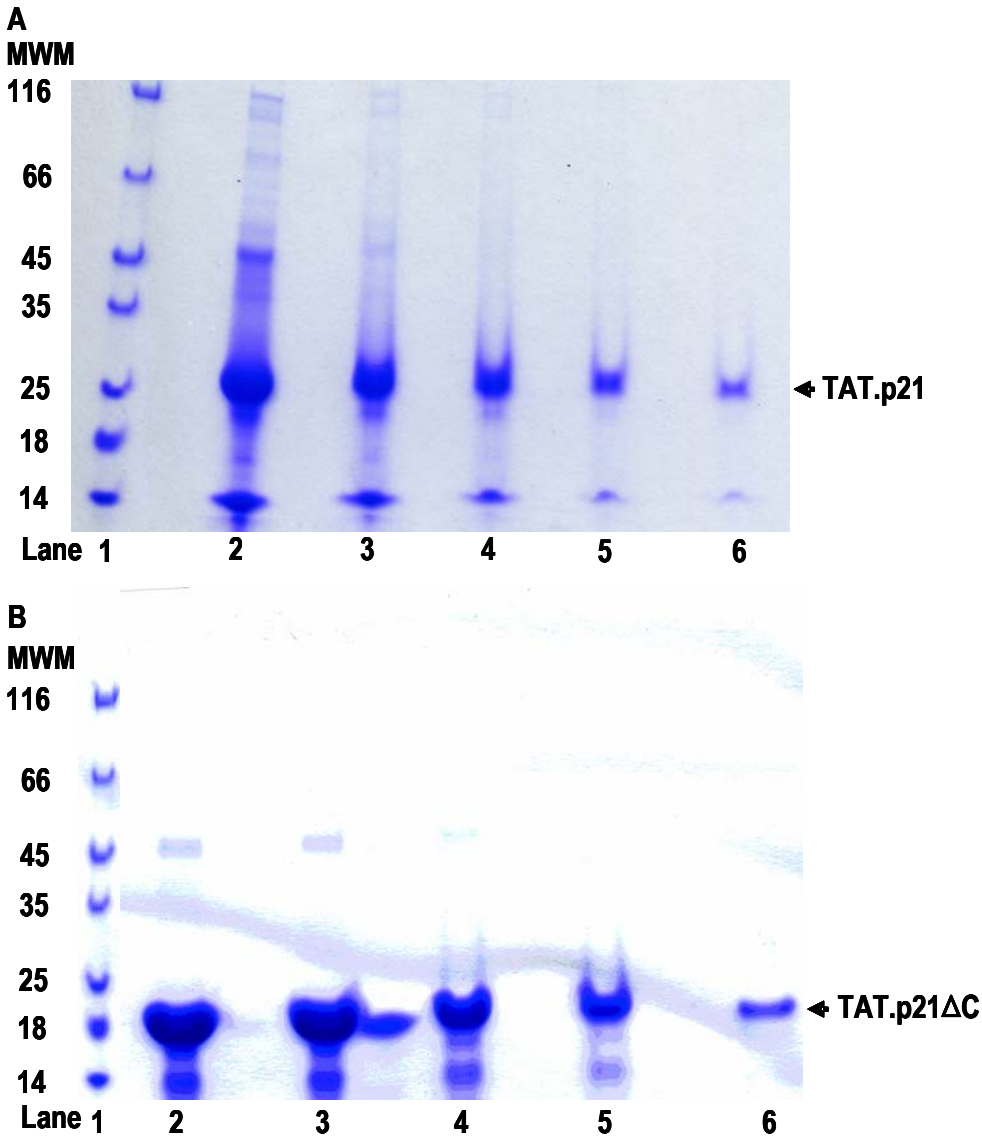

Figure 4.10: Expression of TAT.p21 fusion proteins following purification with the desalting column. Coomassie blue stained SDS-PAGE (4-20% gel) for both TAT.p21 (**A**) and TAT.p21ΔC (**B**). Lanes are loaded as indicated: 1) molecular weight marker (MWM, kDa), 2) 20 µl eluted fraction, 3) 10 µl eluted fraction, 4) 5 µl eluted fraction 5) 2 µl eluted fraction, 6) 1 µl eluted fraction.

The protein composition of these fusion proteins from the final purification step (desalting column) was further confirmed using Western blot analysis. The membranes were probed with non-specific anti-His and gene-specific anti-p21 antibody **(Figure 4.11, page 40)**.

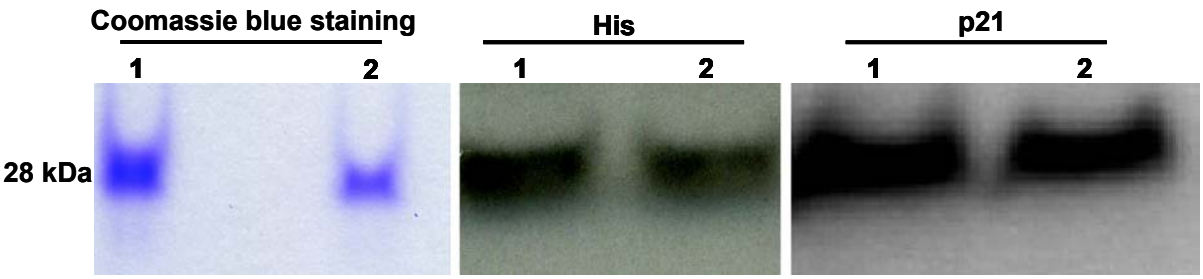

Figure 4.11: Expression and purification profile following the final purification step. TAT.p21 fusion protein purification and expression were detected by Coomassie blue staining and Western blot analysis. Membranes were probed with either mouse monoclonal anti-His or rabbit polyclonal anti-p21 antibody. Lanes are loaded as indicated: 1) 2 µl sample, 2) 1 µl sample from desalting column).

4.3 Effects of TAT.p21 delivery on cardiac hypertrophy

p21 can inhibit growth of normal proliferating cells (Xiong et al., 1993; Yang et al., 1995). However, less is known about its role in growth control of postmitotic cells. The expression levels and activity of p21 have been reported in the processes of cardiac myocyte growth and hypertrophy (Brooks et al., 1998; Koh et al., 1998; Tamamori et al., 1998 and Nozato et al., 2000). These studies suggest that p21 may have unknown functions in postmitotic non-proliferating cells. We generated recombinant TAT.p21 and inactive TAT.p21ΔC fusion proteins with the HIV-1 TAT protein transduction domain to analyze whether ectopic p21 can abrogate maladaptive cardiac hypertrophy. In this regard we also examined whether delivery of TAT fusion proteins represents a useful method of cardiac gene therapy. The cellular transduction and hypertrophy-suppressing capabilities of p21 fusion proteins were evaluated *in vitro* and *in vivo*.

4.3.1 *In vitro* transduction of TAT.p21 inhibits increases in Cdk2 activity, fetal cardiac gene expression, protein synthesis and cardiomyocyte cell size following Ang II

The Cdk-inhibitor p21 was originally identified through its interaction with Cdk2, thereby regulating DNA synthesis in mammalian cells (Xiong et al., 1993; Harper et al., 1995). Since p21 effectively antagonizes the activity of its target kinase Cdk2, we tested whether TAT.p21 can also inhibit Cdk2 in cardiomyocytes. Increasing amounts of TAT.p21 were added to cardiomyocytes and 4 hr later Cdk2 activity was induced with Ang II (100 nM). At 18 hr after addition of Ang II Cdk2-immunecomplex kinase assays were performed using whole cellular

extracts. Full-length TAT.p21 but not TAT.p21ΔC inhibited histone HI phosphorylation in anti-Cdk2 immunoprecipitates in a dosage-dependent manner and was maximally at about 400 nM **(Figure 4.12, page 41)**. Therefore, TAT.p21 can inhibit the catalytic activity of Cdk2 in living cardiomyocytes. In the same experimental setup, the dosage-effect of TAT.p21 on ANF gene transcription was investigated. As depicted in **Figure 4.12, page 41**, full-length TAT.p21 but not TAT.p21ΔC inhibited ANF mRNA expression in a dosage-dependent manner, the maximum concentration being about 500 nM. Thus, TAT.p21 can block the Ang II-dependent increase of Cdk2 activity and ANF mRNA expression in cardiomyocytes *in vitro.*

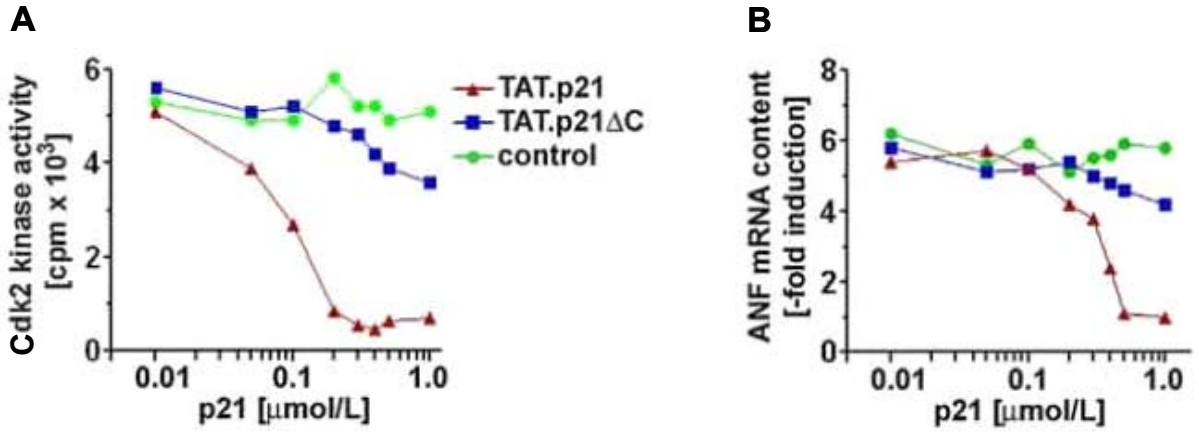

Figure 4.12: Dose-dependent inhibition of Cdk2 kinase activity and ANF gene transcription by ectopic TAT.p21 in isolated neonatal rat ventricular cardiomyocytes exposed to Ang II (100 nM) for 18 hr. Increasing amounts of recombinant TAT.p21 and TAT.p21ΔC were added to cardiomyocytes. Anti-Cdk2 immunoprecipitates (500 µg total protein) were assayed in the presence of [γ-^{32}P] ATP (111 MBq/mM) and histone HI (2.5 µg) as substrate (50 µl reaction volume). The amount of phosphorylated histone HI was determined after SDS-PAGE by PhosphorImager analysis. Northern blot analysis was performed using full-length mouse ANF cDNA**.** Controls were only treated with Ang II. Data are representative of three independent experiments.

The half-life of TAT.p21 is an important issue when evaluating its potential use in living animals (Noguchi et al., 2004). To determine the half-life of TAT.p21 on the activation of Cdk2 and expression of ANF mRNA *in vitro*, we transduced ventricular cardiomyocytes with TAT.p21 and TAT.p21ΔC at 1.0 µM in the presence of Ang II. The functional half-life of TAT.p21 was ~ 48 hr as evaluated by immune complex kinase assay of Cdk2-dependent histone HI phosphorylation and Northern blot analysis of ANF transcription levels **(Figure 4.13 A and B, page 42).** Inhibition of both functional parameters was no longer detected 72 hr

after transduction with TAT.p21. In contrast, the same concentration of TAT.p21ΔC inhibited neither Cdk2 activation nor ANF expression relative to the non-transduced ventricular cardiomyocyte control culture.

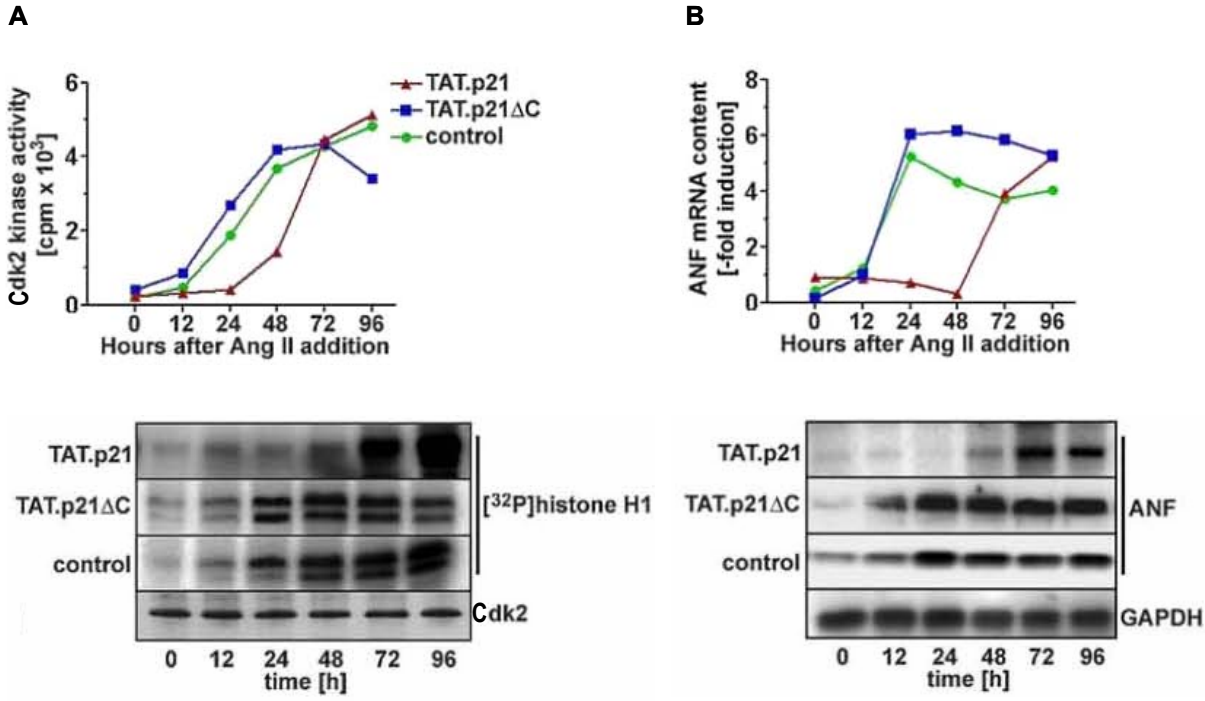

Figure 4.13: Half-life of TAT.p21 in neonatal rat cardiomyocytes determined by Cdk2 kinase activity and ANF transcription. Inhibition of Cdk2 activity (**A**) and ANF mRNA transcription (**B**) was measured during the indicated treatment time with TAT.p21 or TAT.p21ΔC (both at 1 μM) and non transduced cardiomyocytes as negative controls. Immune complex *in vitro* Cdk2 kinase assays were performed by incubation of cellular extracts (500 μg total proteins) with Cdk2-specific antibodies. Kinase activity was measured using histone HI as substrate. Northern blot analysis was performed using full-length mouse ANF cDNA. One representative result of three independent experiments is shown.

To examine whether exogenous treatment of Ang II could provoke hypertrophic response in cardiac myocytes, we first tested the effect of Ang II on both β-MHC and ANF mRNA expression levels, which are well established as molecular markers of cardiac hypertrophy (Sadoshima et al., 1993; Brooks et al., 1998; Nozato et al., 2000). Ang II treatment significantly increased the expression levels of both β-MHC and ANF mRNA when compared to the control group (3.8 ± 0.4 and 5.6 ± 0.5-fold in Ang II + saline group vs. 1.0 ± 0.2 and 1.1 ± 0.2-fold in saline group, P <0.001; **Figure 4.14 A, page 44**). Importantly, incubation of

cardiomyocytes with TAT.p21 (1.0 μM) resulted in a substantial inhibition of hypertrophic growth (1.7 ± 0.4 and 0.9 ± 0.2-fold in Ang II + TAT.p21 vs. 3.8 ± 0.4 and 5.6 ± 0.5-fold in Ang II + saline, P <0.001). This effect could not be observed for TAT.p21ΔC (3.6 ± 0.5 and 5.4 ± 0.2-fold in Ang II + TAT.p21ΔC respectively vs. 3.8 ± 0.4 and 5.6 ± 0.5-fold in Ang II + saline respectively, P >0.05) as determined by levels of hypertrophic marker genes β-MHC and ANF **(Figure 4.14 A, page 44)**.

Cardiac myocyte hypertrophy is also characterized by increasing protein content (Sadoshima et al., 1993; Brooks et al., 1998). Treatment with Ang II-induced cardiac myocyte hypertrophy, as indicated by increases in total protein when compared with the control group (4.7 ± 0.4-fold in Ang II + saline vs. 1.0 ± 0.2-fold in saline, P <0.001; **Figure 4.14 B, page 44**). Co-treatment with TAT.p21 (1.0 μM) significantly inhibited the Ang II-induced increase in total protein content (1.2 ± 0.3-fold in Ang II + TAT.p21 vs. 4.7 ± 0.4-fold in Ang II + saline, P <0.001; **Figure 4.14 B, page 44**). Treatment with TAT.p21ΔC, however, did not affect total protein content (4.1 ± 0.3-fold in Ang II + TAT.p21ΔC vs. 4.7 ± 0.4-fold in Ang II group + saline, P >0.05; **Figure 4.14 B, page 44**). We also evaluated cardiac myocyte size, which is another marker of hypertrophy at the cellular level. Our results indicate that TAT.p21 significantly inhibits an Ang II-induced increase in cardiomyocyte size (486 ± 28 μm^2 in Ang II + TAT.p21 vs. 1476 ± 79 μm^2 in Ang II + saline, P <0.001; **Figure 4.14 B, page 44**). However, TAT.p21ΔC failed to abrogate cardiomyocyte hypertrophy by Ang II (1350 ± 86 μm^2 in Ang II + TAT.p21ΔC vs. 1476 ± 79 μm^2 in Ang II + saline group, P >0.05; **Figure 4.14 B, page 44**). Moreover, since endogenous p21 expression decreases during Ang II stimulation (data not shown), we conclude that TAT.p21 can inhibit cardiac myocyte hypertrophy.

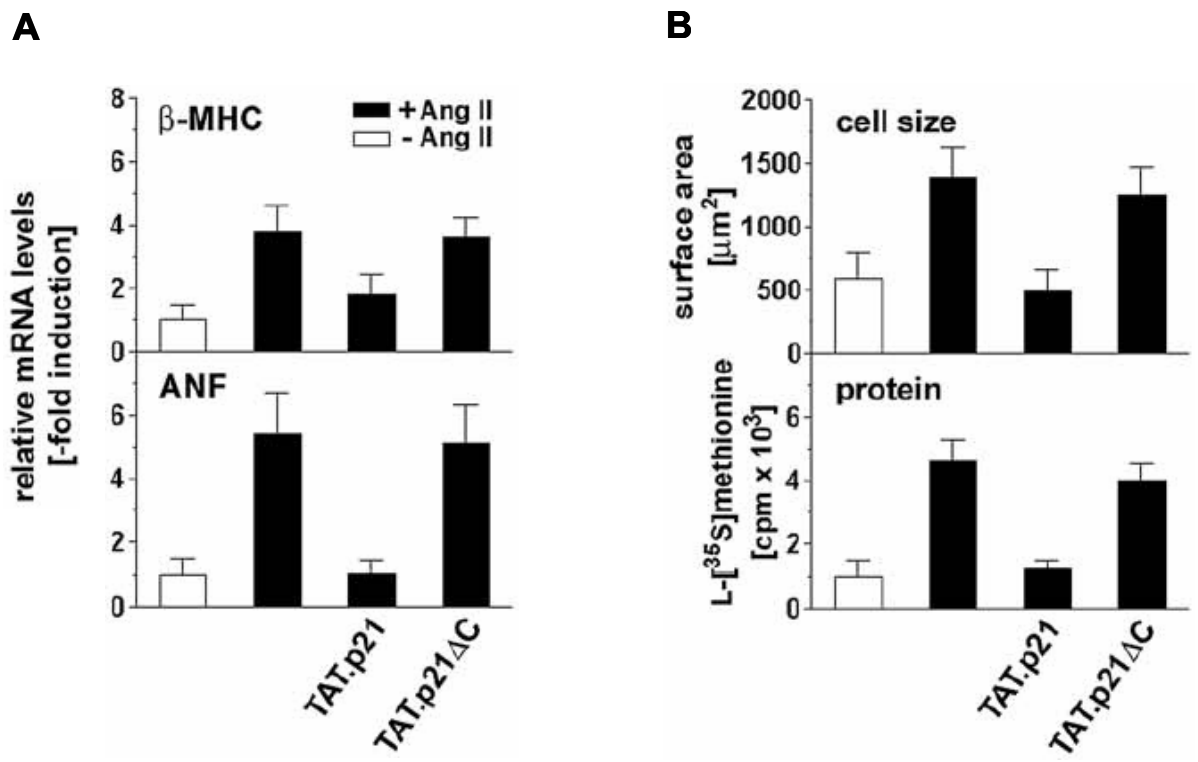

Figure 4.14: Inhibition of Ang II-dependent hypertrophic growth of cardiomyocytes *in vitro* by TAT.p21. Primary cardiomyocytes were cultivated in serum-free medium and transduced with wild-type or mutant TAT.p21 (1.0 μM). Cells were stimulated with Ang II for 48 hr to trigger hypertrophic growth. **A.** Transcript levels of biochemical hypertrophy markers β-MHC and ANF were analyzed by Northern blotting of total RNA. Calculated values of mRNA levels were corrected for GAPDH expression (mean values ± SEM, n=3). **B.** Cardiomyocyte cell size and protein synthesis following Ang II treatment. De novo protein synthesis was measured by labelling of cardiomyocytes in methionine-free medium supplemented with 5 μCi/ml L-[^{35}S] methionine (37 TBq/mM, mean values ± SEM, n=3).

4.3.2 Analysis of the effects induced by TAT.p21 on the heart *in vivo*.

4.3.2.1 *In vivo* transduction of TAT.p21 fusion protein in the murine heart

The *in vivo* transduction capability of TAT.p21 to the heart was evaluated in adult mice. Our preliminary studies suggested that TAT.p21 could achieve robust protein transduction in the heart 2-4 hr after intraperitoneal injection. TAT.p21 injected hearts showed a strong staining pattern using an anti-his antibody throughout the whole myocardium. Inspection of immunostained myocardial sections indicated that > 95% of cells were transduced by TAT.p21 (**Figure 4.15, page 45**). Cardiomyocyte specific staining against cardiac sarcomeric myosin heavy chain (anti-MHC) confirms efficient protein transduction. Procedure-related

mortality, gross neurological problems, systemic distress, cardiac necrosis, or cardiac apoptosis for TAT.p21 transduction were not observed.

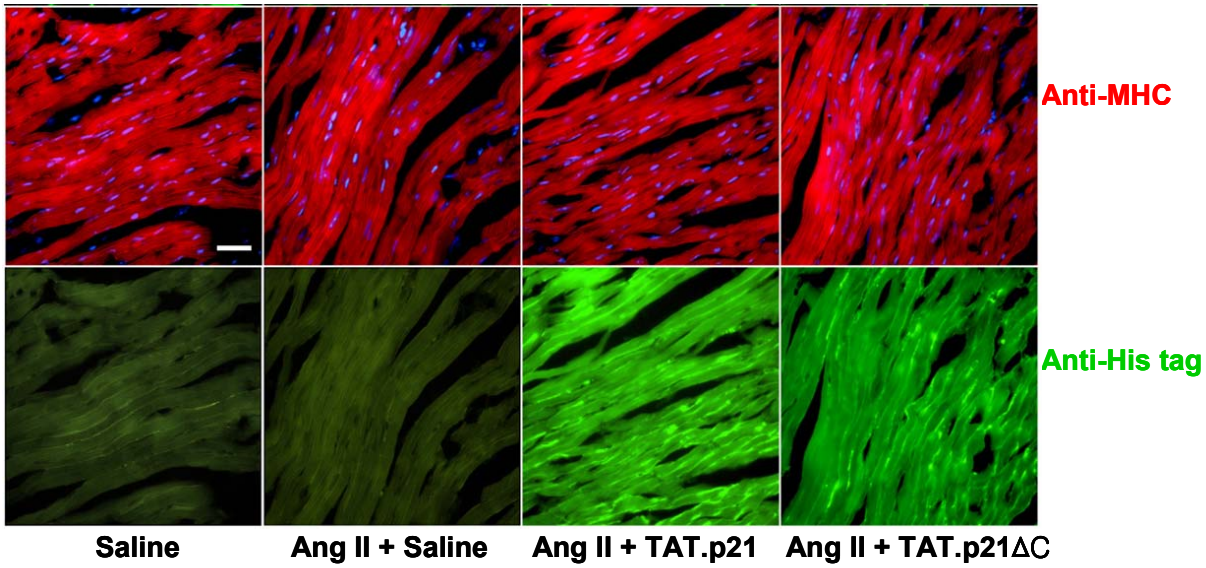

Figure 4.15: Myocardial sections following ectopic delivery of TAT.p21 fusion proteins detected with an anti-His antibody and stained against cardiac sarcomeric myosin heavy chain (anti-MHC). Sections were analyzed by immunofluorescence microscopy, scale bar = 200µm.

4.3.2.2 Systemic delivery of TAT.p21 fusion protein protects against cardiac hypertrophy *in vivo*

To further determine whether p21 protein transduction can block cardiac hypertrophy *in vivo*, we injected male C57BL/6 mice with TAT.p21 (10 mg/kg) once daily for 14 days. In parallel, Ang II (2 mg/kg) was continuously infused by mini-osmotic pumps (Alzet 2000, Charles River) for 14 days. After 14 days of Ang II stimulation myocardial cross-sections showed a marked increase in left ventricular wall thickness that was unaltered by treatment with TAT.p21ΔC. In contrast, myocardial cross-sections from mice treated with Ang II and TAT.p21 showed significantly less hypertrophied ventricular walls that were similar to unstimulated controls **(Figure 4.16, page 46)**.

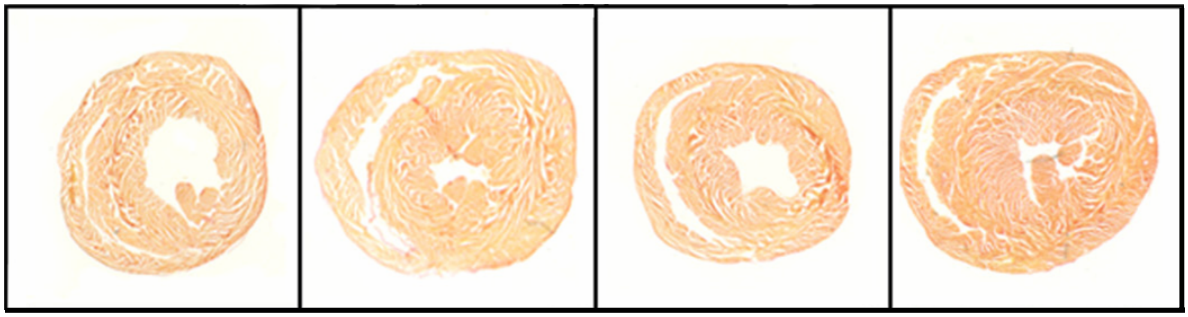

Figure 4.16: Myocardial cross-sections stained with hematoxylin 14 days after treatment with Ang II and TAT.p21 or TAT.p21ΔC fusion proteins.

To characterize cardiac hypertrophy at the cellular level, we performed wheat germ agglutinin staining of myocardial sections in different groups and measured their cell surface areas. Representative images are shown in **Figure 4.17, page 47**.

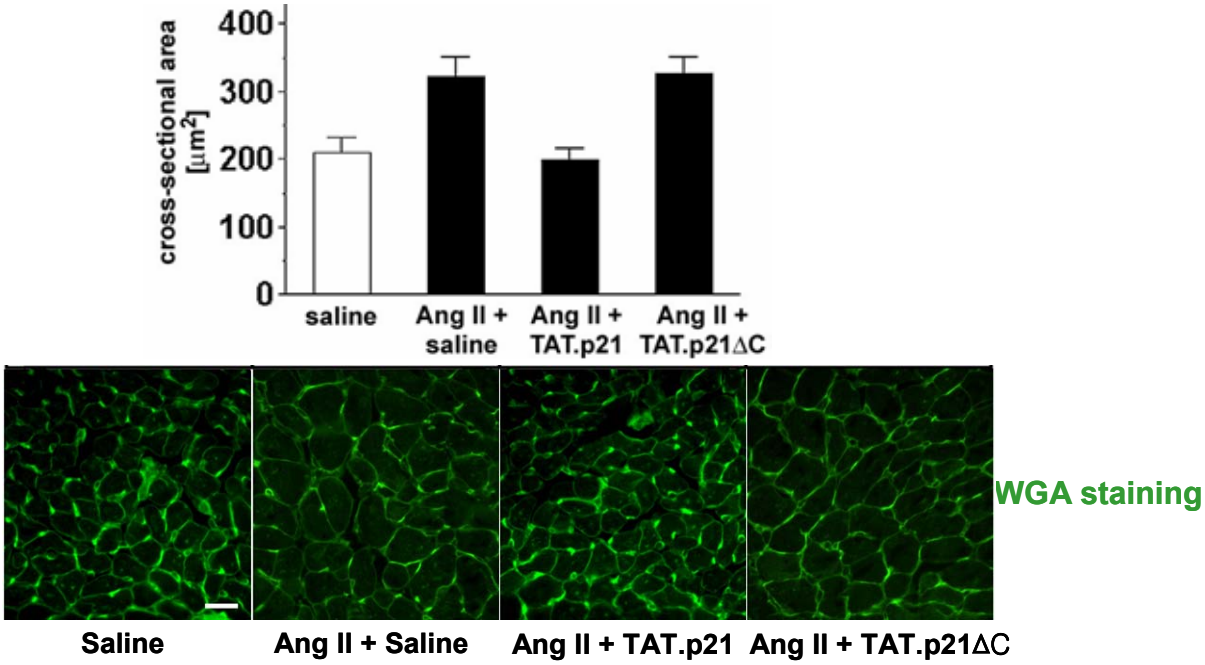

Figure 4.17: Wheat germ agglutinin staining following 2 weeks after treatment with Ang II and ectopic TAT.p21 fusion proteins. Wheat germ agglutinine (WGA) staining was analyzed by immunofluorescence microscopy and cell surface areas were measured by tracing the outline of the myocytes (n=5 for saline and Ang II + saline; n=8 for Ang II + TAT.p21 and Ang II + TAT.p21ΔC).

The cell surface area of cardiomyocytes in the Ang II + saline-treated group were significantly increased compared with those from the same area of control hearts (330 ± 16 µm^2 for Ang II + saline vs. 210 ± 12 µm^2 in the saline group, P <0.01). TAT.p21 treatment reduced the cell surface area significantly compared with the Ang II + saline-treated group (200 ± 10 µm^2 for Ang II + TAT.p21 vs. 330 ± 16 µm^2 for Ang II + saline, P <0.01). Interestingly, no significant difference appeared between the Ang II + TAT.p21ΔC treated group and Ang II + saline (328 ± 14 µm^2 for Ang II + TAT.p21ΔC vs. 330 ± 16 µm^2 for Ang II + saline, P >0.05; **Figure 4.17, page 47**).

Morphometric studies showed significantly increased heart weight to body weight ratios for Ang II + saline compared with saline alone (7.4 ± 0.5 mg/g for Ang II + saline vs. 4.8 ± 0.2 mg/g for saline, P <0.05; **Figure 4.18 A, page 49**). A significant reduction in heart mass occurred after Ang II + TAT.p21 treatment (5.2 ± 0.4 mg/g for Ang II + TAT.p21 vs. 7.4 ± 0.5

mg/g for Ang II + saline, P <0.05). However, no significant difference was seen after treatment with TAT.p21ΔC when compared with Ang II + saline (7.6 ± 0.4 mg/g for Ang II + TAT.p21ΔC vs. 7.4 ± 0.5 mg/g for Ang II + saline, P >0.05; **Figure 4.18 A, page 49**). Furthermore, there was a significant difference between the Ang II + TAT.p21 treated group and Ang II + TAT.p21ΔC (5.2 ± 0.4 mg/g for Ang II + TAT.p21 vs. 7.6 ± 0.4 mg/g for Ang II + TAT.p21ΔC, P < 0.05).

The mRNA expression of β-MHC and ANF, molecular parameters of cardiac hypertrophy, was upregulated in Ang II-treated mice when compared with the saline control group (11.8 ± 1.2-fold and 9.6 ± 0.8-fold in Ang II + saline respectively vs. 1.2 ± 0.1-fold and 1.4 ± 0.2-fold in the saline group respectively, P <0.01; **Figure 4.18 B, page 49**). The magnitude of increased expression of these markers of hypertrophy is similar to that previously observed in other studies (Takemoto et al., 2001). Therefore, these changes correlate with the induction of the hypertrophic response in the myocardium. In contrast, TAT.p21 administration completely inhibited the Ang II-triggered upregulation of β-MHC and ANF mRNA expression when compared with its control groups (1.4 ± 0.2-fold and 1.3 ± 0.1-fold in Ang II + TAT.p21 respectively vs. 11.8 ± 1.2-fold and 9.6 ± 0.8-fold in Ang II + saline respectively, P <0.01). However, injection of TAT.p21ΔC into mice failed to significantly suppress upregulation of cardiac foetal genes following Ang II (10.8 ± 0.9-fold and 8.1 ± 0.7-fold in Ang II + TAT.p21ΔC respectively vs. 11.8 ± 1.2-fold and 9.6 ± 0.8-fold in Ang II + saline respectively, P >0.05; **Figure 4.18 B, page 49**). Furthermore, there is a significant difference between the TAT.p21 and TAT.p21ΔC group (1.4 ± 0.2-fold and 1.3 ± 0.1-fold in Ang II + TAT.p21 respectively vs. 10.8 ± 0.9-fold and 8.1 ± 0.7-fold in Ang II + TAT.p21ΔC respectively, P <0.01; **Figure 4.18 B, page 49**).

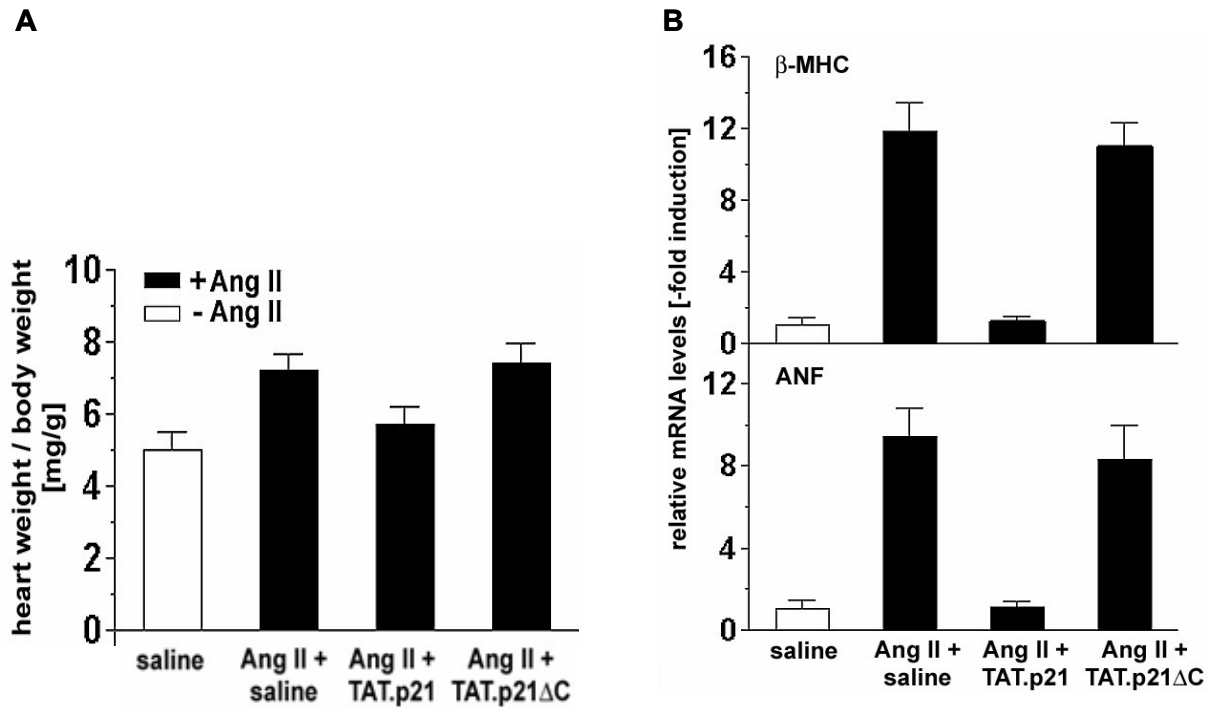

Figure 4.18: TAT.p21 inhibits Ang II-dependent cardiac hypertrophy in mice. Age-matched (8 to 10 weeks) C57BL/6 mice and Ang II (2 mg/kg per day) dissolved in saline or saline alone (control) was continuously infused subcutaneously into mice via mini-osmotic pump. Recombinant TAT.p21 or TAT.p21ΔC proteins (10 mg/kg daily for 14 d) were injected intraperitoneally. The heart weight/body weight indexes (**A**) and β-MHC and ANF mRNA expression levels (**B**) are shown. Calculated values of mRNA levels were corrected for GAPDH expression (n=5 for saline and Ang II + saline; n=8 for Ang II + TAT.p21 and Ang II + TAT.p21ΔC).

In summary, all these results clearly demonstrate that TAT.mediated delivery of wild-type p21 can suppress the development of cardiac hypertrophy in mice following Ang II.

5 DISCUSSION

5.1 p21 inhibits cardiac hypertrophy

Previous studies demonstrate that cardiac hypertrophy is associated with an activation of the cell cycle machinery leading to increased Cyclin-dependent kinase signalling. In this study we tested the hypothesis that repression of Cyclin-dependent kinase signalling by the Cyclin-dependent kinase inhibitor p21 could be an effective molecular approach to inhibit the development of cardiac hypertrophy. Our present results from neonatal rat cardiomyocyte cell culture studies as well as *in vivo* experiments in living adult mice document a strong anti-hypertrophic effect following p21 overexpression. The anti-hypertrophic effect of p21 can be referred to an inhibition of Cyclin-dependent kinase signalling as demonstrated by dose-dependent inhibition of Cdk2 kinase activity. Specificity of action is demonstrated by the fact that cardiac hypertrophy is abrogated only by wild-type p21. In contrast, non-functional mutant p21 neither inhibits Cyclin-dependent kinase signalling nor does it block the cardiac growth response following Ang II stimulation. Importantly, the anti-hypertrophic effect of p21 overexpression is not only observed at the cellular and molecular level but also seen with regard to changes in cardiac architecture and morphology following Ang II administration. Application of TAT.p21 fusion protein provided efficient and homogenous gene transfer *in vitro* and *in vivo*. Our results demonstrate that p21 is a potent inhibitor of cardiac hypertrophy and that the TAT protein transduction technique is a powerful tool for efficient somatic gene transfer.

Cardiac hypertrophy and cell cycle control

Cardiomyocytes undergo terminal differentiation soon after birth, irreversibly withdrawing from the cell cycle so that growth stimulation induces cellular hypertrophy (Brooks et al., 1998). In the adult rat heart, there appears to be a block in the cell cycle, with the majority of myocytes being locked in either the G_0 or the G_1 phase of the cell cycle (Capasso et al., 1992). They do not divide any longer and augmentation of the heart muscle only occurs in form of hypertrophic cell expansion. Thus, a heart injured by a number of stimuli including infarct and pressure overload is not able to regenerate damaged tissue by proliferation (Takeishi and Walsh, 2001; Takaoka et al., 2002). Instead, cardiac myocytes try to compensate for loss of tissue by further outstretching, a process called "cardiac remodelling", where cells re-enter the cell cycle and are known to synthesize DNA but do not undergo mitosis (Marino et al., 1991). Examinations of cultured cardiac myocytes prepared from neonatal rats demonstrated mitotic

rates of less than 2% of cardiac myocytes, whereas mitosis occurred in approximately 50% of fibroblasts (Tamamori et al., 1998). Sadoshima et al. reported that addition of FCS or Ang II 72 hr after dissociation of cardiac myocytes followed by 48 hr incubation with BrdU resulted in no BrdU-positive staining (Sadoshima et al., 1997). Their results indicate that cardiac myocytes taken from newborn rats are not able to proliferate in cell culture. Cardiac hypertrophy is a compensatory response to a variety of physiological or pathological stimuli. The hypertrophic effect helps to preserve heart function. However, prolonged hypertrophic responses lead to a vicious circle yielding exhausted cells that fail to sustain heart function, which forces even more cells to stretch and finally results in overt heart failure (Frey and Olson, 2003). Intensive *in vitro* and *in vivo* investigations have shown that humoral factors, such as Ang II, fibroblast growth factor (β-FGF) and endothelins play an important role in the pathogenesis of cardiac hypertrophy (Baker et al., 1990; Parker et al., 1990; Sadoshima et al., 1993; Leite et al., 1994). In particular, Ang II is a strong stimulus of protein synthesis and hypertrophic growth in cultured cardiomyocytes (Baker et al., 1990).

Effects of TAT.p21 on Ang II-induced cardiac hypertrophy

We found that p21 inhibits cardiac hypertrophy induced by Ang II stimulation. p21 is a growth inhibitor of proliferating cells (Xiong et al., 1993; Yang et al., 2005). However, less is known about its role in growth control of postmitotic cells. p21 expression levels have been extensively investigated in the process of cardiac myocyte growth and hypertrophy (Brooks et al., 1998; Koh et al., 1998; Tamamori et al., 1998 and Nozato et al., 2000). These studies suggest that p21 may have different unknown functions in non-proliferating cells like cardiomyocytes. In order to investigate this hypothesis, we analysed the effect of ectopic p21 on cardiac myocyte growth *in vitro* and *in vivo*. *In vitro* studies were performed in rat neonatal cardiomyocytes, as this cell culture system is a well established model for studies on cardiac growth. Because the renin-angiotensin-aldosterone system is a major physiological mediator of cardiac hypertrophy in mammals (Sadoshima, et al., 1993; Frey and Olson, 2003), Ang II was chosen as stimulus to induce cardiac growth. *In vivo* experimentation was performed in adult mice as the mouse is well suited for manipulation and its physiology resembles that of humans with regards to the cardiac growth response and signalling. Most cardiomyocyte cell culture manipulations are based on adenoviral gene delivery because of its high infection rates. However, its applicability is limited to cell culture studies. For efficient *in vivo* delivery of ectopic p21 protein into the adult murine heart, we generated recombinant TAT.p21 and inactive TAT.p21ΔC N-terminal fusion proteins with the HIV-1 TAT protein

transduction domain (Sherr and Roberts, 1999; Besson et al., 2004). To test the applicability of TAT-mediated protein transduction, both *in vitro* and *in vivo* studies were performed applying this method.

To test protein transduction *in vitro*, neonatal rat cardiomyocytes were transduced with TAT.p21 and Cdk2 activity was detected. Importantly, Cdk2 activity was significantly decreased in a dose- and time-dependent manner following TAT.p21 transduction indicating biologically functional TAT.p21 fusion protein. Furthermore, administration of TAT.p21 fusion protein resulted in a significant inhibition of ANF and β-MHC fetal cardiac gene expression following Ang II stimulation. Abrogation of the hypertrophic response after Ang II administration and transduction of TAT.p21 was further demonstrated by an inhibition of protein synthesis and well retained cardiomyocyte sizes. In contrast, fetal cardiac gene expression, protein synthesis and cardiomyocyte surface area were significantly increased in controls following Ang II treatment. Similarly to the results of Nozato et al. our results confirm that p21 is a potent anti-hypertrophic factor *in vitro* (Nozato et al., 2000).

Next, we tried to confirm these results in a murine model *in vivo*. Adult C57BL/6 mice were continously infused with Ang II by mini-osmotic pumps and injected intraperitoneally with both TAT.p21 proteins or saline once daily respectively for 14 days. By 14 days of Ang II treatment, heart weight to body weight ratios and myocyte cross-sectional areas were significantly higher compared to saline treated control mice. In contrast, administration of TAT.p21 fusion protein completely inhibited the development of Ang II-triggered cardiac hypertrophy when compared to their control counterparts. However, injection of TAT.p21ΔC into the murine peritoneum failed to significantly suppress cardiac hypertrophy following Ang II treatment.

Inhibition of the classical hypertrophic response by p21 wild-type was also confirmed at the molecular level. Re-induction of ANF and β-MHC mRNA expression as seen after Ang II treatment are molecular markers of cardiac hypertrophy. The magnitude of the increased fetal gene expression of these markers was similar to that previously observed in other studies (Nozato et al., 2000). However, the re-expression of fetal isoforms of myofibrillar genes was significantly inhibited by TAT.p21 in Ang II-infused siblings. In contrast, TAT.p21ΔC did not reduce ANF and β-MHC mRNA levels following Ang II-treatment. The observation that induction of the hypertrophic response following Ang II is dependent on p21 expression levels suggests that inhibition of myocardial hypertrophy is a specific physiological function of transduced TAT.p21 protein. Importantly, ectopic p21 abrogates the development of cardiac hypertrophy not only *in vitro* but also in living adult mice. Therefore, inhibition of

myocardial hypertrophy by ectopic p21 in mice seems to be a specific physiological function of transduced wild-type p21 protein.

5.2 Possible mechanisms of p21 to inhibit cardiac hypertrophy

Maladaptive signalling

In response to a variety of mechanical, hemodynamic, hormonal, and pathologic stimuli, the heart adapts to increased demands for cardiac work by increasing its muscle mass through the initiation of a hypertrophic response. This process is an independent major risk factor of cardiac morbidity and mortality and can lead to clinical heart failure (Hunter and Chien, 1999). A key mediator of cardiac remodelling is the angiotensin aldosterone system. Numerous studies applied Ang II administration to imitate adverse cardiac remodelling in cell culture studies or in the living animal. However, the effects on cardiac remodelling observed following Ang II stimulation are mediated by multiple signalling pathways such as the G_1 Cyclin/Cdks pathway, Gp130/STAT3 signalling, Ras/Raf/MEK/ERK signalling and NFAT and calcium signalling. We found that Ang II-mediated cardiac hypertrophy can be inhibited by p21 overexpression. Therefore, a better understanding of the underlying molecular mechanisms necessitates an understanding of p21's interactions with these pathways.

Interaction of p21 with the G_1 Cyclin/Cdks pathway

We found that p21 inhibits cardiac hypertrophy. Some studies suggest that negative regulators of cell cycle or cell proliferation also may play an important role in the pathophysiology of cardiac workload (Ohki et al., 2004). Cdks facilitate progression through the cell cycle and are activated at specific points during the cell cycle (Ohki et al., 2004). p21 is involved in regulating cell cycle progression. p21, which functions by binding to and inactivating a number of the Cdks including Cdk2, is a regulator of the G_1–S cell cycle checkpoint. Several lines of evidence suggest that p21 may have an important role in Cdk2 regulation. *In vitro*, p21 has a very high affinity for CyclinE/Cdk2 complexes (Gu et al., 1993). More than 95% of active Cdk2 in normal cells is found associated with p21 (Harper et al., 1995). Our results show that p21 significantly suppresses cardiac hypertrophy triggered by Ang II. This finding is consistent with the detected decrease of Cdk2-activity. Our data support the assumption that p21 plays a pivotal role by acting as a ‘‘brake’’ and suppresses the catalytic activity of Cdk2, which acts as the gatekeeper of the G_1 phase (Brugarolas et al., 1995). Tamamori et al. have shown that serum stimulation promoted the G_1 Cyclin-dependent Cdk activity without induction of DNA synthesis in cardiomyocytes (Tamamori et al., 1998). Furthermore,

overexpression of p16 by use of the adenovirus vector effectively prevented cell enlargement, depressed serum-induced protein synthesis and expression of skeletal actin and ANF. These results suggest that G_1 Cyclin-dependent Cdk activity promoted by serum stimulation is required for the induction of cardiomyocyte hypertrophy. Reportedly, nuclear p21 plays a potent role in the regulation of Cdk2-kinases (Coqueret, 2003). Indeed, p21 inhibits Cdk2 activity efficiently in cardiac myocytes thereby retaining the growth-inhibitor function of pRb. Our work shows that TAT.p21 completely inhibits Cdk2 activities following Ang II stimulation. Some experiments also have shown that p21-dependent growth-regulation involves Cdk2-unrelated mechanisms (Coqueret, 2003). These data provide new evidence for an understanding of the regulation of cardiac hypertrophy by the G_1 Cyclin/Cdks pathway (Tamamori et al., 1998). Although we did not evaluate the kinase activity of Cdk4, p21 appears to be a universal inhibitor of Cyclin/Cdk activity (Xiong et al., 1993; Harper et al., 1995). However, numerous studies have shown that p21 also is complexed with a number of Cyclins and Cdks during normal development of the cardiac myocyte. In this regard, p21 forms complexes with Cdk2 and Cdk4 in neonatal myocytes and was also found in complexes with Cdk4 in adult cells. Our data indicate that p21 overexpression leads to loss of Cdk activities and inhibition of cardiac hypertrophy (Medema et al., 1995; Harper et al., 1995; Brooks et al., 1997; Grana et al., 1998; Brooks et al., 1998). Taken together, it appears that p21 inhibits cardiac myocyte hypertrophy at least partially via interference with the G_1 Cyclin/Cdks/pRb pathway.

Interaction of p21 with the Gp130/STAT3 signalling pathway

We found that p21 inhibits cardiac hypertrophy induced by Ang II. Ang II has been shown to activate cardiac JAK/STAT (Janus kinase/signal transducer and activator of transcription) signalling. Moreover, Ang II also has been implicated in the activation of the JAK/STAT pathway in pressure overloaded hearts and mechanically stretched cardiac myocytes (Pan et al., 1997; Pan et al., 1999). Ang II activates JAK/STAT signalling via the Ang II type 1 (AT1) receptor. JAK recruitment to AT1 occurs after its activation and association of JAK with AT1 is required for STAT translocation to the nucleus in response to Ang II stimulation (Sayeski et al., 2001). STAT is thought to regulate proliferation by modulating the expression profile of Cdk inhibitors (Quentmeier et al., 1998). Recently, some studies have shown that p21 can interact with STAT3 proteins and block their transcriptional activity. These results point to a novel biological role for p21 in the feedback regulation of JAK/STAT signalling pathways. Meanwhile, these findings indicate that gene activation by STAT3 proteins is affected by

signals that control cell cycle progression (Coqueret and Gascan, 2000). STAT proteins can recognize a conserved element in the promoter of p21 and increase the expression of this gene **(**Bellido et al., 1998). Thus, p21 may be one of the target genes activated by the JAK/STAT cascade. Coqueret et al. have shown that following leukemia inhibitory factor (LIF) stimulation, p21 interacts with STAT3 and inhibits the transcriptional activity of this factor (Coqueret and Gascan, 2000). These results reveal that p21 is part of a feedback network controlling the down-modulation of STAT activity. Several lines of evidence support a role of p21 in the inhibition of cytokine signalling. Activation of STAT factors leads to transcriptional activation of the p21 gene and promotes protein synthesis within a few hours of stimulation **(**Bellido et al., 1998). The well-conserved amino-terminal region among STAT proteins is involved in dimer-dimer interactions, which lead to cooperative DNA binding (Darnell, 1997). Interaction of p21 with this domain may inhibit cooperative DNA binding and prevent transcriptional activation. However, recent results have shown that gene activation by STAT proteins requires CBP (CREB (cyclic adenosine 3′, 5′-monophosphate–regulated enhancer binding protein)-binding protein) and histone acetyltransferase activity (Korzus et al., 1998). Other results indicated that the CBP coactivator can interact with and block the inhibitory effect of p21 on STAT3 functions. It is thus tempting to speculate that p21 binds to the carboxyl-terminal part of STAT3 proteins, which prevents the interaction with CBP and inhibits the transcriptional activity of these factors (Coqueret and Gascan, 2000). This way, p21 acts as an inhibitor of the Gp130/STAT3 signalling pathway and attenuates cardiac myocyte hypertrophy through a classical feedback mechanism. These findings further confirm that p21 is a converging point for the regulation of several intracellular signalling cascades.

Interaction of p21 with the Ras/Raf/MEK/ERK signalling pathway

We found that p21 inhibits cardiac hypertrophy induced by Ang II. Several laboratories have shown that prolonged activation of MAPKs by high-intensity Raf signals induce p21 and result in a p21-dependent growth-arrest (Sewing et al., 1997). The serine/threonine protein kinase Raf is an essential component of the signal transduction pathway leading to mitogen activated protein (MAP) kinase activation by growth factors which work through Ras. Raf is a direct downstream effector of Ras and phosphorylates MAP kinase–extracellular signal-regulated kinase (ERK) (MEK) which in turn activates p42 and p44 ERK kinases resulting in their translocation into the nucleus (Sewing et al., 1997). Hypertrophic agonists like Ang II exert their effects through the Raf (Ras/Raf/MEK/ERK) signalling pathway. In particular, the

induction of protein synthesis by Ang II in cardiac myocytes requires Raf, which in turn activates p42 and p44 ERK kinases resulting in their translocation into the nucleus (Sewing et al., 1997; Bueno et al., 2000). This cascade of events leads to the activation of transcription factors and eventually to cellular proliferation (Treisman, 1996). Blocking endogenous Raf mRNA expression with antisense constructs or dominant-negative Raf mutants interferes with mitogen-induced proliferation of NIH 3T3 cells while microinjection of bacterially expressed c-Raf-1 protein is sufficient to induce DNA synthesis in quiescent cells (Smith et al., 1990; Kolch et al., 1991). In addition to the notion that Raf signalling plays a key role in the stimulation of cell proliferation, Raf also has been linked to growth inhibition and differentiation (Sewing et al., 1997). It is surprising that p21 utilizes this pathway to lead to a G_1-specific cell cycle arrest. The induction of p21 is at least in part due to stimulation of p21 transcription. Following hormone application the levels of p21 mRNA increase with kinetics similar to those of the protein. Furthermore, p21 induction is essential for Raf-dependent arrest (Sewing et al., 1997). Thus, high-intensity Raf signalling usually functions as a positive effector that can also translate a p21-mediated growth arrest. Earlier studies have shown that initiation of proliferation of resting quiescent primary fibroblasts is associated with induction of p21 and that this event requires continuous ERK signalling (Sewing et al., 1997; Pumiglia, 1997). Therefore, it seems that p21 can convert agonistic signalling through the Ras/Raf/ERK/MEK pathway into growth arrest.

Interaction of p21 with the NFAT and calcium signalling pathway

We found that p21 inhibits cardiac hypertrophy induced by Ang II. Numerous studies indicate that alterations in intracellular calcium signalling are a primary stimulus for the hypertrophic response. Hypertrophic agents, including Ang II, β-adrenergic agonists, and endothelin-1 (ET-1) also activate calcium-dependent intracellular signalling systems (Karliner et al., 1990; Sadoshima et al., 1993; Leite et al., 1994). The calmodulin-dependent protein phosphatase calcineurin acts as a sensor of sustained elevations in intracellular calcium concentration, which triggers the transcriptional cascades that govern muscle growth, contractility, and metabolism. Calcineurin has been shown to transduce hypertrophic signals leading to cardiac growth *in vitro* and *in vivo* (Molkentin et al., 1998; Olson and Williams, 2000). Elevations in cytoplasmic calcium concentrations promote the association of calmodulin with calcineurin and consequent activation of the enzyme (Olson and Williams, 2000). Calcineurin is the only known serine/threonine phosphatase under calcium/calmodulin control (Crabtree and Olson, 2002). Among the proteins that are dephosphorylated as a consequence of calcineurin

activation are the nuclear factors of activated T cells (NFATs). Dephosphorylation in turn results in translocation of NFAT proteins to the nucleus and activation of immune response genes such as interleukin-2 (Crabtree and Olson, 2002). Furthermore, it has been shown that the same principal pathway is also operative in cardiomyocytes. Activation of calcineurin in transgenic mouse hearts is sufficient to induce massive cardiac enlargement and eventually heart failure (Molkentin et al., 1998). Recent studies have clearly shown that activation of the calcineurin/NFAT pathway is sufficient for the development of cardiac hypertrophy (Frey and Olson, 2003).

Numerous studies have demonstrated that the signalling pathways, which control proliferation of non-muscle cells are also involved in the withdrawal of cardiomyocytes from the cell cycle and cardiomyocyte hypertrophy (Brooks et al., 1998). Growth factor signalling pathways that induce hypertrophy are intimately interconnected with intracellular pathways, which link changes in calcium homeostasis with the reprogramming of cardiac gene expression (Lim et al., 2001). Calcineurin serves as a point of convergence of these different intracellular pathways and has been shown to be necessary and sufficient for hypertrophy in response to a wide range of signals *in vitro* and *in vivo* (Olson and Williams, 2000; Leinwand, 2001). Recent studies showed that the calcineurin pathway also plays an important role in cell cycle regulation (Jiang et al., 2006). On one hand, mitogenic-signalling pathways drive cell cycle progression as a consequence of their effects on Cyclins, which form complexes with Cdks (Morgan, 1997). Growth factors up-regulate the activities of G_1 Cyclins, which activate Cdks, resulting in phosphorylation of pRb, and S phase entry. On the other hand, NFATc1 (NFAT family has four members, NFATc1-c4) controls cell cycle progression by induction of cell cycle-related genes, such as CyclinD1, CyclinD2, pRb and c-myc which are required for passage of the G_1/S checkpoint (Neal and Clipstone, 2003; Lipskaia and Lompre, 2004). Indeed, forced expression of constitutively active NFATc1 in 3T3-L1 preadipocyte cells promotes growth even in the presence of low serum concentrations (Neal and Clipstone, 2003). p21 appears to be a universal inhibitor of Cyclin/Cdk activity (Xiong et al., 1993; Harper et al., 1995). It is possible that p21 inhibits NFAT signalling by controlling the cell cycle. p21 was also found to bind directly to calmodulin in a calcium-dependent manner. The calmodulin-p21 interaction appears to be required for p21 and Cyclin/Cdk nuclear localization (Taules et al., 1999). The calmodulin binding region of p21 was mapped to the last 20 amino acids of the protein (amino acids 145-164) which contain the p21 NLS and consist of a stretch of basic and hydrophobic amino acids (Gulbis et al., 1996; Taules et al., 1999). Binding to calmodulin may induce a conformational change and expose the NLS of p21, thus allowing

its nuclear translocation. The calcium dependent binding of p21 to calmodulin could in turn affect the activity of calmodulin-dependent enzymes, thus explaining the observed biological effects on cardiac myocyte hypertrophy (Taules et al., 1999). Most recent studies found that pharmacological inhibition of calcineurin by cyclosporine A blocks growth factor-induced p21 expression significantly (Jiang et al., 2006). Thus, it is possible that p21's inhibitory effect on cardiac hypertrophy is mediated via the calcineurin/NFAT signalling pathway.

5.3 Purification and transduction of TAT proteins

Generation of TAT.p21 proteins

To introduce p21 into cardiac myocytes, a fusion protein with the short basic TAT sequence originating from the TAT protein of the HIV-1 was designed. During the last decade, small peptides (10 to 16 amino acids) derived from the HIV-1 TAT protein and from the drosophila Antennapedia homeodomain have been used to internalize various types of molecules into cells (Schwarze and Dowdy, 2000). Despite their demonstrated efficiency in delivering biologically active molecules in *in vitro* experiments, their use for a therapeutic applications *in vivo* has been the object of a relatively small number of studies (Vives, 2005). This could be due to the fact that many proteins overexpress very poorly - typically less than 1 mg/liter - if they do at all (Vives, 2005). A second drawback of eukaryotic proteins that are overexpressed in *E.coli* is the formation of often insoluble so-called inclusion bodies. Inclusion bodies result from the loss of protein tertiary structure and consequently lead to a loss of the protein's biological activity. The major purification problem for directly expressed products is the development of techniques to release them from aggregates into stable active and soluble forms. Third, their disatvantage is that the introduction of fusion proteins into mammalian cells using conventional methods has often proven to be unreliable owing to the bioavailability restriction imposed by the cell membrane (Wadia and Dowdy, 2002).

Recombinant TAT.p21 protein was produced in bacteria and purified under denaturing conditions by means of a Ni^{2+}-charged resins. Denaturation led to an exposure of the six His residues to facilitate purification (Melekhovets and Joshi, 1996). In order to improve the protein expression, we tested different conditions for the optimization of the expressed protein. A genetically modified *E. coli* strain (BL21 (DE3) pLysS) was used which carries a plasmid for lysozyme with a weak promoter that inhibits T7 RNA polymerase and minimizes protein production in the absence of IPTG. Use of this strain eliminated the need for lysozyme digestion of the induced bacteria to release inclusion bodies which resulted in expression of purer protein as compared to the conventional BL21 (DE3) strain (Joshi and Puri, 2005). Our results suggest that using TB medium and induction by 1mM IPTG for 12 hr at 37°C resulted

in maximum protein expression. These proteins were finally purified by *FPLC*. 5 mg highly purified and biologically active proteins were obtained from 5 liters of BL21 (DE3) pLysS bacterial culture. We show here that we can use an efficient, standardized purification protocol to yield 1 mg of highly purified, biologically active protein per liter bacterial culture.

Transduction of TAT.p21 proteins

It has previously been shown that fusion proteins containing the protein transduction domain from the HIV-1 TAT protein could transduce through the cell membrane to deliver their cargo into the cell (Schwarze and Dowdy, 2000). Several proteins can traverse biological membranes by protein transduction. Small regions of proteins, 10 to 16 residues long, are responsible for this phenomenon (Schwarze and Dowdy, 2000). This method prooved suitable to provide soluble TAT.p21 fusion proteins that were able to penetrate cardiomyocytes *in vitro*. Importantly, tests on adult mice *in vivo* showed that TAT.p21 could penetrate the heart and fulfill its gene specific functions. TAT contains several distinct regions based on its amino acid composition. The core, acidic, and cysteine regions correspond to the minimal activation domain, whereas the basic region together with the core and glutamine-rich regions confers RNA-binding activity. In addition, the basic domain contains a nuclear localization signal which mediates the nuclear transport of TAT. TAT is primarily localized in the nucleus/nucleolus, which is a prerequisite for its transactivation function (Gautier et al., 2005). The structural requirement for transduction mediated by the HIV-1 TAT basic domain has been shown to be critical (Ho et al., 2001). Ho et al. demonstrated that enhancement of the α-helical structure resulted in a dramatic increase in protein transduction efficiency (Ho et al., 2001). The basic domain of HIV-1 TAT has been reported to be able to mediate translocation of various proteins not only into cultured cells but also into various organs of mice (Schwarze et al., 1999). TAT fusion proteins have intrinsic ability to enter cells. Uptake was enhanced by the addition of a His-tag on either the amino- or carboxyl-terminal ends of the protein which was enhanced further by the addition of a nuclear localization sequence (Joshi and Puri, 2005). The first convenient method to apply the protein delivery potential of TAT was developed by the group of Dowdy (Nagahara et al., 1998). In this system, in-frame polyhistidine-TAT fusion proteins were purified from a bacterial lysate under denaturing conditions through a series of affinity, ion-exchange, and desalting steps. The reason is that a folded (produced in native conditions) TAT fusion protein can decrease the efficiency and speed of the internalization process compared with completely denatured (unfolded) fusion proteins (Nagahara et al., 1998; Schwarze et al., 1999). Isolated denatured TAT fusion

proteins are made soluble in an aqueous buffer and added directly to the cell culture medium. TAT fusion proteins, purified under denaturing conditions, are internalized in a rapid, concentration-dependent manner to achieve maximum intracellular concentrations in a matter of minutes and are also found in the nucleus (Nagahara et al., 1998; Schwarze et al., 1999). The internalized proteins are then correctly refolded in the cytoplasm, perhaps by intracellular chaperones. The use of denaturing conditions for the purification of TAT fusion proteins is necessary to solubilize proteins from bacterial inclusion bodies and is also involved in increasing transduction efficiency and speed (Nagahara et al., 1998).

5.4 Conclusions and limitations

In conclusion, our study shows that TAT-mediated delivery of p21 can successfully inhibit the development of cardiac hypertrophy in living mice. Our results establish an attractive tool that opens new possibilities for protein therapy of patients and epigenetic experimentation with model organisms.

Transgenic techniques in experimental murine animal models are the preferred methods to alter specific functions of distinct gene products. However, transgenic techniques are laborious and time-consuming (Wadia and Dowdy, 2003). Especially, conditional expression at the appropriate time in a given tissue is sometimes difficult. Alternatively, use of viral vectors may provide a means of circumventing these issues and of accomplishing high expression levels and timed expression. However, due to spatially restricted transfections of adeno- or lentiviral vectors and unforeseeable side effects *in vivo*, their application in the treatment of cardiovascular disorders in human patients appears to be of rather limited value (Wadia and Dowdy, 2003).

To this end, we have described an experimental protein therapy model based on a transducible p21 that selectively inhibits Ang II-dependent myocardial hypertrophy in adult mice. The therapeutic potential of TAT-fusion proteins has been demonstrated by several studies. TAT-bcl-xL was been shown to inhibit neuronal apoptosis in isolated cells and in a cerebral artery occlusion model in mice (Cao et al., 2002). Dowdy´s group has described an experimental anti-HIV protein therapy based on a HIV protease-activated caspase-3 that selectively induces apoptosis in HIV-infected cells (Vocero-Akbani et al., 1999). Two groups have shown that TAT-fusion proteins can be delivered into isolated perfused hearts (Chen et al., 2001; Gustafsson et al., 2002). In each report, perfusion of the excised heart with TAT-conjugated molecules led to reduction of cardiac ischemic cell death. More recently, a transducible peptide inhibitor of NFAT provided immunosuppression for allogeneic islet transplantation in

mice (Noguchi et al., 2004). Consequently, the use of protein transduction technique opens the possibility for introduction of pharmacologically relevant proteins *in vivo* (Snyder and Dowdy, 2004). One of limitations of our present study is that we did not evaluate the cardiac function and prognosis of mice that were treated with TAT.p21. Despite the fact that all mice looked healthy during our experiment, there is a possibility that the inhibition of hypertrophy by p21 may result in left ventricular dysfunction after a longer follow-up. Another limitation of our present *in vivo* study is that we could not rule out the influence of interstitial fibrosis. Cardiac fibrosis and its constituent cells, the fibroblasts, are known to produce Ang II and other growth factors, which play an important role in the induction of cardiac hypertrophy by a paracrine manner (Fujisaki et al., 1995). Future studies have to characterize the molecular pathways by which p21 inhibits Ang II-induced hypertrophy. Finally, potential immune responses and toxicity associated with protein therapy of human patients or animals are also important issues that remain to be elucidated.

5.5 Outlook

Shortly after birth, myocardial cells loose the capability of dividing, and further growth of the heart is due to cellular hypertrophy (Brooks et al., 1998). Left ventricular wall stress, hormones, cytokines, growth factors and cardiovascular diseases increase cardiac workload and induce myocyte hypertrophy that particularly leads to left ventricular hypertrophy. Left ventricular hypertrophy is an integral component of the complex pathophysiology of arterial hypertension and results from mechanical, neurohumoral, and genetic factors which leads to myocyte necrosis and apoptosis (Giles, 1991; Chien et al., 1999). This process is an independent major risk factor of cardiac morbidity and mortality and can lead to clinical heart failure. One clinically relevant approach to treat heart failure is to develop novel strategies that suppress adverse hypertrophy. A current view is that hypertrophy requires entry into G_1 phase of the cell cycle without progression through the S phase (Busk and Hinrichsen, 2003). The G_1 phase of the cell cycle is controlled primarily by the G_1 Cyclin–dependent kinases, Cdk4 and Cdk2 (Sherr, 1994). Some data support a model in which regulation of G_1 progression can be divided into two discrete stages controlled by the activities of Cdk4 and Cdk2, such that inhibition of either stage can prevent cell cycle progression (Brugarolas et al., 1995). As cardiac myocytes enter the cell cycle in response to hypertrophic stimuli but do not proliferate, it is clear that there must be a blockage at some point of the cell cycle. The Cyclin-dependent kinase inhibitor p21 is upregulated at the time of birth when myocyte proliferation ceases and may be important for the hypertrophic response to growth stimuli

(Brooks et al., 1998; Poolman et al., 1998). Our data support the conclusion that p21 plays a pivotal role by acting as a ‘‘brake’’ and suppressor of the catalytic activity of Cdk2, which acts as the gatekeeper of the G_1 phase of the cell cycle (Brugarolas et al., 1995). p21 is not just a Cdk inhibitor but can bind directly and inhibit the activity of a number of transcription factors, including E2F, c-*myc*, Raf and STAT3 (Sewing et al., 1997; Perkins, 2002). Our results further indicate that p21 also inhibits mRNA expression of ANF and β-MHC and protein de novo synthesis (Sadoshima and Izumo, 1993). Taken together, p21 can inhibit cardiac hypertrophy on different levels through multiple mechanisms. Future studies will have to define the target substrates of p21 in differentiated cardiac myocytes. This approach could further clarify the differences between hypertrophic and proliferative processes and provide important insights into the pathogenesis of cardiac hypertrophy.

6 References

Baker KM, Chernin MI, Wixson SK, Aceto JF. Renin-angiotensin system involvement in pressure-overload cardiac hypertrophy in rats. *Am J Physiol* 1990;259:H324-H32.

Becker-Hapak M, McAllister SS, Dowdy SF. TAT-Mediated Protein Transduction into Mammalian Cells. METHODS 2001;24:247-56.

Bellido T, O'Brien CA, Roberson PK, Manolagas SC. Transcriptional activation of the p21(WAF1,CIP1,SDI1) gene by interleukin-6 type cytokines. A prerequisite for their pro-differentiating and anti-apoptotic effects on human osteoblastic cells. J Biol Chem 1998;273: 21137-44.

Besson A, Assoian RK, Roberts JM. Regulation of the cytoskeleton: an oncogenic function for CDK inhibitors? Nat Rev Cancer 2004;4:948-55.

Borriello A, Roberto R, Della Ragione F, Iolascon A. Proliferate and survive: cell division cycle and apoptosis in human neuroblastoma. Haematologica 2002;87:196-214.

Brooks G, Poolman RA, Li JM. Arresting development in cardiac myocyte cell cycle: Role of cyclin-dependent kinase inhibitors. Cardiovascular Res 1998;39:301-11.

Brooks G, Poolman RA, McGill CJ, Lim JM. Expression and activities of cyclins and cyclin-dependent kinases in developing rat ventricular myocytes. J Mol Cell Cardiol 1997;29:2261-71.

Brugarolas J, Chandrasekaran C, Gordon JI, Beach D, Jacks T and Hannon GJ. Radiation-induced cell cycle arrest compromised by p21 deficiency. Nature 1995;377:552-7.

Bueno OF, De Windt LJ, Tymitz KM, et al. The MEK1-ERK1/2 signaling pathway promotes compensated cardiac hypertrophy in transgenic mice. EMBO J 2000;19:6341-50.

Busk PK, & Hinrichsen R. Cyclin D in left ventricle hypertrophy. Cell Cycle 2003;2:91-5.

Burton PB, Yacoub MH, Barton PJ. Cyclin-dependent kinase inhibitor expression in human heart failure. A comparison with fetal development. Eur Heart J 1999;10:604-11.

Cao G, Pei W, Ge H, et al. In Vivo Delivery of a Bcl-xL Fusion Protein Containing the TAT Protein Transduction Domain Protects against Ischemic Brain Injury and Neuronal Apoptosis. J Neurosci 2002;22:5423-31.

Capasso JM, Bruno S, Cheng W, et al. Ventricular loading is coupled with DNA synthesis in adult cardiac myocytes after acute and chronic myocardial infarction in rats. Circ Res 1992;71:1379-89.

Chen L, Hahn H, Wu G, et al. Opposing cardioprotective actions and parallel hypertrophic effects of delta PKC and epsilon PKC. Proc Natl Acad Sci U S A 2001;98:11114-9.

Chien KR, Grace AA, Hunter JJ. Molecular and cellular biology of cardiac hypertrophy and failure. In: Chien KR, editor, Molecular basis of cardiovascular disease, Philadelphia, PA: Saunders, 1999:211-50.

Clark E, Santiago F, Deng L, et al. Loss of G(1)/S checkpoint in human immunodeficiency virus type 1-infected cells is associated with a lack of cyclin-dependent kinase inhibitor p21/Waf1. J Virol 2000;74:5040-52.

Coqueret O. New roles for p21 and p27 cell-cycle inhibitors: a function for each cell compartment? Trends Cell Biol 2003;13:65-70.

Courtney M, Buchwalder A, Tessier LH, et al. High-level production of biologically active human alpha 1-antitrypsin in Escherichia coli. Proc Natl Acad Sci USA 1984;81:669-73.

Crabtree GR, & Olson EN. NFAT signaling: choreographing the social lives of cells. Cell 2002;109(Suppl.):S67-79.

Darnell JE. STATs and gene regulation. Science 1997;277:1630-5.

Dotto GP. p21$^{WAF1/Cip1}$: more than a break to the cell cycle? Biochimica Biophysica Acta 2000;1471:M43-M56.

Fawell S, Seery J, Daikh Y, et al. Tat-mediated delivery of heterologous proteins into cells. Proc Natl Acad Sci USA 1994;91:664-8.

Flink IL, Oana S, Bahl JJ, Morkin E. Terminal differentiation in cardiomyocytes results from hypophosphorylation of retinoblastoma protein by induction of cyclin-dependent kinase inhibitory activities. Circulation 1996;94:A2745.

Frankel AD, & Pabo CO. Cellular uptake of the tat protein from human immunodeficiency virus. Cell 1988;55:1189-93.

Frey N, & Olson EN. Cardiac hypertrophy: the good, the bad, and the ugly. Annu Rev Physiol 2003;65:45-79.

Fujisaki H, Ito H, Hirata Y, et al. Natriuretic peptides inhibit angiotensin II-induced proliferation of rat cardiac fibroblasts by blocking endothelin-1 gene expression. J Clin Invest 1995;96:1059-65.

Gautier VW, Sheehy N, Duffy M, Hashimoto K, Hall WW. Direct interaction of the human I-mfa domain-containing protein, HIC, with HIV-1 Tat results in cytoplasmic sequestration and control of Tat activity.´Proc Natl Acad Sci USA 2005;102:16362-7.

Giles TD. Angiotensin-converting enzyme inhibition, cell growth, and left ventricular hypertrophy in hypertension. Clin Cardiol 1991;14:IV63-67; discussion IV83-90.

Gille H, & Downward J. Multiple ras effector pathways contribute to G_1 cell cycle progression. J Biol Chem 1999;274:22033-40.

Grana X, Garriga J, Mayol X. Role of the retinoblastoma protein family, pRB, p107 and p130 in the negative control of cell growth. Oncogene 1998;17:3365-83.

Green M, & Loewenstein PM. Autonomous functional domains of chemically synthesized human immunodeficiency virus tat trans-activator protein. Cell 1988;55:1179-88.

Gulbis JM, Kelman Z, Hurwitz J, O'Donnell M, Kuriyan J. Structure of the C-terminal region of p21(WAF1/CIP1) complexed with human PCNA. Cell 1996;87:297-306.

Gustafsson AB, Sayen MR, Williams SD, Crow MT, Gottlieb RA. TAT protein transduction into isolated perfused hearts: TAT-apoptosis repressor with caspase recruitment domain is cardioprotective. Circulation 2002;106:735-9.

Gu Y, Turck CW, Morgan DO. Inhibition of CDK2 activity in vivo by an associated 20K regulatory subunit. Nature 1993;366:707-10.

Harper JW, Elledge SJ, Keyomarsi K, et al. Inhibition of cyclin-dependent kinases by p21. Mol Biol Cell 1995;6:387-400.

Ho A, Schwarze SR, Mermelstein SJ, Waksman G, Dowdy SF. Synthetic protein transduction domains: enhanced transduction potential in vitro and in vivo. Cancer Res 2001;61:474-7.

Hochuli E, Döbeli H, Schacher A. New metal chelate adsorbent selective for proteins and peptides containing neighboring histidine residues. J Chromatogr 1987;411:177-84.

Hunter JJ, & Chien KR. Signaling pathways for cardiac hypertrophy and failure. N Engl J Med 1999;341:1276-83.

Jiang Y., Cheng DW, Levi E, Singh LP. IGF-1 increases laminin, cyclin D1, and P21(Cip1) expression in glomerular mesangial cells: An investigation of the intracellular signaling pathway and cell-cycle progression. J Cell Biochem 2006 Jan 11; [Epub ahead of print].)

Joshi BH, & Puri RK. Optimization of expression and purification of two biologically active chimeric fusion proteins that consist of human interleukin-13 and Pseudomonas exotoxin in Escherichia coli. Protein Expr Purif 2005;39:189-98.

Karliner JS, Kariya T, Simpson PC. Effects of pertussis toxin on a1-agonist–mediated phosphatidylinositide turnover and myocardial cell hypertrophy in neonatal rat myocytes. Experientia 1990;46:81-4.

Keyomarsi K, & Herliczek TW. The role of cyclin E in cell proliferation, development and cancer. Prog Cell Cycle Res 1997;3:171-91.

Kobayashi H, Stewart E, Poon R, Adamczewski JP, Gannon J, Hunt T. Identification of the domains in cyclin A required for binding to, and activation of, p34cdc2 and p32cdk2 protein kinase subunits. Mol Biol Cell 1992;3:1279-94.

Kodama H, Fukuda K, Pan J, et al. Biphasic activation of the JAK/STAT pathway by angiotensinII in rat cardiomyocytes. Circ Res 1998;82:244-50.

Koh KN, Kang MJ, Frith-Terhune A, et al. Persistent and heterogenous expression of the cyclin-dependent kinases inhibitor, $p27^{KIP1}$, in rat hearts during development. J Mol Cell Cardiol 1998;30:463-74.

Kolch W, Heidecker G, Lloyd P, Rapp UR. Raf-1 protein kinase is required for growth of induced NIH/3T3 cells. Nature 1991;349:426-8.

Korzus E, Torchia J, Rose D, et al. Transcription factor-specific requirements for coactivators and their acetyltransferase functions. Science 1998;279:703-7.

Larochelle S, & Fisher RP. CDK-activating kinases: detection and activity measurements. Methods Mol Biol 2005;296:279-90.

Lea NC, Buggins AG, Orr SJ, Mufti GJ, Thomas NS. High efficiency protein transduction of quiescent and proliferating primary hematopoietic cells. J Biochem Biophys Methods 2003; 55:251-8.

Leinwand LA. Calcineurin inhibition and cardiac hypertrophy: a matter of balance. Proc Natl Acad Sci USA 2001;98:2947-9.

Leite MF, Page E, Ambler SK. Regulation of ANP secretion by endothelin-1 in cultured atrial myocytes: desensitization and receptor subtype. Am J Physiol 1994;267:H2193-H203.

Lim HW, New L, Han J, Molkentin JD. Calcineurin enhances MAPK phosphatase-1 expression and p38 MAPK inactivation in cardiac myocytes. J Biol Chem 2001;276:15913-9.

Lipskaia L, & Lompre AM. Alteration in temporal kinetics of Ca2+ signaling and control of growth and proliferation. Biol Cell 2004;96:55-68.

Marino TA, Haldar S, Williamson EC, et al. Proliferating cell nuclear antigen in developing and adult rat cardiac muscle cells. Circ Res 1991;69:1353-60.

Medema RH, Herrera RE, Lam F, Weinberg RA. Growth suppression by p16ink4 requires functional retinoblastoma protein. Proc Natl Acad Sci USA 1995;92:6289-93.

Melekhovets YF & Joshi S. Fusion with an RNA binding domain to confer target RNA specificity to an RNase: design and engineering of Tat-RNase H that specifically recognizes and cleaves HIV-1 RNA in vitro. Nucleic Acids Res 1996;24:1908-12.

Meyerson M, & Harlow E. Identification of G1 kinase activity for cdk6, a novel cyclin D partner. Mol Cell Biol 1994;14:2077-86.

Molkentin JD, Lu JR, Antos CL, et al. A calcineurin-dependent transcriptional pathway for cardiac hypertrophy. Cell 1998;93:215-28.

Morgan DO. Cyclin-dependent kinases: engines, clocks, and microprocessors. *Annu. Rev.* Cell Dev Biol 1997;13:261-91.

Nagahara H, Vocero-Akbani AM, Snyder EL, et al. Transduction of full-length TAT fusion proteins into mammalian cells: TAT-p27Kip1 induces cell migration. Nat Med 1998;4:1449-52.

Nakayama K, & Nakayama K. Cip/Kip cyclin-dependent kinase inhibitors: Brakes of the cell cycle engine during development. Bioessays 1998;20:1020-9.

Neal JW, & Clipstone NA. A constitutively active NFATc1 mutant induces a transformed phenotype in 3T3-L1 fibroblasts. J Biol Chem 2003;278:17246-54.

Noguchi H, Matsushita M, Okitsu T, et al. A new cell-permeable peptide allows successful allogeneic islet transplantation in mice. Nat Med 2004;10:305-9.

Nozato T, Ito H, Tamamori M, et al. G1 cyclins are involved in the mechanism of cardiac myocyte hypertrophy induced by angiotensin II. Jpn Circ J 2000;64:595-601.

Obaya AJ, & Sedivy JM. Regulation of cyclin-Cdk activity in mammalian cells. Cell Mol Life Sci 2002;59:126-42.

Ohki R, Yamamoto K, Ueno S, et al. Transcriptional profile of genes induced in human atrial myocardium with pressure overload. Int J Cardiol 2004;96:381-7.

Ohtsubo M, Theodoras AM, Schumacher J, Roberts JM, Pagano M. Human cyclin E, a nuclear protein essential for the G1-to-S phase transition. Mol Cell Biol 1995;15:2612-24.

Olson EN, & Williams RS. Calcineurin signaling and muscle remodeling.Cell 2000;101:689-92.

Pan J, Fukuda K, Kodama H, et al. Role of angiotensin II in activation of the JAK/STAT pathway induced by acute pressure overload in the rat heart. Circ Res 1997;81:611-7.

Pan J, Fukuda K, Saito M, et al. Mechanical stretch activates the JAK/STAT pathway in rat cardiomyocytes. Circ Res 1999;84:1127-36.

Parker TG, Chow KL, Schwartz RJ, Schneider MD. Differential regulation of skeletal alpha-actin transcription in cardiac muscle by two fibroblast growth factors. Proc Natl Acad Sci USA 1990;87:7066-70.

Perkins ND. Not just a CDK inhibitor: regulation of transcription by p21(WAF1/CIP1/SDI1). Cell Cycle 2002;1:39-41.

Poolman RA, & Brooks G. Expressions and activities of cell cycle regulatory molecules during the transition from myocyte hyperplasia to hypertrophy. J Mol Cell Cardiol 1998; 30:2121-35.

Poolman RA, Gilchrist R, Brooks G. Cell cycle profiles and expressions of p21CIP1 and P27KIP1 during myocyte development. Int J Cardiol 1998;67:133-42.

Pumiglia KM, & Decker SJ. Cell cycle arrest mediated by the MEK/mitogen activated protein kinase pathway. Proc Natl Acad Sci USA 1997;94:448-52.

Quentmeier H, Zaborski M, Drexler HG. Effects of thrombopoietin, interleukin-3 and the kinase inhibitor K-252a on growth and polyploidization of the megakaryocytic cell line M-07e. Leukemia 1998;12:1603-11.

Regula KM, Rzeszutek MJ, Baetz D, Seneviratne C, Kirshenbaum LA. Therapeutic opportunities for cell cycle re-entry and cardiac regeneration. Cardiovasc Res 2004;64:395-401.

Rosato RR, Wang Z, Gopalkrishnan RV, Fisher PB, Grant S. Evidence of a functional role for the cyclin-dependent kinase-inhibitor p21WAF1/CIP1/MDA6 in promoting differentiation and preventing mitochondrial dysfunction and apoptosis induced by sodium butyrate in human myelomonocytic leukemia cells (U937). Int J Oncol 2001;19:181-91.

Sadoshima J, Aoki H, Izumo S. Angiotensin II and serum differentially regulate expression of cyclins, activity of cyclin-dependent kinases, and phosphorylation of retinoblastoma gene product in neonatal cardiac myocytes. Circ Res 1997;80:228-41.

Sadoshima J, & Izumo S. Molecular characterization of angiotensin II--induced hypertrophy of cardiac myocytes and hyperplasia of cardiac fibroblasts. Critical role of the AT1 receptor subtype. Circ Res 1993;73:413-23.

Sadoshima J, Xu Y, Slayter HS, Izumo S. Autocrine release of angiotensin II mediates stretch-induced hypertrophy of cardiac myocytes in vitro. Cell 1993;75:977-84.

Sayeski PP, Ali MS, Frank SJ, Bernstein KE. The angiotensin II-dependent nuclear translocation of Stat1 is mediated by the Jak2 protein motif ^{231}YRFRR. J Biol Chem 2001; 276:10556-63.

Schwarze SR, & Dowdy SF. In vivo protein transduction: Intracellular delivery of biologically active proteins, compounds and DNA. Trends Pharmacol Sci 2000;21:45-8.

Schwarze SR, Ho A, Vocero-Akbani A, Dowdy SF. In vivo protein transduction: Delivery of a biologically active protein into the mouse. Scienc 1999;285:1569-72.

Sewing A, Wiseman B, Lloyd AC, Land H. High-intensity Raf signal causes cell cycle arrest mediated by p21Cip1. Mol Cell Biol 1997;17:5588-97.

Sherr CJ. Mammalian G_1 cyclins. Cell 1993;73:1059-65.

Sherr CJ. G1 phase progression: cyclin on cue. Cell 1994;79:551-5.

Sherr CJ, Roberts JM. CDK inhibitors: positive and negative regulators of G1-phase progression. Genes Dev 1999;13:1501-12.

Smith MR, Heidecker G, Rapp UR, Kung HF. Induction of transformation and DNA synthesis after microinjection of *raf* proteins. Mol Cell Biol 1990;10:3828-33.

Snyder EL, & Dowdy SF. Cell penetrating peptides in drug delivery. Pharm Res 2004; 21:389-93.

Stein GH, Drullinger LF, Soulard A, Dulic V. Differential roles for cyclin-dependent kinase inhibitors p21 and p16 in the mechanisms of senescence and differentiation in human fibroblasts. Mol Cell Biol 1999;19:2109-17.

Takaoka H, Esposito G, Mao L, Suga H, Rockman HA. Heart size-independent analysis of myocardial function in murine pressure overload hypertrophy. Am J Physiol Heart Circ Physiol 2002;282:H2190-7.

Takeishi Y, & Walsh RA. Cardiac hypertrophy and failure: lessons learned from genetically engineered mice. Acta Physiol Scand. Acta Physiol Scand 2001;173:103-11.

Takemoto M, Node K, Nakagami H, et al. Statins as antioxidant therapy for preventing cardiac myocyte hypertrophy. J Clin Invest 2001;108:1429-37.

Tamamori M, Ito H, Hiroe M, Terada Y, Marumo F, Ikeda MA. Essential roles for G1 cyclin-dependent kinase activity in development of cardiomyocyte hypertrophy. Am J Physiol 1998;275:H2036-40.

Taules M, Rodriguez-Vilarrupla A, Rius E, et al. Calmodulin binds to p21(Cip1) and is involved in the regulation of its nuclear localization. J Biol Chem 1999;274:24445-8.

Taya Y. RB kinases and RB-binding proteins: new points of view. Trends Biochem Sci 1997;22:14-7.

Treisman R. Regulation of transcription by MAP kinase cascades. Curr. Opin. Cell Biol 1996; 8:205-15.

Verschuren EW, Jones N, Evan GI. The cell cycle and how it is steered by Kaposi's sarcoma-associated herpesvirus cyclin. J Gen Virol 2004;85:1347-61.

Vives E. present and future of cell-penetrating peptide mediated delivery systems: "Is the Trojan horse too wild to go only to Troy?". J Control Release 2005;109:77-85.

Vocero-Akbani AM, Heyden NV, Lissy NA, Ratner L, Dowdy SF. Killing HIV-infected cells by transduction with an HIV protease-activated caspase-3 protein. Nat Med 1999;5:29-33.

von Harsdorf R, Hauck L, Mehrhof F, Wegenka U, Cardoso MC, Dietz R. E2F-1 overexpression in cardiomyocytes induces downregulation of p21CIP1 and p27KIP1 and release of active cyclin-dependent kinases in the presence of insulin-like growth factor I. Circ Res 1999;85:128-36.

Wadia JS, & Dowdy SF. Modulation of cellular function by TAT mediated transduction of full length proteins. Curr Protein Pept Sci 2003;4:97-104.

Wadia JS, & Dowdy SF. Protein transduction technology. Curr Opin Biotechnol 2002;13:52-6.

Wadia JS, & Dowdy SF. Transmembrane delivery of protein and peptide drugs by TAT-mediated transduction in the treatment of cancer. Adv Drug Deliv Rev 2005;57:579-96.

Wadia JS, Stan RV, Dowdy SF. Transducible TAT-HA fusogenic peptide enhances escape of TAT-fusion proteins after lipid raft macropinocytosis. Nature Medicine 2004;10:310-5.

Xiong Y, Hannon GJ, Zhang H, Casso D, Kobayashi R, Beach D. p21 is a universal inhibitor of cyclin kinases. Nature 1993;366:701-4.

Yang W, Velcich A, Lozonschi I, et al. Inactivation of p21WAF1/cip1 enhances intestinal tumor formation in Muc2-/- mice. Am J Pathol 2005;166:1239-46.

7 Appendix

7.1 Abbreviations

°C	Celcius
A	Ampere
ACE	Angiotensin-converting enzyme
Agn	Angiotensinogen
Amp	Ampicillin
ANF	Atrial natriuretic factor
BLAST	Basic local alignment tool
BSA	Bovine serume albumine
BP	Blood pressure
bp	base pairs
CDI	Cdk inhibitor
Cdk	Checkpoint kinase
cDNA	complementary DNA
cM	centiMorgan
cpm	counts per minute
cR	centiRay
d	Days
D	Dalton
DEPC	Diethylene pyrocarbonate
DNA	Deoxyribonucleic acid
DNase	Deoxyribonuclease
DTT	Dithiothreitol
dNTP	Deoxy-nucleoside triphosphate
EDTA	Ethylendiamine-N,N,N',N'-tetraacetate
E2F	E2A binding factor
E.coli	*Escherichia coli*
e.g.	exempli gratia
FAM	6-carboxyfluorescein
g	Gram
GAPDH	Glycerinaldehyde-3'-phosphate dehydrogenase
HDAC	Histone deacetylase
hr	hour
ID element	Identifier element
i.e.	id est
IPTG	isopropyl-β-D-thiogalactoside
kb	kilo bases
kD	kilo dalton
KO	knockout
l	Litre
LB	Luria broth medium
LMP	low-melting point
LVH	left ventricular hypertrophy
m	Milli
M	Molar
Mr	Molecular weight
µ	Micro
µCi	Micro Curie
µg	Micro gram
µl	Micro litre
µM	Micro molar

Mb	Mega bases
MEF	Mouse embryonic fibroblast
MHC	Myosin heavy chain
Min	Minute
NaCl	Sodiumchloride
NaCl	Sodiumchloride
ng	Nano gram
nl	Nano litre
nM	Nano molar
NGFR	Nerve growth factor receptor
No.	Number
OD	Optical density
ORF	Open reading frame
PAGE	Polyacrylamid gel electrophoresis
PCR	Polymerase chain reaction
pH	Logarithm of the reciprocal of the hydrogen ion concentration
PI3-K	Phosphoinositide 3-kinase
PIKK	Phosphatidy inositol-3-kinase-like kinase
PMSF	Phenyl-methyl-sulphonyl-fluoride
Pnmt	phenylethanolamine-N-methyltransferase
PPY	Pancreatic polypeptide
RAS	Renin-angiotensin system
RNA	Ribonucleic acid
RNase	Ribonuclease
rpm	revolutions per minute
RT	Room temperature
RZPD	Resource Centre/Primary Database (Ressourcen-Zentrum Primär-Datenbank)
s	second
SDS	Sodium dodecyl sulfate
Taq	Thermophilus aquaticus
TB	Terific broth
TBE	Tris-borat-EDTA
Tris	Tris-(hydroxymethyl)-aminomethane
U	Unit
UBF	Upstream binding factor
V	Volt
weight	w
wt	wild type

7.2 Table of Figures

7.3 Curriculum Vitae

Due to protection of data privacy the Curriculim Vitae is not published online.

7.4 Publications

Articles related to the MD thesis:

Hauck L, **An J**, Dietz R, von Harsdorf R. Modulation of p21 and p73α activities by MDM2 confers resistance to hypertrophic and apoptotic signaling in cardiomyocytes. Submitted.

Hauck L, Harms C, **An J**, Dietz R, Endres M, von Harsdorf R. p21 is required for the inhibition of heart growth by HMG-CoA reductase inhibitors. Submitted.

Other articles:

Hauck L, **An J**, Punnoose AM, Kronenberg G, Dietz R, von Harsdorf R. The E2F4-p130 transcriptional repressor recruits histone deacetylase 1 to promoters of key apoptotic genes that is required for cardiomyocyte viability. Submitted

An J, Ch J, Li X, et al. Effect of Granulocyte colony stimulating factor on modulation of mdr1 gene expression in primary cells of human acute myeloblastic leukemia. Journal of Experimental Hematology 1999;7:42-6.

An J, Zh S, An H, et al. Relationship between clinical prognosis and expression of p-170 and CD34 in patients with primary acute myeloblastic leukemia. Journal of Guangdong Medical College 1999;17:11-4.

An J, Ch J, Li X, et al. The modulation effect of granulocyte colony stimulating factor on the mdr1/P-gp expression in acute myeloid leukemic cells. Chinese Journal of Hematology 1998;19:342-5.

An J, Ch J, Li X, et al. The modulation effect of granulocyte colony stimulating factor on the P-gp expression in acute myeloid leukemic cells. Chinese Journal of Hematology 1998;19: 98-9.

An J, Wang Z, Zh S, et al. Primary human acute myeloblastic leukemia: An analysis of in vitro granulocyte maturation following stimulation with G-CSF. Journal of Guangdong Medical College 1998;16:191-4.

An J, Ch J, Li X, et al. MDR1 gene _expression in AML patients and its correlation with CD34 immunophenotype. Journal of Clinical Hematology 1998;11:7-9.

An J, Zh S, Zheng H, et al. The clinical significance of plasma tissue factor pathway inhibitor in leukemic patients. Chinese Journal of Thrombosis and Hemostasis 1998;5:79-80.

Zh S, **An J**, Zheng H, et al. The value of clinical implication of plasma tissue factor pathway inhibitor (TFPI) in leukemia and MDS. Journal of Clinical Hematology 1998;12:12-3.

Liu G, Li F, Cai W, Yang Q, Xie Z, **An J.** Identification of FBG-455G/A polymorphisms in 210 samples of Gangdong population and the relationship with plasma fibrinogen level. Chinese Journal of Hematology 1999;20:255-7.

7.5 Acknowledgements

The present study was carried out at the Max Delbrück Center for Molecular Medicine in Berlin, during 2002-2006. I owe my gratitude to Professor Dr. Rainer Dietz and Professor Dr. Rüdiger von Harsdorf for the excellent research facilities, for giving me the opportunity to work in the field of cardiovascular research and for their support during these years. I would like to specially thank Priv.-Doz. Dr. Martin Bergmann for the review of my MD thesis.

My special thanks goes to Dr. Stefan Donath for the great support and valuable comments on the manuscript of this thesis. I also wish to thank Dr. Ludger Hauck for his excellent supervision. I wish to express my gratitude to all those who have given me valuable assistance and help during this project.

I wish to thank Dr. Christoph Harms for his encouragement and his good advices also during difficult times. I would like to acknowledge all of my colleagues who in one or the other way made my work a pleasure. Thanks to Alan M. Punnoose and Thomas Knaus for their support and great sense of humor. It was especially nice to work with Marlies Grieben and Daniela Grothe at some stages of this study.

My sincerest gratitude goes to my parents for their care, love, and everlasting support. I owe my deepest thanks to Shulan for her love, encouragement, help, and understanding during these years.

Statement

Ich, Junfeng An, erkläre, dass ich die vorgelegte Dissertationsschrift mit dem Thema: “Protein transduction of $p21^{CIP1}$ inhibits angiotensin II-induced cardiac hypertrophy in mice” selbst verfasst und keine anderen als die angegebenen Quellen und Hilfsmittel benutzt, ohne die (unzulässige) Hilfe Dritter verfasst und auch in Teilen keine Kopien anderer Arbeiten dargestellt habe.

Datum Unterschrift